GEOLOGICA ULTRAIECTINA

Mededelingen van de Faculteit
Geowetenschappen Universiteit Utrecht

No. 283

Respiration in ocean margin sediments

Johan Henrik Andersson

ISBN: 978-90-5744-148-6

NIOO Thesis 61

Respiration in ocean margin sediments

Sedimentrespiratie in de overgang van het continentale plat naar de diepe oceaan

(met en samenvatting in het Nederlands)

Proefschrift

ter verkrijging van de graad van doctor aan de Universiteit Utrecht op gezag van de rector magnificus, prof. dr. J.C. Stoof, ingevolge het besluit van het college voor promoties in het openbaar te verdedigen op maandag 12 november 2007 des middags te 2 uur

door

Johan Henrik Andersson

geboren op 15 december 1977 te Sölvesborg, Zweden

Promotoren:	Prof. dr. C. H. R. Heip
	Prof. dr. J. J. Middelburg
Co-promotor:	Dr. K. Soetaert

This thesis was supported by the Netherlands Organisation for Scientific Research and the European Union (ORFOIS; EVK2-CT-2001-00100).

Contents

1 General introduction

Despite the fact that marine sediments might look very dull and uninspiring, at a first glance no more than lifeless cold brownish mud, this impression is far from the truth. Marine sediment flourish with life, ranging from bacteria performing a multitude of chemical reactions to a suite of benthic animals such as mussels, worms and sea urchins. Moreover, marine sediment are intimately linked to the presence of oxygen in the atmosphere, provide the key to the past climate and represent a removal site of bioavailable nitrogen and phosphorus.

1.1 Oxygen in the marine environment

Oxygen[1] has been a favored electron acceptor ever since it first appeared in the atmosphere in the beginning of the early Proterozoic era, 2.4 Gyr ago as a byproduct of oxygenic photosynthesis (Catling and Claire, 2005). However, photosynthetic production of oxygen is not enough to produce an oxic atmosphere, since it will be consumed rapidly by respiration of organic matter (OM) and oxidation of reduced substances, unless the OM and reduced substances are out of contact with oxygen. Present estimates of the global net primary production and heterotrophic respiration are 8.4 Pmol O_2 yr^{-1} and 8.39 Pmol O_2 yr^{-1}, respectively (Lenton, 2003). The slight difference (0.1 %) between these two numbers is the key to the presence of oxygen in the atmosphere, due to the process of burial of organic carbon and pyrite in continental margin sediments (Berner and Raiswell, 1983; Middelburg and Meysman, 2007).

With such a powerful electron donor as oxygen available, life was able to evolve from unicellular to multicellular organisms, i.e. metazoans (Knoll and Carroll, 1999). This occurred around 0.6 Gyr ago, after oxygen had

[1]Oxygen in this chapter actually refers to either O_2(g) or O_2(aq)

Table 1.1: Respiration pathways in ocean margin sediments

Pathway	Chemical reaction
Aerobic respiration	$CH_2O + O_2 \rightarrow CO_2 + H_2O$
Denitrification	$5CH_2O + 4NO_3^- \rightarrow 4HCO_3^- + 2N_2 + CO_2 + 3H_2O$
Manganese reduction	$CH_2O + 2MnO_2 + H_2O \rightarrow HCO_3^- + 2Mn^{2+} + 3OH^-$
Iron reduction	$CH_2O + 4Fe(OH)_3 \rightarrow HCO_3^- + 4Fe^{2+} + 7OH^- + 3H_2O$
Sulfate reduction	$2CH_2O + SO_4^{2-} \rightarrow 2HCO_3^- + H_2S$

increased even further, near the end of the Proterozoic era (Canfield and Teske, 1996). Along with the evolution of metazoans with muscular, unidirectional guts came also faecal pellets, which transported OM through the water column at a much faster rate than previously (Logan et al., 1995). Thus, the biological pump became operational, the sea floor was oxygenated and oxygen levels in the surface ocean increased even further, allowing metazoans to diversify even more (Meysman et al., 2006).

Despite this dramatic oxygenation, anoxic environments are still present today in some oceans basins and in sediments. This excludes metazoans from living deep down in the sediment. Various animals, such as polychaete worms, bury themselves beneath the sediment surface, but have to maintain contact with the overlying water to get oxygen. By pumping water, they ventilate their burrows and can in this way breathe and sustain themselves. Ventilation also causes a modification of the redox potential in the immediate surroundings of the burrow, by oxygenating layers of sediment where oxygen would never reach if transport were solely occurring by molecular diffusion. Deeper down in the sediment than the burrows reach, is the exclusive domain of unicellular organisms relying on ancient pathways of respiration, such as denitrification, manganese reduction, iron reduction and sulfate reduction (Table 1.1).

In some places in the ocean, where vertical mixing is limited, e.g. due to stratification, and where oxygen consumption is high, due to high input of OM, poor oxygen conditions develop in the bottom water and drastically modify the benthic community. In areas where the overlying water is permanently close to anoxia, but still some oxygen remaining, such as the Oxygen Minimum Zones of the Pacific Ocean and the Arabian Sea, adaptations to these conditions have arisen. These adaptations to low oxygen concentrations are quite diverse and include thin flat bodies,

enhanced respiratory surface area and the presence of sulfide-oxidizing symbionts (Levin, 2003).

Besides the direct impact of oxygen depletion on the presence of fauna, poor oxygen conditions also interact in a positive feedback with nutrient cycles by releasing phosphorus, otherwise bound to iron hydroxides under oxic conditions (Benitez-Nelson, 2000; Kemp et al., 2005). Lack of oxygen also impedes nitrification, i.e. the conversion of ammonia to nitrate, and thus limits the availability of nitrate for denitrifying bacteria and hence the coupled nitrification/denitrification, which converts biologically available nitrogen to the more inaccessible form of nitrogen gas, N_2 (Kemp et al., 1990; Rysgaard et al., 1994; Middelburg et al., 1996).

1.2 Quantification of organic matter cycling in marine sediments

Once particulate organic matter (POM) has been deposited on the sea floor its long-term fate is either to be preserved and buried or to be mineralized and released, as dissolved substances, back to the overlying water column. The fate of OM depends on several factors, where the amount of OM arriving at the sediment surface is one of the most important (Hedges and Keil, 1995). The input of POM has been measured with sediment traps, devices somewhat similar to large rain gauges. However, this is not as trivial as it might seem. In order to get an accurate estimate of the flux arriving at the sediment surface, the sediment trap should be deployed as close as possible to the bottom, but above the benthic boundary layer to avoid POM entering the trap via resuspension causing the flux estimate to be too high. By placing the trap higher up in the water column, lateral input of POM is neglected and the flux is consequently underestimated (van Weering et al., 2001). Indeed, POM fluxes measured by sediment traps are generally too low to sustain the fluxes measured by sediment incubations (Jahnke et al., 1990; Lampitt et al., 1995; Herman et al., 2001).

A common technique to measure fluxes, such as respiration rates, in marine sediments is the incubation of intact sediments. A known area of sediment is incubated together with a known volume of ambient bottom

water. A large range of solutes, e.g. nutrients, metals and dissolved inorganic carbon have been measured on discrete water samples (Dyrssen et al., 1984). Some solutes such as oxygen can be measured during the incubation with sensors such as electrodes or optodes (Glud et al., 2000, cf. Chapter 6). The flux J of a solute i is calculated from the concentration change over time during the incubation,

$$J_i = \frac{dC_i}{dt}\frac{V}{A} = \frac{dC_i}{dt}h \tag{1.1}$$

where V is the volume of overlying water inside the incubator with area A. This calculation relies on a number of assumptions:

1. Steady-state conditions are valid during the incubation, i.e. the flux of the solute across the sediment-water interface (SWI) is equal to the depth integrated production or consumption due to respiration.

2. Respiration in the overlying water is negligible compared to that within the sediment

3. Differences in hydrodynamic conditions between the inside of the incubator and ambient conditions, have no influence on the fluxes across the SWI

Sediment can either be retrieved from the sea-floor, using e.g. a multiple corer (Barnett et al., 1984), or incubated *in situ* at the sea-floor using bell jars (Pamatmat and Banse, 1969) or benthic chamber landers (Tengberg et al., 1995) (Fig. 1.1).

By comparing *in situ* incubations with cores incubated on deck, deck incubations of deep-sea sediments have been shown to exhibit artificially high rates due to sampling artifacts, such as elevated temperature during the transit through the water column (Glud et al., 1994) or decompression resulting in lysis of bacteria and concurrent release of labile substrates for bacteria (Hall et al., 2007; Epping et al., 2002). However, there are also a number of advantages of incubating cores *ex situ* i.e. on deck:

1. Comparatively low cost of the incubation system.

2. Easy verification of a correct functioning of the system.

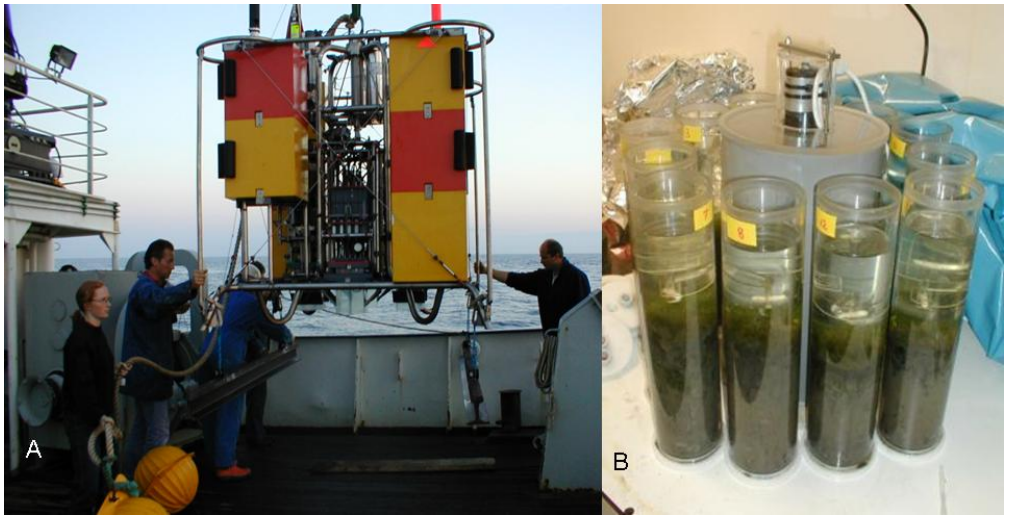

Figure 1.1: Examples of different types of incubation systems. A benthic chamber lander (**A**) and a shipboard incubation setup (**B**).

3. Possibility of manipulating the experimental conditions, such as temperature and light climate.

4. Height, necessary in the calculation of the flux (Eq. 1.1), is known with high accuracy.

Thus, *in situ* incubations are most clearly a necessary tool in the deep-sea environment (>1000m), but the question is still open if there is a difference between *in situ* and deck incubations in shallower environments (Millerway et al., 1994).

By incubating sediments, fluxes from the sediment to the water column of dissolved inorganic carbon or fluxes of oxygen into the sediment have thus been established for a wide range of environments. Sediment oxygen consumption rates range over several orders of magnitude from more than 200 in coastal sediments to 0.02 mmol O_2 $m^{-2}d^{-1}$ in abyssal sediments (Jørgensen, 1983; Middelburg et al., 1997, cf. Chapter 2).

The high activity in coastal sediments are a result of being close or even part of the euphotic zone, so that less respiration occurs in the water

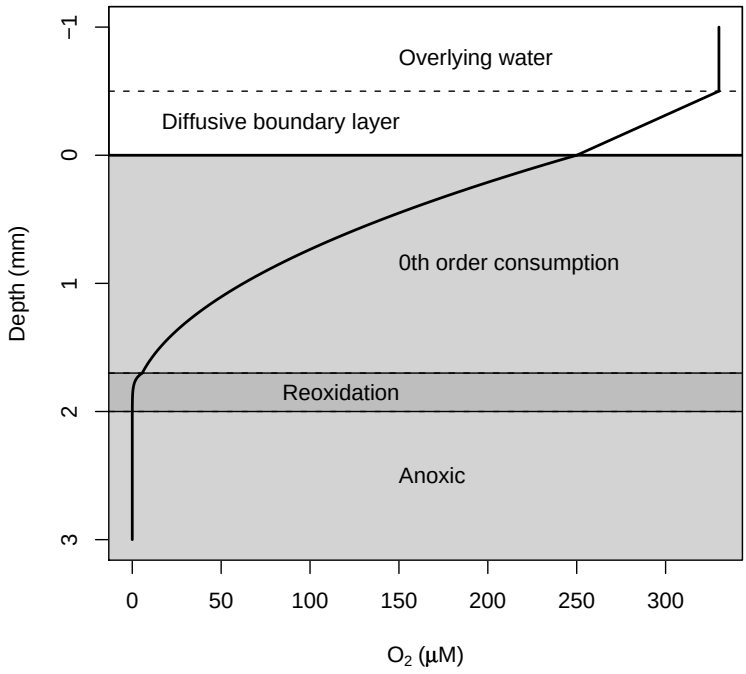

Figure 1.2: Typical oxygen microdistribution in a continental shelf sediment

column before reaching the sediment surface. Conversely, abyssal sediment receive only a very small part of the OM produced in the euphotic zone, the major part being mineralized in the overlying water column (Suess, 1980). The amount of OM deposited on the sediment surface, available for mineralization, is the main determinant of the flux of oxygen into the sediment and the oxygen penetration depth.

Using microelectrodes the oxygen microdistribution in the sediment can be measured, albeit at a single point (Revsbech et al., 1980; Jørgensen and Revsbech, 1985). Considering an idealized microdistribution of oxygen in muddy continental shelf sediments, five distinct vertical zones can be distinguished (Fig 1.2). First a constant concentration in the overlying water,

maintained by the moving water. Progressing down towards the sediment surface, the diffusive boundary layer (DBL) is encountered, where the current speed is low and molecular diffusion dominates the transport. If no consumption of oxygen occurs in the DBL, the concentration change becomes linear down to the actual sediment surface. In the oxic layer of the sediment, the volumetric oxygen consumption rate can be assumed constant, independent of the oxygen concentration, and described as a zero-order reaction (Bouldin, 1968, Model II). Below this layer, a thin layer of enhanced consumption often exists, because of overlap between oxygen and reduced substances such as Fe^{2+}, Mn^{2+} or HS^{-}, diffusing up from below (Jørgensen, 1983; Soetaert et al., 1996b; Berg et al., 1998). The oxygen microdistribution can be used to calculate the diffusive flux across the SWI, using the concentration gradient in the DBL,

$$J_{O_2} = -D_{sw}\frac{dO_2}{dx}, \tag{1.2}$$

where D_{sw} is the molecular diffusion coefficient in sea water, adjusted to *in situ* salinity and temperature. The concentration gradient in the top sediment can also be linearized and used to calculate the flux,

$$J_{O_2} = -\phi\frac{D_{sw}}{\theta^2}\frac{dO_2}{dx}, \tag{1.3}$$

and in this case both the porosity (ϕ) and the tortuosity (θ^2) have to be known and taken into account. This is also the reason why the concentration gradient is slightly steeper just below the sediment surface than in the DBL (Fig 1.2), as the flux is the same on both sides of the SWI but diffusion is impeded by sediment grains inside the sediment.

Nevertheless, none of the above flux calculations take the influence of the benthic fauna into account. Benthic animals increases the oxygen consumption both by their own respiration (Herman et al., 1999) and through enhancement of the flux of oxygen across the SWI by pumping oxygen-rich water from the overlying water in a process coined bio-irrigation. The contribution of bio-irrigation is variable depending on the functional type and number of benthic inhabitants, but can enhance the flux manifold and even be the dominant mode of transport across the SWI (Archer and Devol, 1992; Glud et al., 2003).

1.3 Experimental design and model identifiability

Experimental design involves thinking ahead in order to (1), be able to prove a given hypothesis and (2), to optimize the amount of work required to prove or falsify a hypothesis. Besides the obvious construction of the experimental setup, there are several other components involved in experimental design. One part of experimental design is the use of appropriate controls and procedural controls. Another is the sampling of the population [2] in order to get a representative and unbiased sample. For example, if one has postulated the hypothesis that benthic fauna in a certain area increases the sediment oxygen demand by at least 100% compared to the same sediment without fauna, one first has to acquire representative samples, often randomly assigned positions within the area described in the hypothesis. Secondly some of these samples will be used as controls, with as little as possible disturbance. Some of the samples will be used as experiments, i.e. the fauna will be removed from the sediment and some of the samples will be used as procedural controls, where fauna will be removed and put back in order to be able to show that it is not the procedure of removing the fauna, but the fauna itself that make the difference (Underwood, 1997). So far, experimental design involves only practical and logical thinking and neither mathematics nor statistics. The next step is deciding on the number of replicates to use. The ability to falsify a hypothesis using statistical techniques depends fundamentally on three parameters, (1) the variance within the population, (2) the effect size, i.e. the minimum difference between controls and experimental samples, (3) the number of replicates. The first parameter is an inherent part of the system and can not be influenced. The same goes for the second as it is part of the hypothesis. The third parameter, however, is usually only constrained by time, equipment and resources. If prior knowledge about the variance within the population is available from either literature or a pilot experiment, it is possible to calculate the minimum number of replicates necessary to test the hypothesis with sufficient statistical power, for simpler designs such as one-way ANOVA, formulas are available and

[2] Population in a statistical sense, where the samples are to be drawn from, e.g. shallow muddy sediments

for more complicated designs, computer simulations can be used. If the calculated number of necessary replicates is unfeasibly large, it is rather questionable to go ahead and do the experiment with fewer replicates, as this is almost certain a waste of time and money (Underwood, 1997).

Most questions, related to OM cycling in sediments, can not be answered by such manipulative experiments, but requires the use of non-linear models, typically solved with numerical integration techniques. In this case, the experimental design needs more elaborate techniques in order to test if the given hypothesis can be answered based on the intended sampling scheme. By using models that summarize the current knowledge, so called "state-of-the-art" models, a large number of processes are usually represented. Each process is described with at least one and usually several parameters. Such complex models are then applied to available data and a reasonable fit to the data is obtained by tuning of some of the parameters. In order to get a deeper understanding of the model behavior, model sensitivity analysis is a very useful tool where model parameters are varied systematically and the output examined (Soetaert et al., 1996b, 1998). Model parameters that have a large effect on the output are more likely to be identified uniquely. Examples of such "state-of-the-art" models relevant for OM cycling in sediments, often referred to as models of early diagenesis, are the one-dimensional dynamic reactive transport models developed by Berg et al. (2003b) and Meysman et al. (2003). Using a single data-set it usually not possible to identify all parameters in such models. By using the parameter identifiability technique developed by Brun et al. (2001), the combinations of parameters subsets that are likely to be identifiable can be found. As this technique is independent of actual observations it is very useful for the purpose of experimental design (Brun et al., 2001). This requires prior knowledge about reasonable parameter values for the system intended for the study and the intended sampling scheme. In the context of the models mentioned above, this would include the information on which variables are to be measured along with the depths and times of sampling.

1.4 Outline of this thesis

The aim of this thesis was to advance the knowledge on respiration in ocean margin sediments and the assessments of tools needed for this purpose. This was achieved using literature data, experimental techniques and diagenetic modeling.

In **Chapter 2** literature data of sediment oxygen consumption were compiled and used to estimate the global consumption of oxygen in the deep ocean (below 200m). Regressing sediment oxygen consumption versus water depth, a double exponential was fitted, describing the decrease with depth. By combining this relation with global bathymetric data the global consumption in both sediments and water column was calculated. Assuming that oxygen consumption is a quantitative measure of carbon production, the amount of OM received at the sea floor could be calculated and the efficiency of the biological pump was compared to previous estimates based on sediment traps and ocean general circulation models.

The short-term fate of phytodetritus was studied in the Arabian Sea and is presented in **Chapter 3**. This was done by amending sediment in incubations with diatoms labelled with ^{13}C. The sediment was incubated for a duration of two to five days. After incubating sediment cores, they were sectioned and overlying water, porewater and sediments were analyzed for label in dissolved organic and inorganic carbon, bacterial biomarkers and foraminiferal and macrofaunal biomass. The study sites ranged in depth from 140m to 1850m, encompassing the Oxygen Minimum Zone, which enabled us to study the effect of oxygen on the fate of phytodetritus under natural conditions.

Benthic respiration measurements were performed during three cruises, in the years 2003-2005, to the Gulf of Finland. The results from these cruise are presented in **Chapter 4**. Benthic fluxes of oxygen and dissolved inorganic carbon were derived from *in situ* incubations using a combination of two benthic landers. Three different stations were visited, representing three different sediment accumulation regimes, namely erosion, transport and accumulation stations. As mentioned earlier, interpreting benthic fluxes as respiration rates relies on a number of assumption, where one is the assumption of steady-state during the incubation. Since bottom water concentrations are variable in the Gulf of Finland, the effect of a variable bottom water concentration on the fluxes was investigated using

a dynamic diagenetic model.

Chapter 5 is a study of experimental design and parameter identifiability, where bio-irrigation measurements using inert tracers where chosen as an illustrative example. Bio-irrigation is often quantified through incubations where an inert tracer such as bromide is added to the overlying water of a core or a benthic chamber. Rates are derived by fitting the observed tracer distribution, after incubation for some time, with a model containing several parameters, where some, such as the enhancement over molecular diffusion or non-local exchange are *a priori* unknown. Identifiability analysis was used to investigate the minimum data requirements for two contrasting types of sediment, representative for deep-sea and shallow-water settings. Using two different datasets, uncertainties of the fitted parameters were calculated, based on Bayesian inference

In **Chapter 6**, a commercially available oxygen sensor was evaluated. This sensor uses an optical technique to measure the oxygen concentration. The availability of a oxygen sensor with a low detection limit is very useful in e.g. the study of low-oxygen environments, where large shifts in benthic communities occur with very small changes in oxygen concentration (Woulds et al., 2007). A set of ten different tests were performed, including both laboratory evaluations and field studies. The field studies, covered a wide range of situations, from shallow coastal waters and wastewater treatment plants to autonomous lander deployments at abyssal depths.

The thesis ends with a summary of the results from these various chapters.

2 Respiration patterns in the deep ocean

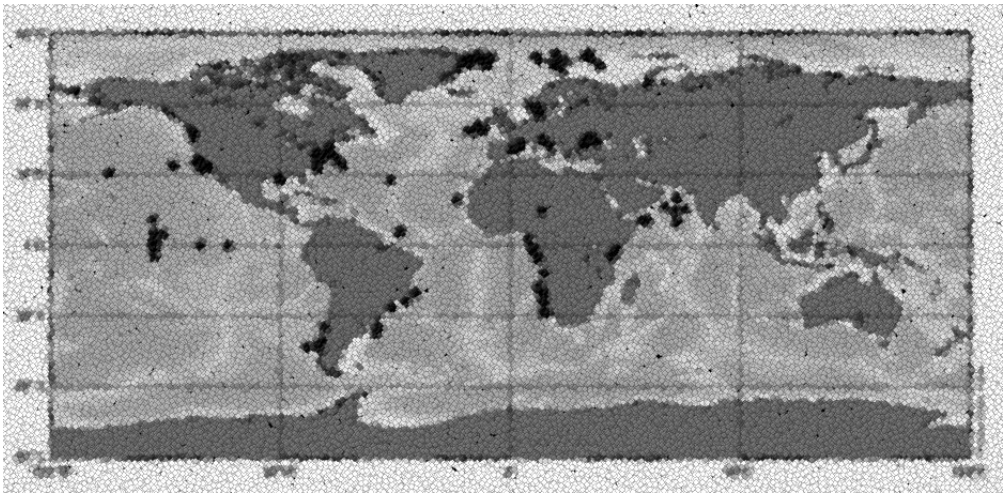

Johan Henrik Andersson, Jeroen W. M. Wijsman, Peter M. J. Herman, Jack J. Middelburg, Karline Soetaert and Carlo Heip, 2004, *Geophysical Research Letters*, 31, L03304, doi:10.1029/2003GL018756

2.1 Introduction

The net removal of carbon dioxide from the atmosphere in the oceans is due to the combined effect of the solubility and the biological pumps. The biological pump refers to the carbon fixed by primary producers in the euphotic zone and exported to the dark ocean below, where it is respired (Volk and Hoffert, 1985). The efficiency of this carbon pump depends not only on the rate of carbon fixation and export out of the surface layer, but also on the depth at which the organic carbon is respired because this determines the time during which carbon is isolated from the atmosphere (Yamanaka and Tajika, 1996).

However, our knowledge of respiration patterns below the photic zone and the governing processes (settling, degradation and particle aggregation / disaggregation) is limited (Boyd and Stevens, 2002). Because of that, biogeochemical ocean general circulation models (BOGCMs) usually impose the carbon fluxes using simple exponential (Heinze et al., 1999) or power law (Yamanaka and Tajika, 1996) relationships with depth.

Sediment traps are normally used to measure particulate organic matter (POM) fluxes (Suess, 1980). However, this approach has several drawbacks: hydrodynamic conditions, resuspension, swimmers and degradation of organic matter all decrease the predictive ability and fluxes have to be corrected for possible bias (Antia et al., 2001). Indeed, sediment carbon budgets, based on sediment traps, and when uncorrected, often reveal that POM fluxes are insufficient to support effluxes of total dissolved inorganic carbon or influxes of oxygen (Smith et al., 1992) or to sustain the fauna (Heip et al., 2001).

An alternative way to derive the flux of POM at a certain water depth is to use sediment oxygen consumption (SOC) measurements at the same depth. The rationale is that sediments are the ultimate sediment traps, that almost all carbon arriving at the sediment surface is respired and that oxygen consumption gives an integrative measure of carbon degradation (Herman et al., 2001). Because they integrate the POM influx over a considerable period of time, SOC data are much more invariant than fluxes of POM (Sayles et al., 1994). Moreover, they can be accurately measured by a variety of techniques: in situ with benthic landers (Tengberg et al., 1995) or by shipboard incubations of retrieved sediment cores.

A potential drawback of using SOC is that sediment deposition at a

particular depth in the ocean is affected by the local primary productivity, which decreases offshore (Wollast and Chou, 2001). Because of that, simply extrapolating sediment oxygen consumption rates from the productive shelf regions into organic matter fluxes in deep-sea waters may lead to overestimates.

In this paper we will use SOC data, compiled from the literature, to re-evaluate respiration patterns in the oceans below the shelf-break (200 m), both in the sediments and water. In a subsequent paper respiration on the continental shelf will be addressed. We will compare our estimates with those based on corrected sediment trap results, to test the applicability of SOC as a measure of water column processes.

2.2 Methods

2.2.1 Flux parameterizations

As there is insufficient understanding of the governing processes, the decrease of the organic matter deposition flux with depth, is often described statistically. The two common parameterizations are the exponential decrease (Volk and Hoffert, 1985) and the power law (Martin et al., 1987).

These parameterizations imply constancy with depth of the processes that shape the deposition or mineralization flux profiles. Recent findings suggest that the relationship of deposition fluxes with depth are not as simple, but are affected by the changes in physical or biological properties with depth of the water column (see section 2.3.1).

To include such depth-dependency of rates, we propose a different semi-empirical model, the double exponential decrease:

$$F(z) = F_0 \left[(1-p)e^{-b_1 z} + p\, e^{-b_2 z}\right] \tag{2.1}$$

In such formulation, the flux ($F(z)$) or remineralization gradually changes between two end member states, where p is a partitioning coefficient of the flux at the surface (F_0) and b_1 and b_2 are the slopes of the two exponentials. We are not explicit as to which end member states this equation refers to and as will be discussed below, it can be explained in a number of non-exclusive ways. We have adopted a weighted rather than a two-layer formulation to generate a gradual change.

2.2.2 Data

Sediment oxygen consumption rates from all parts of the ocean were collected in a database. From this database we excluded estimates obtained from modeling oxygen depth profiles, measured with microelectrodes, as these data do not account for the activity of large benthic animals (Archer and Devol, 1992). Moreover, as deck-measurements of cores from the deep sea may have too high oxygen consumption due to either pressure or temperature effects (Epping et al., 2002), we also excluded shipboard measurements of sediments below 1500 m. The data used then consisted of 490 measurements obtained from benthic landers (all depths) and from deck incubations (<1500 m). References to the data sources can be found in the electronic supplement. Data were log-transformed prior to analysis to get homogeneous variances. The bias introduced by this transformation was corrected following Middelburg et al. (1997).

2.3 Results and discussion

2.3.1 Remineralization profile

The semi-empirical fit of the double exponential function to the SOC data (Fig. 2.1) produces the parameter estimates displayed in Table 2.1. A double exponential ($R^2 = 0.68$, $p < 0.001$, $n = 490$) is significantly better compared to a single exponential even when taking into account two additional parameters (Sum of squares reduction test, $F_{2,485} = 103$, $p < 0.001$ (Schabenberger and Pierce, 2001)).

Table 2.1: Parameter estimates of equation (2.1)

Parameter	Central estimate	Low confidence limit[a]	High confidence limit[a]
F_0 [mmol m^{-2} d^{-1}]	38	30	45
p [-]	0.17	0.13	0.21
b_1 [m^{-1}]	0.018	0.012	0.024
b_2 [m^{-1}]	0.00046	0.00039	0.00053

[a] 95 % confidence interval

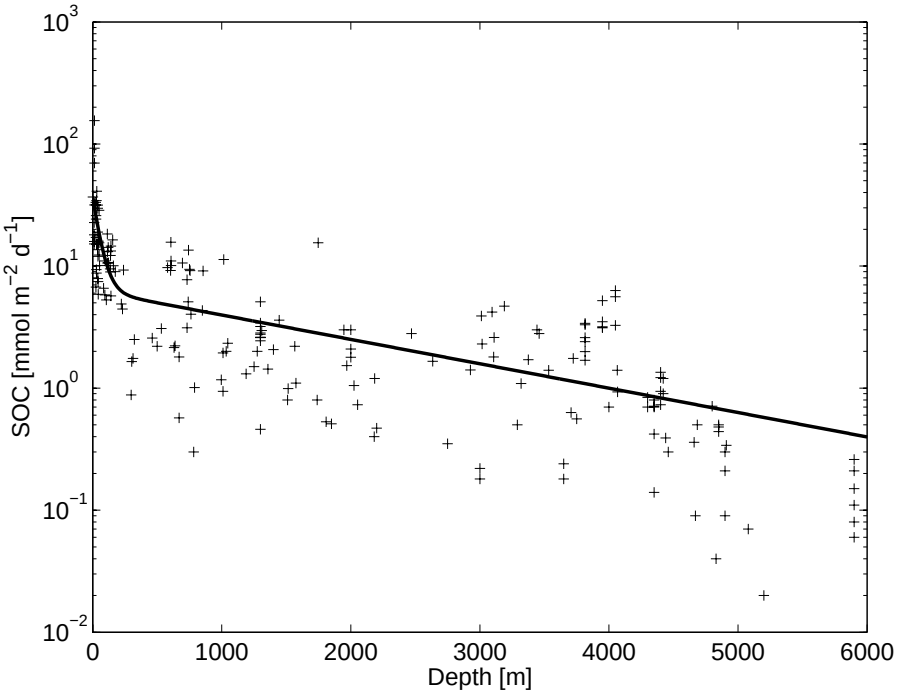

Figure 2.1: Depth attenuation of sediment oxygen consumption fitted by a double exponential profile.

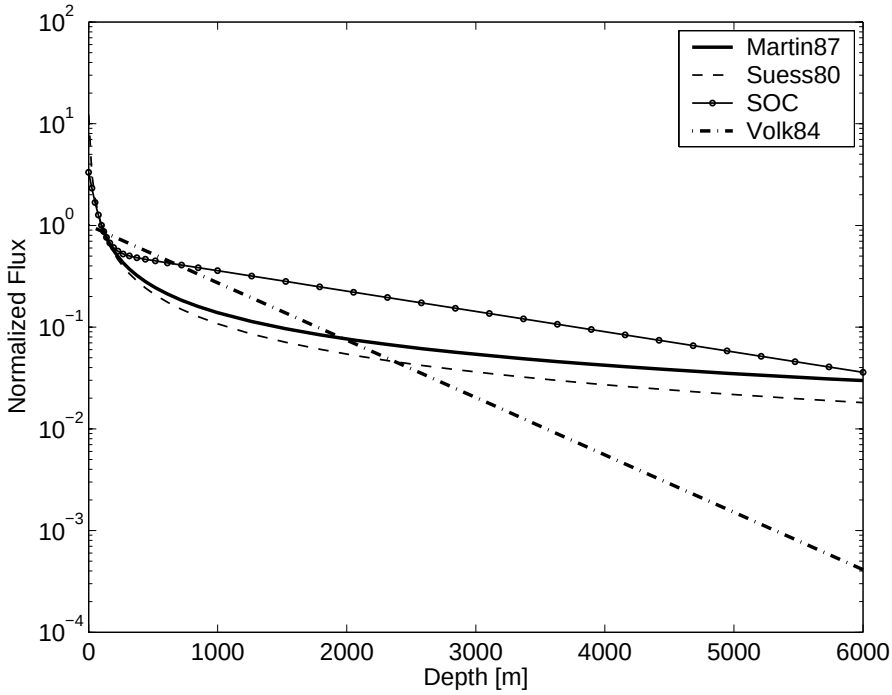

Figure 2.2: Comparison of flux-depth relationships. SOC is the double exponential fit of this paper, the other curves are the empirical fits by Suess (1980),Martin et al. (1987), and a single exponential fit as used in BOGCMs (Heinze et al., 1999; Volk and Hoffert, 1985) Fluxes are normalized to a common flux at 100 m.

The depth profile in upper waters is similar to sediment-trap based flux-depth profiles (Fig. 2.2), such as the ocean composite profile of Martin et al. (1987) based on fluxes in the upper 2 km, or the profiles as derived by Suess (1980). However, the double exponential deviates substantially for deeper water, where fluxes are well above previous carbon-flux depth relations. When fitting a single exponential profile to the SOC data the resulting e-folding depth (1/b) is 1333 m, twice the value in use in BOGCMs (cf. Heinze et al. (1999), 770 m). A power law fit yields a depth attenuation coefficient of -0.53, which is lower than the open ocean composite value (-0.858), based on sediment trap data (Martin et al., 1987). We investigated whether the deviation at large depth was due to our use of sediment oxygen consumption rates, rather than sediment trap fluxes by fitting the double exponential equation to particulate organic carbon fluxes based on ^{230}Th corrected sediment trap data (Antia et al., 2001). As in this data set there were no data above 500 m, the p and b_1 (Eq. 2.1) was imposed from the SOC-fit. The resulting b_2 is 0.00053 m^{-1}, similar to that based on SOC data (Table 2.1). Moreover, our power law slope is in the range of recent estimates (-0.36, -0.93) based on sedimentary fluxes (Devol and Hartnett, 2001) . Finally, electron transport activity data has also been summarized by Aristegui et al. (2003) where the data are fitted to a single exponential with a depth attenuation coefficient of 0.00053 m^{-1}, very similar to the derived parameter (b_2) from our second term exponential (Eq. 2.1), which clearly dominates the flux below 1000 m. A single exponential fit to SOC data below 200 m also results in an attenuation of 0.00037 m^{-1}.

Table 2.2: Respiration in Different Compartments of the Ocean in Tmol O_2 yr^{-1}

Depth interval	Total	Sediment	Water	Sediment/Total
200–1000 m	359	28	331	0.08
>1000 m	468	129	338	0.28
Total	827	157	670	0.19

The double exponential profile predicts a deeper penetration of biologically fixed carbon into the ocean interior. This implies that more carbon

is sequestered for a longer time in the deep ocean and this should be taken into account when evaluating the sensitivity of the oceans carbon dioxide uptake due to the biological pump. The double exponential not only provides a better fit, but it is also consistent with reported changes in the physical, biogeochemical and biological properties with water depth. Based on a particle settling and degradation model, the attenuation coefficients bi can be decomposed as the ratio of a first-order respiration rate constant to a net settling velocity. The difference in attenuation coefficient can then be attributed to a difference in net settling velocities, degradation constants or a combination thereof. For instance, assuming a uniform first order degradation coefficient of 0.07 d^{-1}, typical for fresh algal detritus (Middelburg, 1989), this implies that the net settling velocities would be 4 and 152 m/d for the two fractions. This could then in turn be attributed to two size fractions with different settling velocities or to a difference in net settling velocities between the turbulent well-mixed surface ocean and the deep ocean. This, together with increases in particle sinking speed with depth (Berelson, 2002) impacts the depth attenuation of particle deposition fluxes. Alternatively, the difference in attenuation coefficients could be due to differences in the first-order rate constant. It is well known that the degradation of organic matter decreases with time due to preferential mineralization of the more reactive compounds of organic matter and this is often described by a double exponential model (2-G model) (Westrich and Berner, 1984). This difference in degradation coefficient can in turn be due to compositional differences in the organic matter (Dauwe et al., 1999), due to sorption of organic matter to particles (Armstrong et al., 2002; Mayer, 1994) or to differences in the biological community, such as decreasing intensity of zooplankton grazing on POM with water depth (Jackson and Burd, 2002). Accordingly, there are a number of plausible mutually non-exclusive causes for a change in the carbon-flux attenuation coefficient with depth.

2.3.2 Global ocean respiration budget

By combining ocean hypsometry with Equation 2.1 using parameters from Table 2.1, we calculate global respiration patterns in the sediment (Table 2.2). Assuming that the SOC at a particular depth reflects a flux of organic matter through the water column at this depth at any place in the

ocean, we can also multiply with the area of the ocean at this depth and get the total flux of organic matter. By making the difference of fluxes across two depth planes we calculate the total respiration in this interval (Table 2.2). The difference between the total respiration and sedimentary respiration must then be consumed in the water column.

Assuming that the obtained relationship of deposition fluxes with depth represents long-term averaged conditions, we proceed by calculating carbon mineralization or oxygen utilization rates in the water column (OUR, units of mmol O_2 m^{-3} d^{-1}).

To do so, we solve the following constitutive equation,

$$-\frac{\partial F}{\partial z} - OUR = 0, \tag{2.2}$$

for OUR by differentiating Equation 2.1 with depth (Suess, 1980).

$$OUR = 0.56\left[(1-0.005)e^{-0.018z} + 0.005e^{-0.00046z}\right] \tag{2.3}$$

The decrease of OUR with water depth is shown in Figure 2.3 where a comparison is made with other volumetric respiration data from electron transport system (ETS) activity (Aristegui et al., 2003), reflecting instantaneous respiration of both particulate and dissolved organic material, and estimates from Munk (1966) based on profiles of dissolved oxygen in the water column from the Pacific ocean, reflecting a more long term average.

The ETS data support the slope of the SOC data, but the absolute values differ because of the inherent uncertainty in the back calculation from ETS values to O_2 consumption. The mean of the estimates by Munk (1966) compares well with our estimate.

Eight tenths of the global respiration below 200 m (Table 2.2) occurs in the water column, with similar contributions from the mesopelagic zone (200-1000 m) and the deeper ocean for water column respiration. Sedimentary respiration on the other hand mainly takes place in the deeper part because of the vast areas of the abyssal plains.

These estimates of the global respiration in the deep sea are higher than the ones obtained by Jahnke (1996), 129 Tmol O_2 yr^{-1} compared to 54.3 Tmol O_2 yr^{-1} for deep sea sediments, and 468 Tmol O_2 yr^{-1} compared to 120.2 Tmol O_2 yr^{-1} for water and sediments below 1000 m.

Possibly, the fact that Jahnke (1996) lacked data from productive regions such as the Arabian Sea and upwelling areas west of Africa and

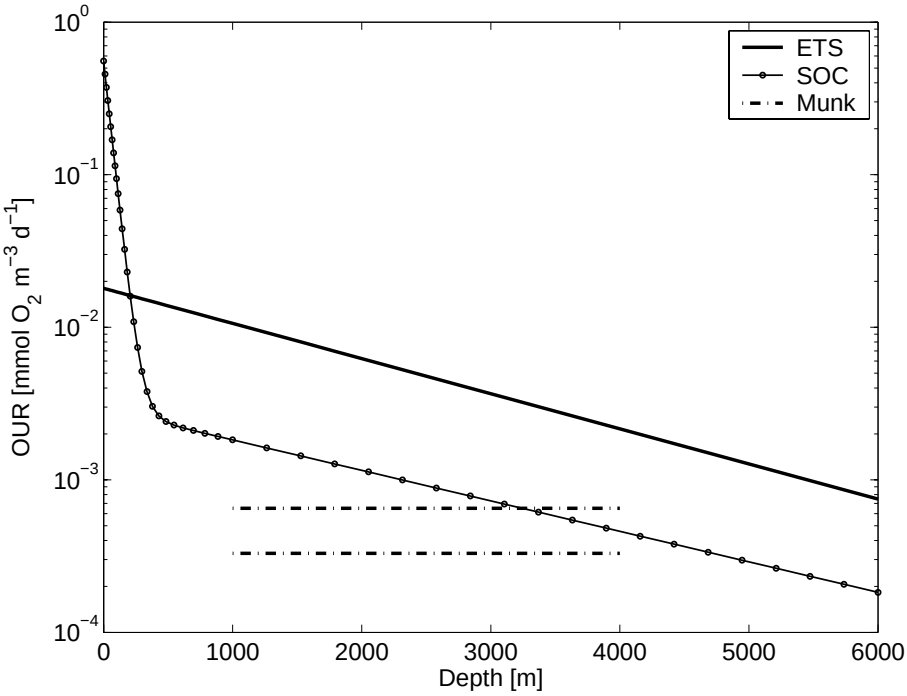

Figure 2.3: Oxygen utilization rates (OUR), derived from sediment oxygen consumption. Our estimated curve has a similar slope to the one based on electron transport system activity (Aristegui et al., 2003) and the mean compares well to estimates from oxygen distribution fields in the Pacific (Munk, 1966), where the two lines indicate the estimated range of OUR.

South America might explain this discrepancy. The estimates by Jahnke (1996) show that sediments and water column respiration are of equal importance below 1000 m while our calculations show a more modest (28 %) influence of sediments. Total sediment respiration below 200 m is 1.41 Gt C yr^{-1} , consistent with Middelburg et al. (1997) (1.5 Gt C yr^{-1}). Total respiration below a water depth of 200 m is 827 Tmol O2 yr^{-1} , or 7.4 Gt C yr^{-1} with an O_2/C ratio of 1.34 (Körtzinger et al., 2001). In a recent review del Giorgio and Duarte (2002) reported global respiration rates in the mesopelagic zone of 21 to 28 Gt C yr^{-1}. This range is much higher than our estimate that includes particulate organic matter degradation only. The estimate of del Giorgio and Duarte (2002) includes subducted DOC-fluxes as well, but these support only about 10 % of the respiration in the mesopelagic zone (Aristegui et al., 2003).

2.4 Conclusions

1. Sediment oxygen consumption data can provide an independent way to derive global respiration in the deep sea, taking on a bottom-up perspective contradictory to the more common focus on export production.

2. Fluxes of organic matter have a less steep attenuation in the bathypelagic zone than current fits based on biased sediment trap data suggest, but are comparable to fits based on ^{230}Th-corrected sediment traps. We estimate an export production of 7.4 Gt C yr^{-1}, 80 % of which is respired in the water column, with similar contributions of the mesopelagic (200-1000 m) and deeper ocean.

3 Short-term fate of phytodetritus in the Arabian Sea Oxygen Minimum Zone

Johan Henrik Andersson, Clare Woulds, Matt Schwartz, Greg Cowie, Lisa A. Levin, Karline Soetaert, Jack J. Middelburg, 2007, *Biogeosciences Discussion*, 4:2493-2523

3.1 Introduction

Phytodetritus arriving in pulses is a major food source for the benthic communities living at ocean margins and deep-sea basins (Gooday, 2002). The occurrence of such intense phytodetritus pulses requires episodic production events and a short transit time through the water column where it would otherwise be degraded, i.e. the settling speed needs to be high. Aggregation of phytoplankton into larger particles (Kriest and Evans, 1999) and ballasting (Francois et al., 2002) contribute to high settling speeds. As diatoms easily form aggregates, they are the most important part of phytodetritus settling at the seafloor (Beaulieu, 2002).

Following the fate of naturally occurring phytoplankton blooms and the resulting detritus deposited on to the sea floor is logistically difficult due in part to the unpredictable nature of these sedimentation events. Time-series observations of sediment measures (e.g. as total sediment oxygen consumption) have revealed inconclusive results when compared to measured deposition fluxes (Smith, 1992; Sayles et al., 1994; Soetaert et al., 1996a). An experimental approach, where algae enriched in ^{13}C are added directly to the sediment surface facilitates the establishment of carbon budgets, whilst it also enables studying several parts of the benthic food web, such as uptake into bacteria, fauna and respiration, simultaneously (Moodley et al., 2002; Witte et al., 2003b; Moodley et al., 2005).

The biogeochemistry of the Arabian Sea is strongly influenced by the two monsoon periods. Periods vary, but the southwest monsoon occurs from late May to early September and the northeast monsoon from December to March (Wiggert et al., 2005). Primary productivity increases dramatically in these two periods due to higher nutrient levels, caused primarily through coastal upwelling of nutrient-rich waters and subsequent advection by large-scale circulation (Kawamiya and Oschlies, 2003). At the end of the algal blooms, detritus sinks through the water column and on to the sea floor (Haake et al., 1993). The sediments of the Arabian Sea therefore receive fluxes of organic material that display strong seasonal variability.

Another prominent feature of the Arabian Sea is the midwater Oxygen Minimum Zone (OMZ), from a water depth of around 100 m down to 1100 m, due to intense respiration of organic matter in combination with

a reduced ventilation of intermediate water bodies. The OMZ coincides roughly with maxima in sedimentary organic carbon, suggesting a link between organic carbon preservation and oxygen availability (Cowie et al., 1999).

The short term fate of phytodetritus has been studied at several places in the ocean (Blair et al., 1996; Moodley et al., 2000, 2002; Witte et al., 2003b), but no study have yet directly compared sites in suboxic and oxic environments. At present low-oxygen environments are only a minor part of the world ocean (Helly and Levin, 2004), but are biogeochemically important for a number of processes such as organic carbon preservation (Hartnett et al., 1998; Burdige, 2007) , metal cycling (Aller, 1994), removal of biologically available nitrogen through denitrification and natural production of N_2O, contributing to global warming (Naqvi et al., 2000). It is also important to note, that the area of oxygen-poor waters is likely to expand due to global warming, both as a direct effect of decreased solubility and indirectly because of enhanced stratification (Keeling and Garcia, 2002).

In this paper we present results from an experimental study on the short term fate of phytodetritus on the sea floor, at sites spanning the OMZ on the Pakistan margin of the Arabian Sea, before and after the SW monsoon. Phytodetritus sedimentation events were simulated by adding a known amount of ^{13}C labelled diatoms and subsequently tracing the ^{13}C into bacteria, via incorporation into phospholipid-derived fatty acids (PLFAs) specific to bacteria, into Foraminifera and macrofauna, and into dissolved organic, inorganic carbon pools. Site depths ranged from 140 to 1850 m, which encompasses the OMZ and provided us with a natural laboratory where the effect of oxygen and temperature could be tested under natural conditions.

3.2 Material and methods

3.2.1 Study site

Experiments were conducted on cruises CD146 and CD151, before and immediately after the summer monsoon of 2003 on-board RRS Charles Darwin. Thus it was possible to assess changes in benthic community

Table 3.1: Station characteristics. Bottom water temperature and oxygen concentrations were taken from CTD casts.

Station depth (m)	Temperature (°C)	Oxygen (μM)	Latitude (°N)	Longitude (°E)
Pre-monsoon				
140	22	92	23°17′	66°43′
300	15	4.5	23°12′	66°34′
850	10	5.8	22°57′	66°54′
940	9.0	5.8	22°54′	66°37′
1000	8.7	6.7	22°52′	66°33′
1200	7.2	15	23°0′	66°25′
1850	3.5	79	22°52′	66°0′
Post-monsoon				
140	18	4.9	23°17′	66°43′
300	15	4.9	23°12′	66°34′
940	9.3	7.6	22°54′	66°37′
1850	3.7	76	22°52′	66°0′

response associated with the biannual monsoon-driven delivery of OM to the sediment. Experiments were conducted at sites along an offshore transect off the Indus River, across the Pakistan margin of the Arabian Sea (Table 3.1).

3.2.2 Experimental conditions

Cores (i.d. 10 cm) were taken using a multiple-barrel "megacorer", providing virtually undisturbed samples (Barnett et al., 1984), and immediately transferred to a temperature controlled laboratory set to *in situ* temperature, where the experiments were conducted.

Diatoms grown in a ^{13}C enriched medium were freeze dried onto silica or kaolin ballast and injected into the barrels, as a slurry dissolved in purified water, through a port in the core lid. The labelled diatoms consisted of 75 % ^{13}C, except at the 1850 m station in the post-monsoon season, where a different batch of algae were used consisting of 31% ^{13}C. This

resulted in a loading of between 3.6 and 5.8 mg of ^{13}C added to each core (43.9 ± 6.8 mmol $^{13}C\,m^{-2}$).

During the incubation, each core was connected to its own oxystat gill consisting of a network of gas-permeable silicon tubing immersed in a tank where concentrations of oxygen were set to *in situ* levels (Schwartz et al., 2007). Overlying water was continuously circulated though the silica tubing in order to maintain bottom-water oxygen levels. Oxygen concentration was continuously monitored, using Unisense microelectrodes.

Each experiment was conducted simultaneously on two replicate cores, emanating from separate megacorer casts, and incubated in the dark for 2 or 5 days, exact durations varied slightly due to logistical constraints. All cores were incubated with a gentle stirring of the overlying water. Samples of the overlying water were taken at the beginning and end of, and at pre-determined intervals during, each experiment. The samples were immediately poisoned with 50 μL of a saturated solution of $HgCl_2$ to vials with volumes of 5 mL, in order to prevent further microbial activity. After termination of each experiment, cores were sectioned at 0.5 cm intervals to 2 cm depth, then at 1 cm intervals to 10 cm depth, and then at 2 cm intervals to 20 cm depth. One half of each slice was placed in a centrifuge tube for porewater extraction, and the other half was placed in a petri dish for faunal sampling. After centrifugation, the supernatant was transferred to vials for subsequent $\delta^{13}C$-DIC analysis (see below). The remaining sediment, used for the analysis of $\delta^{13}C$-POC and bacterial lipids, were transferred to plastic bags and freeze dried. Fauna samples were sieved using filtered sea water, and residues from 300 μm, 150 μm and 63 μm sieves were retained. From the 300 μm and some 150 μm residues all fauna were extracted by sorting at 12-20X magnification to the lowest possible taxonomic level, and frozen in pre-weighed tin capsules or combusted glass vials.

In addition to the shipboard incubations, labelling experiments were also conducted *in situ* using a benthic chamber lander (Elinor). The lander system has been described in detail by Glud et al. (1995). On arrival at the sea floor the lander inserted a 30x30 cm chamber into the underlying sediment. Pre-programmed syringes, a stirring motor, an oxygen electrode and an external oxystat gill allowed maintenance of ambient oxygen levels, slurry introduction, sample withdrawal and stirring comparable to the shipboard experiments. In these experiments, 19–27 mg ^{13}C were added,

giving a dose of 18–25 mmol $^{13}C\,m^{-2}$. After a 2-day incubation a shovel closed the bottom of the chamber, weights were dropped and the lander ascended to the surface. Sediment from the lander chamber was subsampled using two short megacore tubes. These cores were sectioned, and the samples were processed as described above.

3.2.3 Analytical methods

Sediments and fauna

Aliquots of 200–400 μg C, of gently disaggregated freeze-dried sediment, were weighed into silver capsules. De-carbonation was achieved by carefully adding 2–5 drops of double distilled 6 M HCl. Samples were dried overnight at 60 °C and stored in a vacuum desiccator prior to analysis.

Faunal samples were air dried at 45 °C and stored in a vacuum desiccator. Soft bodied fauna were de-carbonated in two layers of tin capsule using 2-5 drops of 1 M HCl, followed by drying at 40 °C. Macrofauna and Foraminifera, were de-carbonated with 6 M HCl, the original tin capsule having been placed inside silver capsules. All samples were analyzed on a dedicated Europa Scientific (Crew, UK) Tracermass isotope ratio mass spectrometer with a Roboprep Dumas combustion sample converter.

Bacteria

Bacterial biomass and uptake were quantified by measuring the concentration and isotopic composition of three PLFAs, iC14:0, iC15:0 and aiC15:0 specific to bacteria, following Middelburg et al. (2000).

PLFAs were extracted from 4 g freeze-dried sediment using a modified Bligh and Dyer extraction (Boschker et al., 1999). The lipid extract was fractionated on silicic acid into different polarity classes by sequential elution with chloroform, acetone and methanol. The methanol fraction containing the PLFAs was derivatized to yield fatty acid methyl esters (FAMEs).

The isotopic composition and concentrations were determined using a Varian 3400 gas chromatograph equipped with a HP5 column, coupled via a combustion interface to a Finnigan Delta+ isotope ratio mass spectrometer (IRMS).

Dissolved inorganic/organic carbon

Samples for the determination of dissolved inorganic and organic carbon were stored refrigerated in darkness and upside-down in head-space vials. The vials were sealed with butyl rubber membranes covered with Teflon to prevent gas diffusion through the membrane. Concentrations of dissolved inorganic carbon were measured by coulometric titration. Isotopic compositions were measured independently by injecting head-space gas directly in a continuous stream of helium into a Finnigan Delta+ IRMS via a ConFloII interface following Moodley et al. (2000).

Concentrations and isotopic composition of dissolved organic carbon (DOC) were measured on the same samples used for the determination of δ^{13}C-DIC. Dissolved inorganic carbon was removed by adding sulfuric acid in excess and subsequent stripping with helium. The samples were analyzed with a Skalar Formacs^{LT} TOC analyzer coupled through a ConFloII interface to a Finnigan Delta S IRMS. The calibration standards were prepared with potassium phtalate dissolved in purified water (MilliQ).

3.2.4 Data treatment

Incorporation of ^{13}C is reflected as excess (above background) ^{13}C and is expressed in terms of total uptake in millimoles of ^{13}C per square meter as well as specific uptake (i.e. $\Delta\delta^{13}\mathrm{C} = \delta^{13}\mathrm{C}_{\mathrm{sample}} - \delta^{13}\mathrm{C}_{\mathrm{control}}$, where δ^{13}C is expressed relative to Vienna Pee Dee Belemnite (VPDB)). Total uptake was calculated as the product of excess ^{13}C (E) and carbon concentrations. Excess ^{13}C is the difference between the fraction ^{13}C of the control (F_{control}) and the sample (F_{sample}) : $E = F_{\mathrm{sample}} - F_{\mathrm{control}}$, where the fraction of ^{13}C (F) was calculated from the ratio (R) of ^{13}C/^{12}C,

$$F = {}^{13}\mathrm{C}/({}^{13}\mathrm{C} + {}^{12}\mathrm{C}) = R/(R+1). \tag{3.1}$$

The carbon isotope ratio (R) was derived from the measured δ^{13}C values as:

$$R = (\delta^{13}\mathrm{C}/1000 + 1) \cdot R_{\mathrm{VPDB}}, \tag{3.2}$$

where $R_{\mathrm{VPDB}} = 0.0112372$.

Incorporation into bacterial biomass was calculated in the following way,

$$I_{\mathrm{bact}} = \frac{\sum_{i=1}^{3} I_{\mathrm{PLFA,i}}}{F_{\mathrm{PLFA}} \cdot C_{\mathrm{PLFA}}} \tag{3.3}$$

where $F_{\mathrm{PLFA}} = 0.12$ is the fraction of the three PLFA's to total bacterial PLFA's, (Moodley et al., 2005) and $C_{\mathrm{PLFA}} = 0.038$ is the fraction of PLFA carbon to total bacterial carbon (Boschker and Middelburg, 2002).

3.3 Results

The δ^{13}C-DOC values in overlying waters were elevated well above background values (-20 ± 1 ‰, assuming that natural sedimentary DOC has a similar isotopic composition to that of POC in underlying sediments) at the start of all incubations (Fig. 3.1), indicating that the added phytodetritus was a source of some DOC as well as POC. The δ^{13}C-DOC values decreased over time as a result of dilution with unlabeled DOC present in the porewater. In several cases the δ^{13}C-DOC increased again after the initial decrease as a result of degradation of labelled POC.

As the overlying water was sampled for δ^{13}C-DIC and DIC at several times during the incubations, it was possible to investigate the extent and timing of respiration more closely than components such as faunal and bacterial uptake, which were sampled only at the end of the 2- and 5-day incubations. The evolution of excess ^{13}C in DIC over time was in general very comparable between replicate cores although these were collected purposely from different casts. The most intense respiration was found at the shallowest station, at 140 m. This is also the station where respiration of the added phytodetritus was immediately evident already from the start of the incubation (Fig. 3.2 and 3.3). Later, however the respiration rate slowed down. The fast initial response followed by gradual slowing down and an apparent eventual halt is found in both the pre- and post-monsoon data at the 140 m station. Respiration of added phytodetritus at 300 m in the OMZ also started immediately, but with a much lower rate. In contrast, respiration at the deeper stations all showed an initial lag phase with very low rates of respiration but a marked increase after this phase. Overall, the length of the lag phase increased with increasing water depth; about one day at the 940 m station increasing to about two days at the 1200 m and 1850 m stations (Fig. 3.2).

Due to technical difficulties with the lander, the number of successful *in situ* deployments was limited. However, respiration of added algal material was evident at both the 140 m and 940 m stations with relative differences

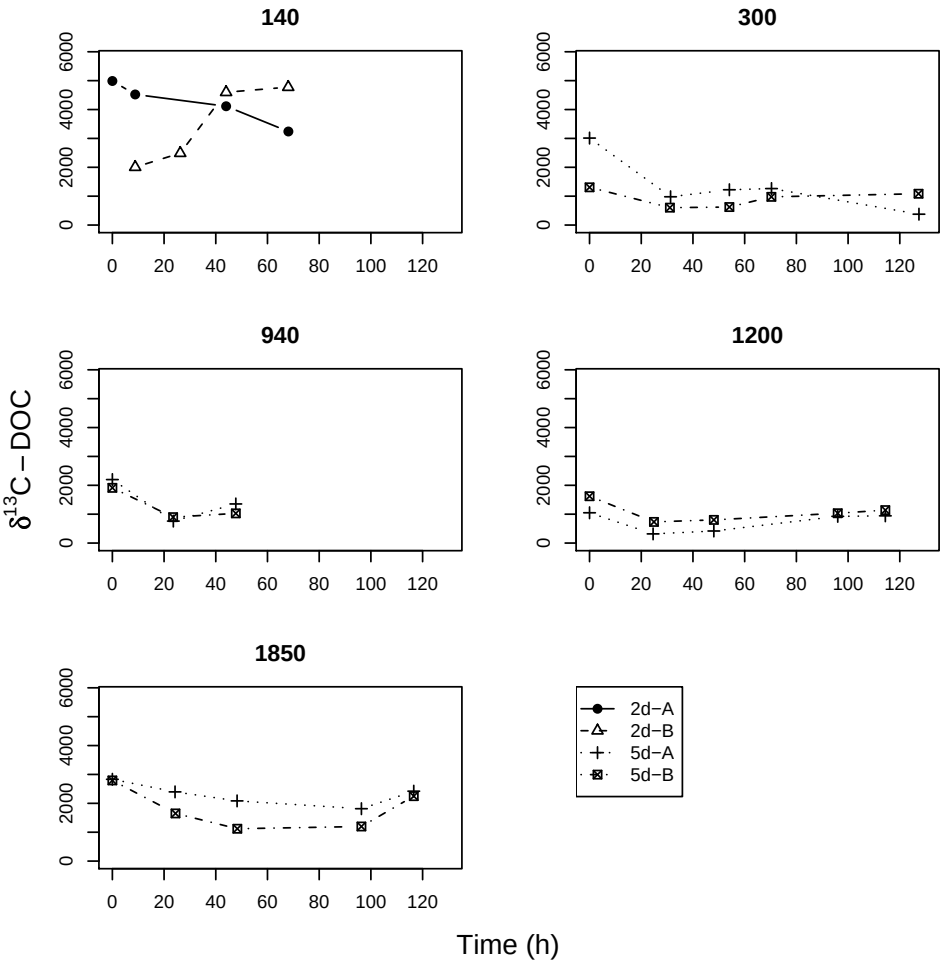

Figure 3.1: Isotopic composition of dissolved organic carbon in the overlying water from the pre-monsoon cruise. A, B indicate replicate cores.

in rates similar to those observed in the shipboard incubations (Fig. 3.4).

Downcore profiles of sediment δ^{13}C-POC, obtained at the end of the experiments show limited downward mixing of the added algae (Fig. 3.5) in either 2- or 5-day incubations. Moreover, there was no apparent change over time. Despite the limited vertical displacement, small amounts of labelled material were brought down from the surface to deeper layers at all stations except in the core of the OMZ at 300 m station where all the added phytodetritus remained in the topmost sediment layer (0-0.5 cm).

The δ^{13}C-DIC of porewaters was highly enriched relative to background values. Enrichment was highest in the top centimeters, exponentially decreasing with depth in the sediment (Fig. 3.6). Except for one profile from 140 m in the pre-monsoon cruise exhibiting sub-surface peaks, all porewater profiles appear to be the combined result of respiration at the sediment-surface and downward diffusion into the sediment.

Transfer of ^{13}C from phytodetritus to bacteria was highest in the upper two centimeters (Fig. 3.7). Label assimilation in bacteria was also detectable in the 2–5 cm depth layer, but contributed <1% to the depth-integrated bacterial uptake. The labelling pattern of the three bacteria-specific fatty acids, iC14:0, iC15:0 and aiC15:0 was consistent across stations and depth layers in the sediment. The fatty acid with the highest specific uptake ($\Delta\delta^{13}$C) in general is iC15:0. Bacterial uptake was quite similar across the stations above 1000m depth. Uptake was much lower at greater station depths, even after five days (Table 3.2). Bacterial uptake of the added algal carbon was on average comparable to macrofaunal and foraminiferal uptake (Woulds et al., 2007). At the 300 m station, where exceptionally low oxygen levels resulted in a near-total absence of macrofauna, bacterial and foraminiferal uptake was similar. At the 940 m station, the macrofauna were much more prominent and dominating the carbon processing.

Respiration was measured in incubations lasting both 2 and 5 days. To allow the comparison of all incubations, all respiration values were linearly interpolated from the two closest sampling times to a common time of 44 hours (Fig. 3.8). As some incubations nominally lasting 5 days had to be terminated earlier due to limited processing manpower, these were interpolated to 86 hours (Fig 3.9). Respiration after 44h was most intense at the shallowest station and decreased with station depth. However, after 86h the decrease with station depth is only evident at the

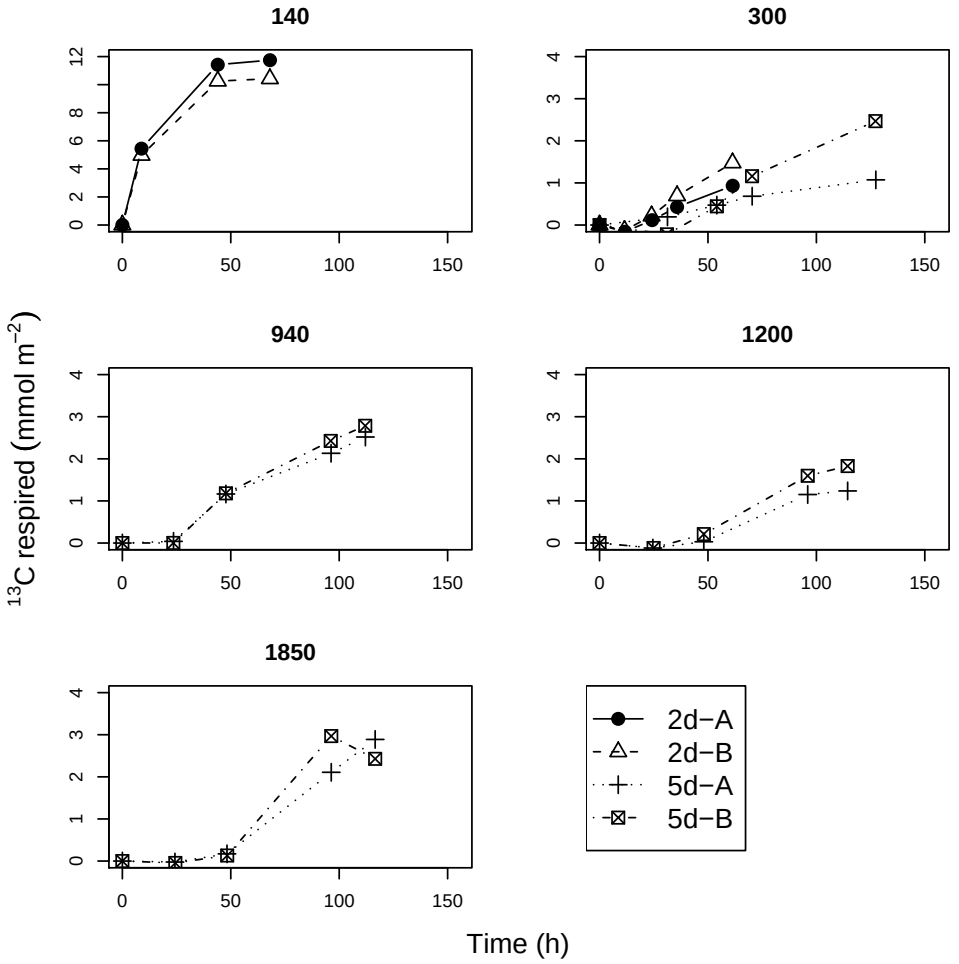

Figure 3.2: Respiration of the added tracer during the pre-monsoon cruise. Note the different scale for station 140. See Table 3.1 for details about the stations.

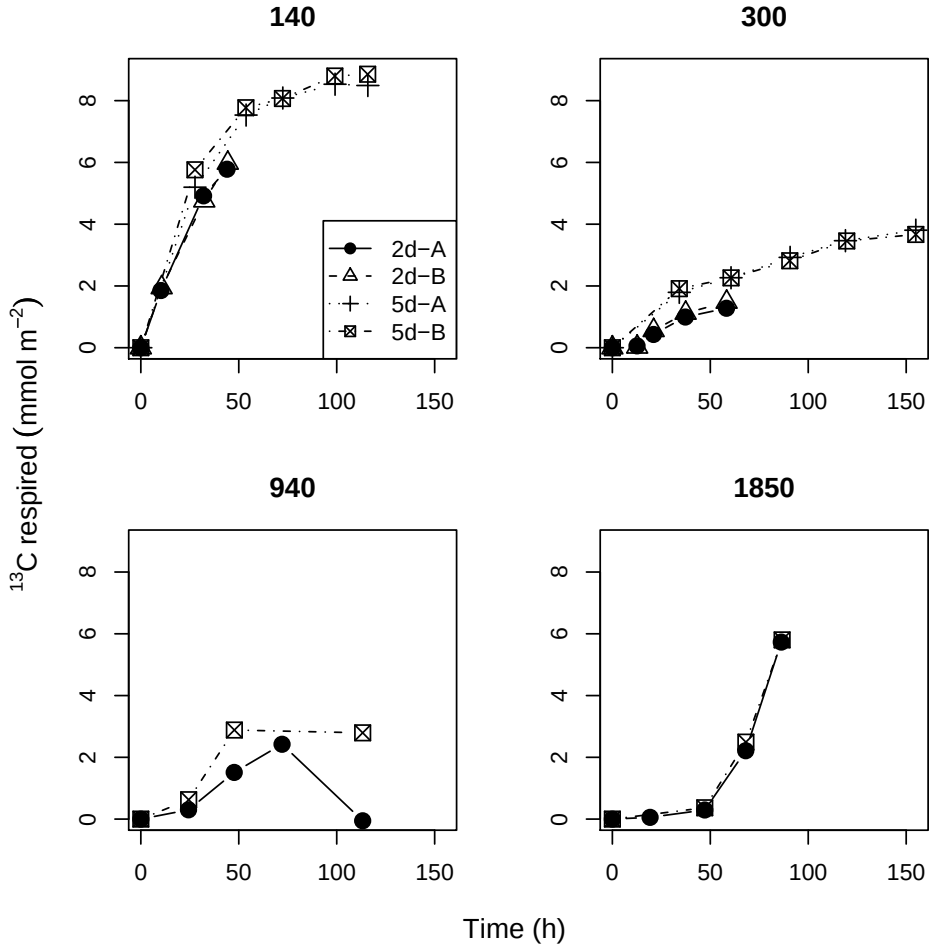

Figure 3.3: Respiration of the added tracer during the post-monsoon cruise. See Table 3.1 for details about the stations

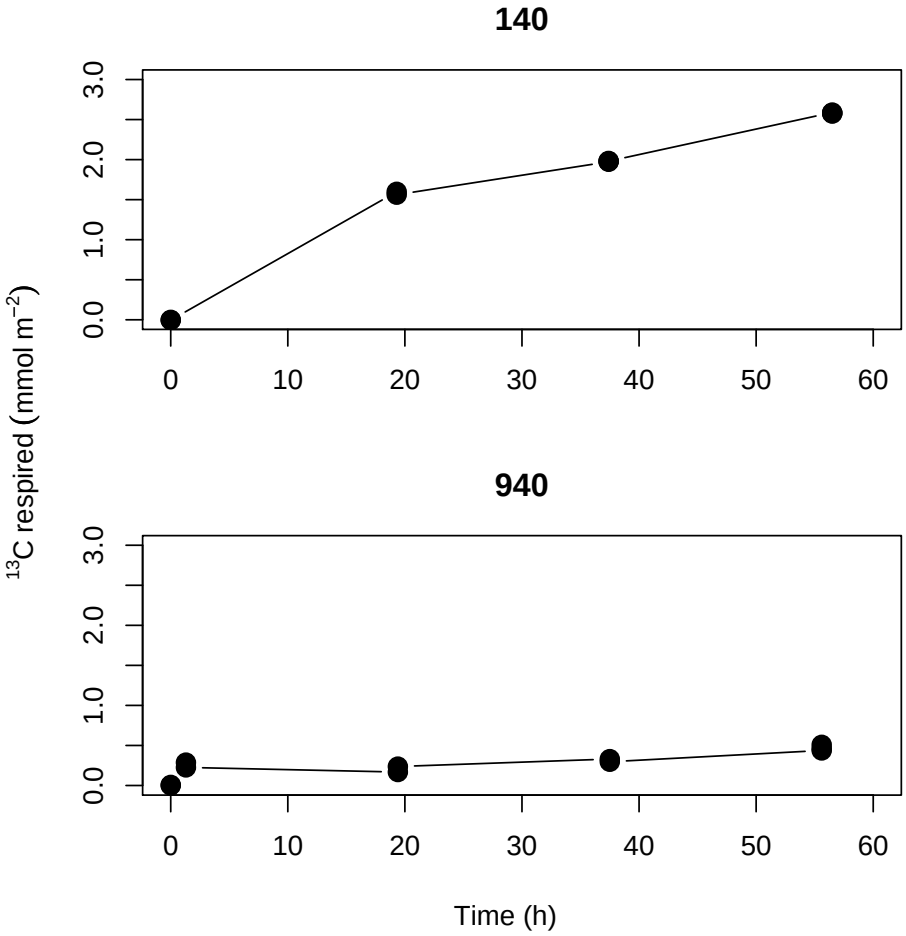

Figure 3.4: Respiration of the added tracer during the post-monsoon cruise in *in situ* incubations. See Table 3.1 for details about the stations

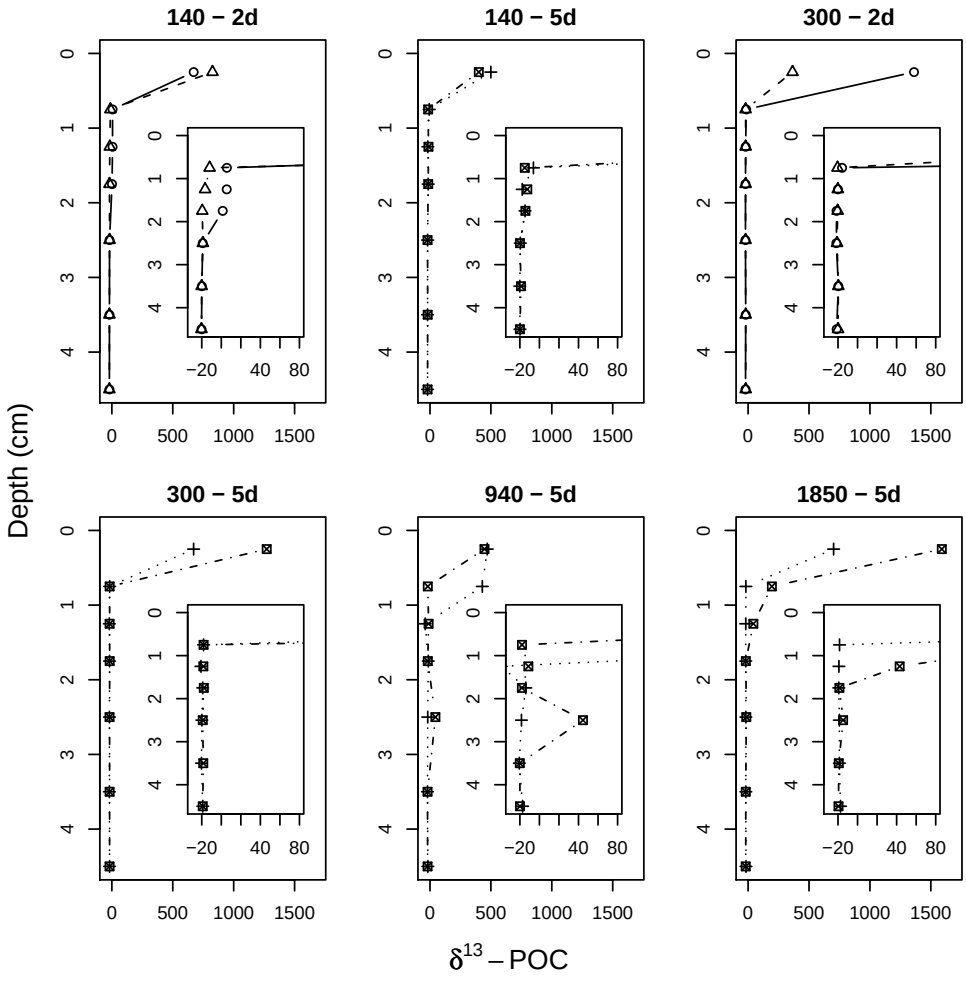

Figure 3.5: Excess δ^{13}C-POC from the post-monsoon cruise. Insets zoom in on a limited range in delta values to allow distinguishing small differences between stations with limited and no vertical displacement of added algal ^{13}C.

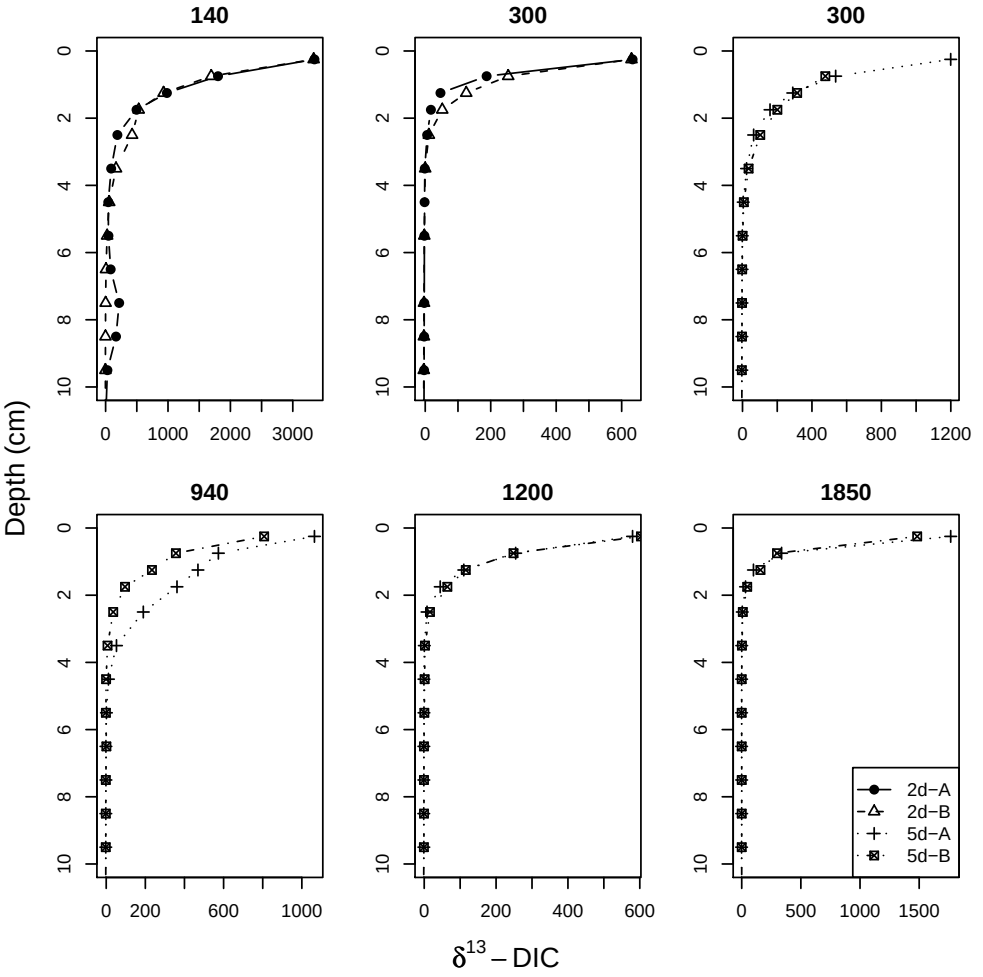

Figure 3.6: Isotopic composition of the porewater DIC at the end of the experiments at four different water depths from the pre-monsoon cruise. Results are shown for a maximum depth of 10 cm, although samples were analyzed to a depth of 20 cm.

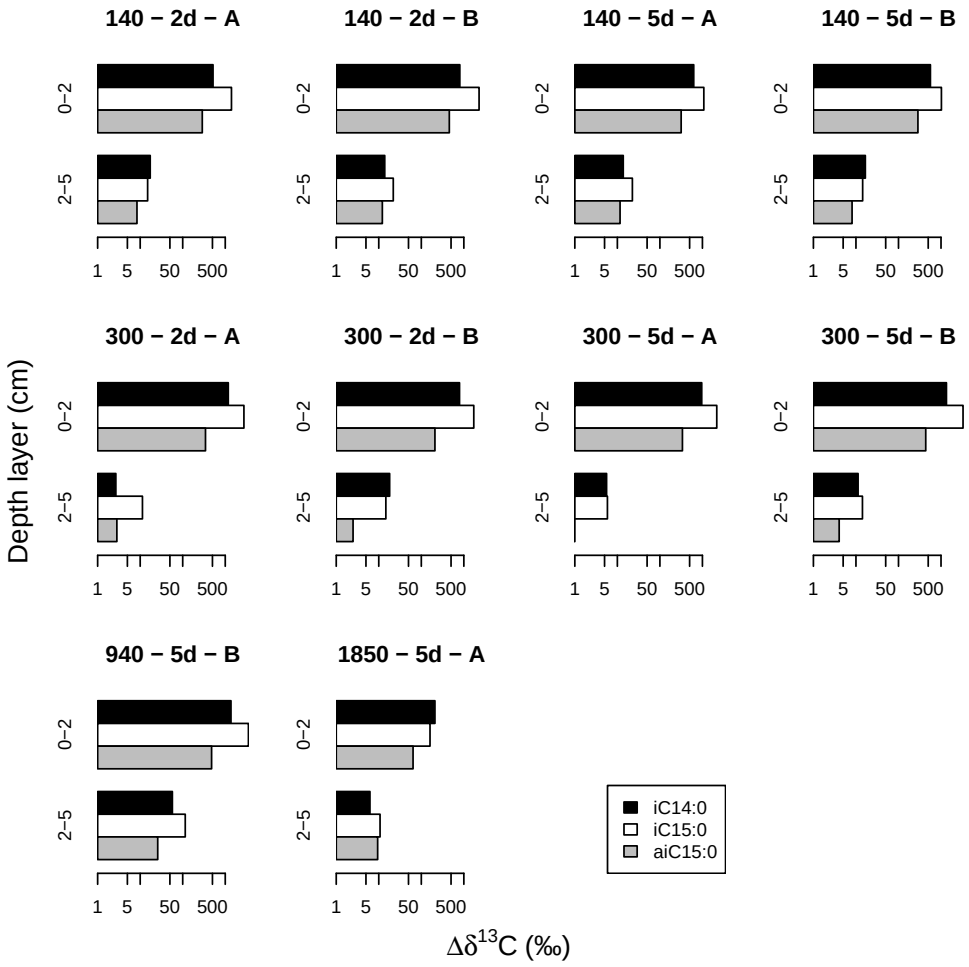

Figure 3.7: Specific uptake of ^{13}C into bacterial fatty acids in two depth layers at all stations during the post-monsoon cruise. A, B indicate replicate cores. Note the use of a logarithmic x-axis.

Table 3.2: Means and standard deviations of phytodetrital pools (Foram:Foraminfera, Macro:Macrofauna) in mmol ^{13}C m^{-2} and recovery in % of the added carbon. Recovery is calculated as the sum of macrofaunal uptake, respired carbon and bulk excess POC, as POC already includes the contribution from both bacteria and Foraminifera. The contribution from macrofauna and Foraminifera were taken from Woulds et al. (2007).

Station	Days	POC	Bacteria	Foram	Macro	Respired	Recovery
Pre-monsoon							
140	2	24.1(10.1)	1.26(0.2)	0.38	2.61	11.1(0.936)	81.6(23.9)
300	2	16(0.854)	0.27(0.03)	0.31	0	1.2(0.383)	44(3.47)
300	5	24.4	0.41(0.15)	0.38	0	1.77(0.986)	61.6
850	2		0.18(0.05)				
940	5	8.34	0.26(0.21)	0.08	3.00	2.65(0.188)	35.0
1000	2		0.17(0.03)				
1200	5	10.2(2.18)	0.05(0)	0.41	0.17	1.53(0.418)	29.7(6.76)
1850	5	48.2(15.5)	0.14(0.08)	0.37	0.068	2.66(0.326)	84.6(27.7)
Post-monsoon							
140	2	32.9(3.22)	1.71(0.815)	1.17	0.587	5.88(0.139)	96(8.52)
140	5	18.6(2.64)	1.6(0.509)	2.19	0.605	8.67(0.258)	69.3(6.53)
140	2 *in situ*	0.5(0.42)	0.29(0.24)	0.628	0.489	2.58	72.0
300	2	33(25.3)	1.93(1.33)	0.321	0	1.38(0.141)	84.8(63)
300	5	36.2(15.8)	2.79(1.36)	1.30	0	3.74(0.0973)	96.8(38.6)
940	5	31.9(4.48)	0.95(1.34)	0.0677	4.38	2.61(0.261)	94.1(11.9)
940	2 *in situ*	0.11(0.01)	0.07(0.01)	0.039	2.96	0.46	36.0
1850	5	32.7(21.6)	0.08	0.228	0.0984	5.77(0.0493)	78.4(44)

140 to 300 meter stations. Note that a different batch of algae was used for the 1850 m station in the post-monsoon cruise, which apparently was more easily mineralized.

3.4 Discussion

3.4.1 Experimental approach

Potential artifacts in shipboard incubations of oceanic sediments have been reported repeatedly (e.g. Glud et al., 1994) and include possible changes due to decompression or warming of the sediment during retrieval and incubation of the cores. At most stations, we also performed *in situ* incubations to be able to verify the shipboard results. However, the distribution

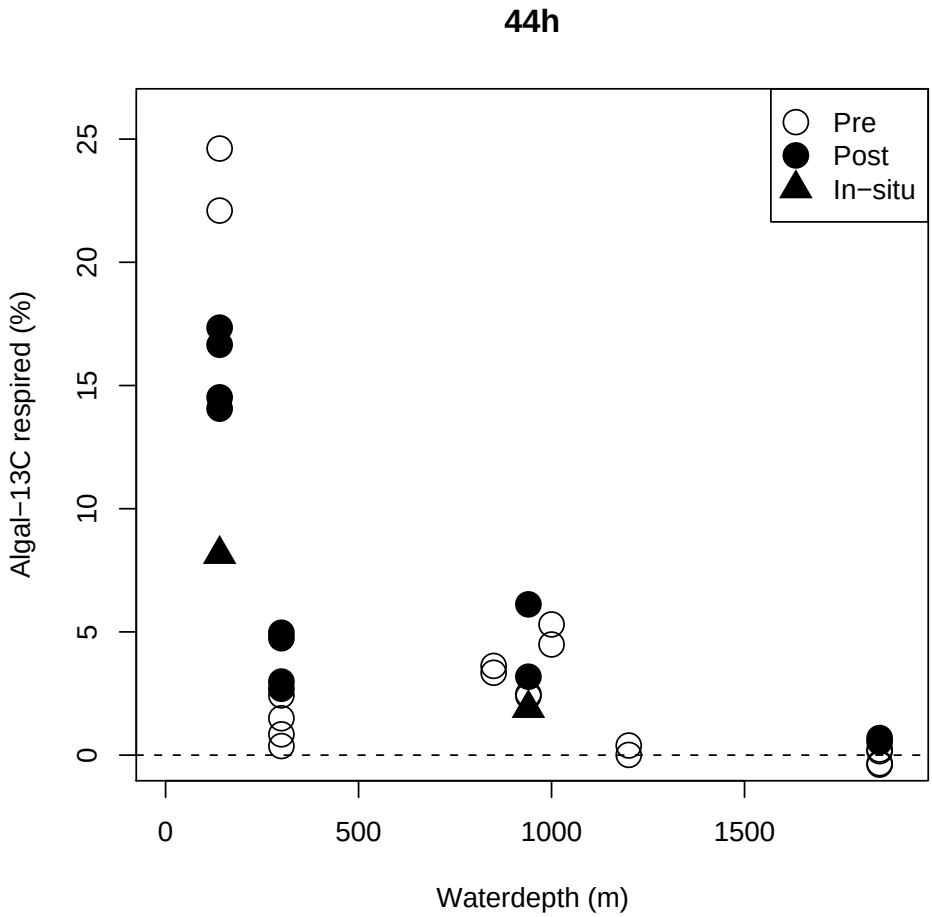

Figure 3.8: Percentage of total label respired after 44 hours across the ocean margin. A different batch of algae was used for station 1850 at the post-monsoon cruise. All experiments were performed in duplicate.

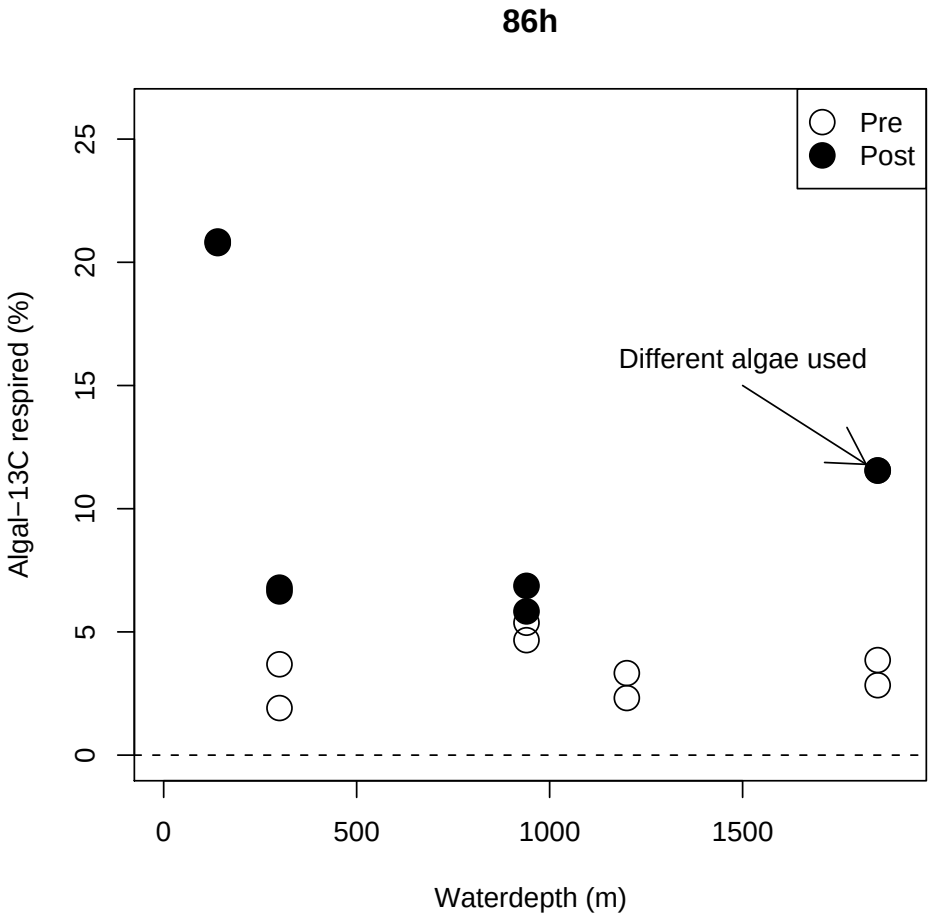

Figure 3.9: Percentage of total label respired after 86 hours across the ocean margin. A different batch of algae was used for station 1850 at the post-monsoon cruise, which apparently was more easily mineralized. All experiments were performed in duplicate.

of added phytodetritus in the *in situ* incubation the chamber was very patchy, as highlighted by large differences in excess ^{13}C-POC and bacterial uptake between subcores (Table 3.2). This heterogeneity introduces large uncertainty when data from subcores are extrapolated to the entire chamber area.

Incubation of sediments from low-oxygen environments pose a major challenge because measures should be taken to maintain oxygen levels close to ambient. Therefore, water from each core was pumped through gas-permeable silicon tubing placed in a reservoir where oxygen concentrations were kept at *in situ* concentrations. This ensured ambient oxygen levels and thus a close-to-natural functioning of the benthic community. However, since the partial pressure of carbon dioxide was higher in the cores compared to the controlled reservoir, it is possible that carbon dioxide effluxed from the experimental cores and consequently that absolute values of respiration are underestimated.

While core incubations are able to replicate both the temperature and oxygen conditions of the *in situ* environment, the stirring rate is constant and is set to prevent resuspension. Should resuspension occur in the natural environment, it could alter the fate of phytodetritus by keeping it exposed longer to decomposition in the benthic boundary layer (Beaulieu, 2003).

The natural status of phytodetritus arriving at the sea floor has been found to be highly variable in terms of degradation state and composition, and it is thus not easy to select the appropriate pre-treatment of experimental phytodetritus such that it resembles natural conditions best (Beaulieu, 2002). Similarly, it was not possible to select proportionally representative amounts of labeled C to add to the different sites. Instead, we chose to add the same material and the same quantity to all sediments, allowing a direct comparison among sites. Adding the same amount of phytodetritus at all depths does not simulate natural inputs, as these would generally be lower at greater depths due to respiration within the water column (Andersson et al., 2004). Our experiments were therefore designed to directly compare the relative potential for phytodetritus processing at different study sites. However, it has been shown that degradation of particulate organic material is slowed down in suboxic water columns such as the one found in the Arabian Sea (Devol and Hartnett, 2001). Thus, in OMZ areas, the flux of organic material arriving at the

sea floor is of a more similar magnitude at different depths, than it would be for an entirely oxic water column.

That the nature of reactive organic matter added may be important to experimental results was possibly demonstrated in the response recorded during the post-monsoon period at the 1850 m station. Due to problems with algal cultures, a different batch of labeled diatoms was used, which apparently was much more readily respired. Moreover, the immediate ^{13}C enrichment of DOC in incubations at all stations (Fig. 3.1) indicates that DOC was added with the freeze-dried algal material despite thorough rinsing procedures. Although this unintended addition of ^{13}C-DOC amounted to less than 5 % of total added ^{13}C in all cases, the combined results highlight that benthic carbon processing studies using artificially introduced phytodetritus are not necessarily comparable, because the results may depend on the type of algae used, their preconditioning and the specific carbon loading (Bühring et al., 2006).

Summing up the contribution from all the compartments, i.e. uptake into bacteria, Foraminifera, macrofauna, respiration and unprocessed algal carbon remaining in sediment a recovery can be calculated. POC measurement includes the contribution from both unprocessed algal carbon and carbon taken up by bacteria and Foraminifera (macrofauna was picked out). Thus, the recovery was calculated by the sum of the POC pool, the uptake into macrofauna and the DIC pool. The recovery was high in most of the experiments from the post-monsoon cruises and some of the pre-monsoon stations (Table 3.2). Apparent label losses are primarily due to uncertainty in the measurement of excess ^{13}C-POC. Another potential loss of ^{13}C-DIC was losses of gaseous ^{13}C-CO_2 through the silicon tubing (see above).

3.4.2 Fate of phytodetritus

Our results clearly show that, within 2-to-5 day timescales, a minor fraction of total added carbon was processed at all sites, and the fate of the majority of the processed carbon was respiration, in both pre- and post-monsoon seasons. The notable exception was at the 940 m station where in both pre- and post-monsoon seasons, uptake by the abundant macrofauna dominated the phytodetritus processing. The occurrence of the amphinomid polychaete *Linopherus* sp. at this station accounted for most of the

macrofaunal uptake and influenced the entire carbon processing (Woulds et al., 2007). When present, animals such as these amphinomid polychaete have a large impact on the the mineralization pathway, by subducting organic matter below the oxic zone (Levin et al., 1997). This demonstrates that short-term carbon cycling pathways can differ dramatically, with possible consequences for the fate of carbon (e.g. burial vs. respiration).

At the 140 m site there was a marked shift in the uptake patterns from pre- to post-monsoon due to an upward shift in the upper boundary of the OMZ, which caused bottom waters to become considerably less oxygenated (Table 3.1). Concurrent with this decrease in oxygen, the uptake shifted from macrofauna-dominated to more equally divided between bacteria, Foraminifera and macrofauna. The shift in uptake pattern indicates that changes in oxygen, from fully oxygenated to hypoxic conditions, has a major impact on the pathway of benthic phytodetritus processing (Woulds et al., 2007). Respiration also responded to the shift in oxygen concentration, but in a less dramatic sense.

Specific uptake into bacterial lipids expressed as $\Delta\delta^{13}$C in the 0–2 cm layer was always less than 3500 ‰. Using equation (3.1) and (3.2) this corresponds to a fraction of ^{13}C of 4.8 %. Thus, even the most active of the bacterial lipids did not experience more than 5% turnover during five days of incubation. The turnover calculation assumes an equal contribution of all bacteria in the 0–2 cm layer.

Transfer of labeled carbon below the surface layer was limited, even at stations where macrofauna was present. Even though the impact of fauna might be less than that found elsewhere (Witte et al., 2003a; Kamp and Witte, 2005), the fauna left a clear imprint at station 940 in the profiles of δ^{13}C-POC, bacterial lipids and in the porewater profiles of δ^{13}C-DIC (Fig. 3.5, 3.7, 3.6), where the penetration is of label is deeper and values more variable.

3.4.3 Factors governing respiration

The importance of benthic respiration as a fate for phytodetritus on the timescale of days to months is still largely unknown and results reported from the literature are ambiguous. Moodley et al. (2002) examined the fate of phytodetritus in a deep-sea environment (NE Atlantic, 2170m) on a relatively short timescale, by incubating sediment amended with

labelled algae for 35 hours. They found that 1.5% of the added algae were respired during these 35 hours. However, 40% of the algal carbon was left unaccounted for after the experiment, implying that it might have been lost prior to injection. Assuming that this was the case the respiration would increase to 2.4%. Moodley et al. (2005) later repeated this experiment at several locations, with a large range in water depths and temperatures, and found that ∼15% of the added algal carbon was respired at all location after 24 hours. Similarly, in our study , respiration accounted for up to 25% of the added algae within 5 days at the 140 m station. It was the dominant fate of the processed phytodetritus. This result is similar to the study of Moodley et al. (2005) where respiration dominated the budget of processed phytodetritus as well, in sites ranging from estuarine to deep-sea environments.

Chemical reaction rates increase with increasing temperatures, including microbially mediated reactions in marine sediments such as organic matter mineralization (Westrich and Berner, 1988). Effects of temperature on short-term processing of phytodetritus have been studied by Moodley et al. (2005), where they found that a decrease in temperature slowed down respiration considerably. By decreasing the temperature from an *in situ* of 16 °C to a temperature of 6 °C, respiration as a fate of phytodetritus decreased from 17 to 3 % of the added algal carbon respectively. In our experiments the length of the lag time in the appearance of excess ^{13}C into the DIC pool showed a smooth transition from warm, shallow sediments where no delay was observed to a lag time of almost two days at the deepest and coldest station. The increase in lag time with increasing station depth, and concurrently decreasing temperatures (Table 3.1), might be explained by a decoupling in the temperature response between the different functional groups of bacteria taking part in the mineralization process. One group is responsible for performing the initial hydrolysis of organic matter to DOC and another group the respiration of these compounds to CO_2. Such a decoupling results in an accumulation of low-molecular weight DOC at low temperatures (Weston and Joye, 2005).

Bottom water oxygen concentrations may have an effect on sediment organic matter (OM) processing, but literature evidence is scattered and sometimes conflicting. Hartnett et al. (1998) and Hedges et al. (1999) have reported correlative evidence that oxygen exposure time determines the extent of OM processing. Experimental studies examining the effect of

oxygen on OM degradation have shown it to be small when the material is fresh and larger when it is more refractory (Hulthe et al., 1998; Kristensen et al., 1995), but these experiments were not done with undisturbed sediment originating from naturally suboxic environments. In this study, the effect of oxygen on respiration was not as pronounced as the effects of temperature, but was apparent at the 300 m station where oxygen levels were so low that virtually no macrofauna could exist. An unexpected decrease in oxygen levels at the 140 m station (Table 3.1), from 92 μM in the pre-monsoon cruise to 5 μM in the post-monsoon cruise, might have caused the respiration to decrease. However, not to the same level as at the 300 m station, which would be expected if the only factor determining respiration factor was oxygen. Concurrent with the decrease in oxygen at the 140 m station was also a decrease in temperature, which probably had a similar effect as the change in oxygen on the respiration.

4 Respiration of organic carbon in sediments of the Gulf of Finland, Baltic Sea

Johan Henrik Andersson, Anders Tengberg, Henrik Stahl, Jack J. Middelburg, Karline Soetaert, Per O.J. Hall, *In preparation*

4.1 Introduction

Sediments are an important component in the cycle of organic matter, as a place of intensified mineralization and the concurrent release of nutrients back to the pelagic system. In eutrophied systems benthic nutrient fluxes impose a burden in addition to the external loading from rivers or atmosphere and are referred to as internal loading.

The Gulf of Finland is the most eutrophied basin of the Baltic Sea as it receives a substantial amount of nutrients from e.g. three capital cities including St. Petersburg. This has resulted in severe changes in a number of ecologically important attributes, e.g. increased occurrence of harmful algal blooms and decreased water transparency (Wulff et al., 2001). Despite recent decreases in the external loading due to the collapse of the former Soviet Union, no improvement has been observed in the nutrient status in the Gulf of Finland. The explanation put forward is internal loading from remineralization of organic matter stored in sediments (Pitkänen et al., 2001). In order to further understand the impact of eutrophication and to suggest cost-effective abatement measures, several biogeochemical models of varying complexity have been developed for the entire Baltic Sea (e.g. Stigebrandt and Wulff, 1987; Wulff and Stigebrandt, 1989; Neumann, 2000; Savchuk and Wulff, 2001) or sub-basins including the Gulf of Riga (Savchuk, 2002) and the Gulf of Finland (Kiirikki et al., 2001, 2006). To obtain reliable results with any of these models, they need to be calibrated with data of high quality.

Production or respiration rates adds the dimension of time to the available data, traditionally consisting primarily of hydrographical profiles, which only tell the combined result of production, respiration and transport processes. Respiration rates in general and benthic respiration rates in particular have not been measured routinely in the Baltic sea except for a limited number of research studies (Conley et al., 1997; Koop et al., 1990; Balzer, 1984).

The method most commonly used to determine benthic respiration rates is the measurement of benthic O_2 fluxes. This method assumes that products of anaerobic respiration, the dominating pathway in coastal environments, are quantitatively re-oxidized. Measurements of benthic fluxes of dissolved inorganic carbon (DIC), also referred to as total carbonate, (C_t) or $\sum CO_2$, have also been used, but less frequent. This method cov-

ers both aerobic and anaerobic respiration and circumvents assumptions about respiration quotients, however, DIC fluxes are also affected by the dissolution or precipitation of carbonate minerals (Anderson et al., 1986).

In this paper we investigate sediment activity in three contrasting stations in the Gulf of Finland, a sub-basin of the Baltic Sea. We present depth profiles of total organic carbon and dissolved inorganic carbon as well as rates of benthic respiration based on *in situ* benthic chamber lander incubations. Respiration rates are quantified by a combination of O_2 and DIC fluxes. Furthermore, we address the long-term combined effect of deposition, resuspension and subsequent re-deposition, reflected in the sediment accumulation rate, on the rates of respiration. By using a dynamic diagenetic model we also investigate the influence of highly variable bottom-water concentrations of O_2 and DIC on the respective fluxes of these compounds.

4.2 Materials and methods

4.2.1 Study area

The Gulf of Finland is a sub-basin of the Baltic Sea, one of the world's largest brackish water basins. The exchange of Baltic Sea water with the adjacent North Sea, through the shallow Danish straits, is very limited and the residence time of the Baltic sea water is in the order of 35-40 years (Voipio, 1981). Because of the long residence time of the water combined with large inputs of nutrients, eutrophication is a severe problem in the Baltic Sea. The poor water exchange also contributes to a permanent stratification in large parts of the Baltic Sea including the Gulf of Finland which causes permanent anoxia in some of the deeper parts, e.g. the Gotland deep and periodic anoxia in other areas (Conley et al., 2002).

The fauna inhabiting Baltic Sea sediments is relatively scarce, and consists of few species with a distribution mostly determined by salinity, but also drastically limited by areas of prevailing or recurrent anoxia (Karlson et al., 2002).

Three stations were selected within the study area (Fig. 4.1), each reflecting a different bottom type with respect to sediment accumulation. Station PV1 located at the western end of the Gulf of Finland was selected

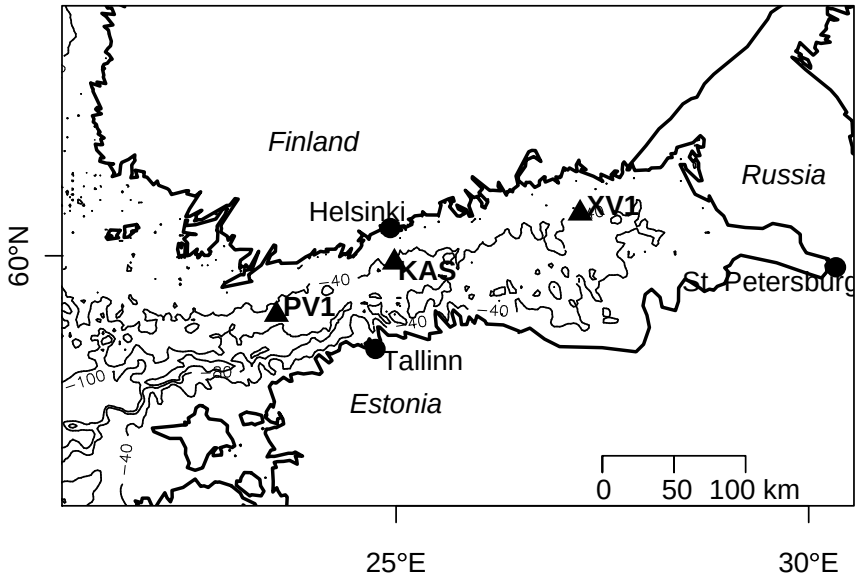

Figure 4.1: Map of the study area. Station locations are denoted by filled triangles. Bathymetric data were obtained from Seifert et al. (2001)

Table 4.1: List of lander deployments in the Gulf of Finland along with hydrographic data of the bottom water. Salinity (S), temperature (T) and O_2 were measured with sensors mounted on the lander. DIC were sampled from a Niskin bottle mounted on the lander. Indicated errors are standard deviations based on replicate samples.

Stn.Dep	Time	Location (°N, °E)	Depth (m)	S	T (°C)	O_2 (μM)	DIC (μM)
PV1.1	Jun03	59°35′,	79	9.3	4.1	0	1792±32
PV1.2		22°28′		9.1	4.0	2	1867±34
PV1.1	Sep04			8.0	3.7	121	1717±2.1
PV1.2				7.4	3.1	186	1725±0.3
PV1.1	May05			10.5	5.1	9	1932±0.3
PV1.2				10.3	5.1	8	1945±0.1
KAS.1	Jun03	59°57′,	56	8.4	2.7	142	1668±10
KAS.2		24°59′		7.5	2.4	131	1762±25
KAS.1	Sep04			7.2	2.8	131	1629±7.4
KAS.2				6.5	4.8	205	1605±3.4
KAS.1	May05			7.8	3.0	215	1715±4.0
KAS.2				7.9	3.0	197	1700±0.8
XV1.1	May05	60°16′,	48	7.0	2.2	285	1586±5.0
XV1.2		27°14′		6.3	1.9	330	1542±2.0

as an example of an accumulation bottom. Station Kasuuni (KAS), located south of Helsinki, was selected as a transport bottom, i.e. with no net long-term accumulation. Station XV1 in the eastern Gulf of Finland, close to the Finnish-Russian border, was chosen as representing an erosion bottom. All three stations are situated in the open Gulf of Finland and they are exposed to a variable degree of periodic anoxia; the most severe conditions generally occurring in the western Gulf of Finland (Vallius, 2006).

4.2.2 Sampling and analysis

Benthic chamber landers were deployed during three cruises to the Gulf of Finland. The first cruise took place during 23 June – 8 July 2003, the second in 15–28 September 2004 and the third in 13–23 May 2005. Details about the individual deployments are found in Table 4.1. A combination of two benthic landers was used, one with four incubation chambers and a smaller version with a single chamber. The landers have been described in more detail by Stahl et al. (2004b). The overlying water was stirred by a "Mississippi"-type wheel ensuring a complete mixing of the chamber. Nine syringes per chamber were used to withdraw samples during the incubation. To replace the sampled water, ambient bottom water was drawn through a narrow steel tube acting as a diffusion barrier. The volume of the overlying water was determined from the dilution of a known amount of an inert tracer. A syringe filled with 60 ml of NaBr solution (300mM) was injected into the chamber at the beginning of the incubation. The first sample was withdrawn after 10 minutes to ensure complete mixing of the NaBr solution. The Br concentrations were fitted with a inert tracer model developed by Andersson et al. (2006) in order to obtain the overlying water volumes. It has been shown that simple linear regression in some cases result in significant underestimation of the initial tracer concentration as the initial decrease is very rapid (Rao and Jahnke, 2004).

Sediment cores (i.d. 10 cm) intended for sediment and pore-water analysis, were sampled using a multiple corer, providing virtually undisturbed cores (Barnett et al., 1984). The cores were then immediately transferred to a temperature controlled laboratory set at *in situ* temperature, where they subsequently were sectioned into 18 intervals with a thickness of 0.5 cm down to 3 cm depth, 1 cm down to 10 cm and 2 cm down to a total depth of 20 cm. Slicing and centrifugation (2100-2500 rpm, 670xG, 30 min) were done at *in situ* temperature to minimize temperature artifacts. The ambition was to sample two replicate cores for each analyte during each cruise, but due to time constraints only one core was sampled in some cases. In the case of replicate cores, the cores were taken from separate deployments of the multiple corer. Bottom water was sampled using Niskin bottles mounted on the landers. All solute samples (except for O_2) from the chamber incubations, centrifuged pore-waters and bot-

tom waters were filtered through pre-rinsed 0.45 μm pore size cellulose acetate filters.

Optodes (Aanderaa Data Instruments Inc.) were used in order to continuously measure O_2 concentrations both inside and outside of the chambers (Tengberg et al., 2006). Samples for DIC concentrations were stored refrigerated in glass vials with butyl rubber stoppers until shipboard analysis, generally less than 24 hours after sampling. To determine the concentration of DIC, phosphoric acid was added to the sample in order to convert all dissolved carbonate species to CO_2. The CO_2 was then quantified with a non-dispersive infrared detector (LiCor) as described by O'Sullivan and Millero (1998). Calibration was made using Certified Reference Material available from A. G. Dickson Laboratory, Scripps Inst. of Oceanography, USA.

In addition to measuring the concentration of DIC, samples were also taken independently for the determination of the isotopic composition of DIC. These samples were stored refrigerated, upside-down in head-space vials with a butyl rubber membrane covered with Teflon, until analysis back in the laboratory. Isotopic composition was measured by injecting head-space gas directly in a continuous stream of helium into a Finnigan Delta+ IRMS via a ConFloII interface. Measured values were corrected for isotopic equilibrium fractionation according to Miyajima et al. (1995).

Sedimentary organic carbon concentration and isotopic composition were determined on gently disaggregated freeze-dried sediment, weighed into silver cups and subsequently decarbonated via the *in situ* acidification technique of Nieuwenhuize et al. (1994) using a Carlo Erba elemental analyzer.

Bromide, chloride and sulfate were determined on diluted samples by anion-chromatography with electro-chemical detection (DIONEX P850, ED40).

4.2.3 Benthic fluxes and carbonate dissolution

Benthic fluxes were calculated using the concentration change during the incubation based on linear regression of solute concentrations vs. time. Fluxes that were not significant ($p>.05$) were ignored and not presented. Solute concentration changes in the chamber were corrected for dilution effects by ambient water during sampling.

Carbonate dissolution was calculated based on the change in the isotopic composition of DIC. The isotopic composition of DIC produced in the sediment during an incubation or added to the pore-waters was calculated by a Keeling plot technique (Mortazavi and Chanton, 2004). Thus, the δ^{13}C-DIC of the produced DIC was obtained as the intercept of the linear regression of δ^{13}C-DIC vs. 1/DIC. The amount of carbonate dissolution was subsequently calculated based on an end-member approach, where the isotopic composition of organic carbon and calcium carbonate in surface sediments (0-0.5 cm) were the two end-members.

4.3 Results

4.3.1 Sediment profiles of organic carbon

Sediment surface concentrations of organic carbon were highest at station PV1 (accumulation bottom) with values of 6.5–9.1 % C d.w (Fig. 4.2). At station KAS (transport bottom) surface values were 3.8–5.5 % C d.w. and at station XV1 (erosion bottom) the lowest values of 1.0–4.0 % C d.w. were found. Variability was also largest here.

Organic carbon concentrations decreased quasi-exponentially with increasing depth in the sediment as a result of degradation of the labile fractions of the organic matter and reaching concentrations of 0.2–1 % at station KAS and XV1 while at station PV1 they remained higher (2–3 %) down to 20 cm depth.

4.3.2 Pore-water profiles

Concentrations of DIC at station PV1 increased from concentrations of around 2500 μM in the surface to around 5000 μM at a depth of 20 cm (Fig. 4.3). The steepest increase occurred in the upper five centimeters. One out of the two pore-water profiles from the cruise in 2005, differed markedly from the rest of the profiles at this station by having a subsurface maximum at around a depth of 3 cm.

At station KAS, surface concentrations of DIC were similar or slightly higher than those at station PV1. In four out of five profiles from this station, the concentration increased slightly with increasing depth. Con-

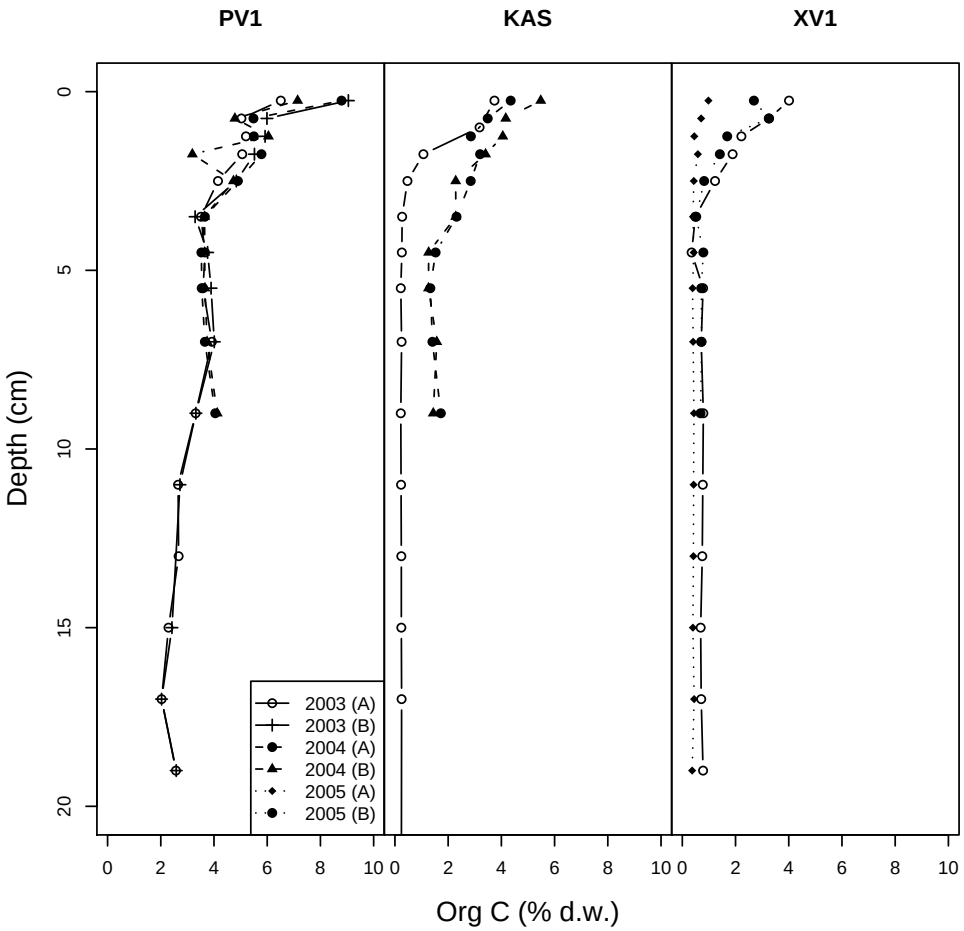

Figure 4.2: Depth distributions of organic carbon in surface sediments of the three stations in the Gulf of Finland.

centrations at depth were higher in 2005 than in the profiles from 2004. Comparing results from replicate cores, such large differences were not found. Thus, a large shift occurred between the 2004 and 2005 cruise. The results from 2003 show a similar profile to the deviating profile at station PV1 with a maximum at a depth of around 3 cm.

At station XV1, results are inconclusive with one profile with almost constant concentration of around 2500 μM, a second profile with a minimum at a depth of 1-1.5 cm and a third one , sampled in 2003, where concentration at depth is clearly lower than close to the sediment surface.

Pore-water profiles of chloride, bromide and sulfate were measured in samples taken during the cruise in 2004. Comparing station PV1 with station KAS, concentrations of these three anions were higher at PV1 reflecting the more saline conditions at this station (Fig. 4.4). Concentrations of bromide and chloride were very variable with depth but increased somewhat with increasing depth down in the sediment. Sulfate decreased strongly with depth as a result of sulfate reduction but was always present down to the sampled depth of 20 cm at station PV1.

4.3.3 Benthic respiration rates

During three cruises, a total of 47 benthic chamber incubations were performed *in situ* with the two landers. Based on the concentration change in the chamber during these incubations a total of 36 DIC and 38 O_2 fluxes were derived (Table 4.2). During the 2003 cruise the DIC analyzer malfunctioned, leaving us with O_2 fluxes alone. During the cruise in 2003 the bottom water was anoxic at station PV1, implying that the benthic flux of O_2 was zero. In general concentration changes in oxygen were very clear due to the high accuracy of the optical oxygen sensor (Tengberg et al., 2006). The change in DIC concentrations where very reliable (Fig. 4.5), except at station XV1 where the coarse sediment embedded with ferromanganese crustations impeded the penetration of the chamber into the sediment, resulting in a higher overlying water height than intended and thus, smaller concentration changes than at the other two stations.

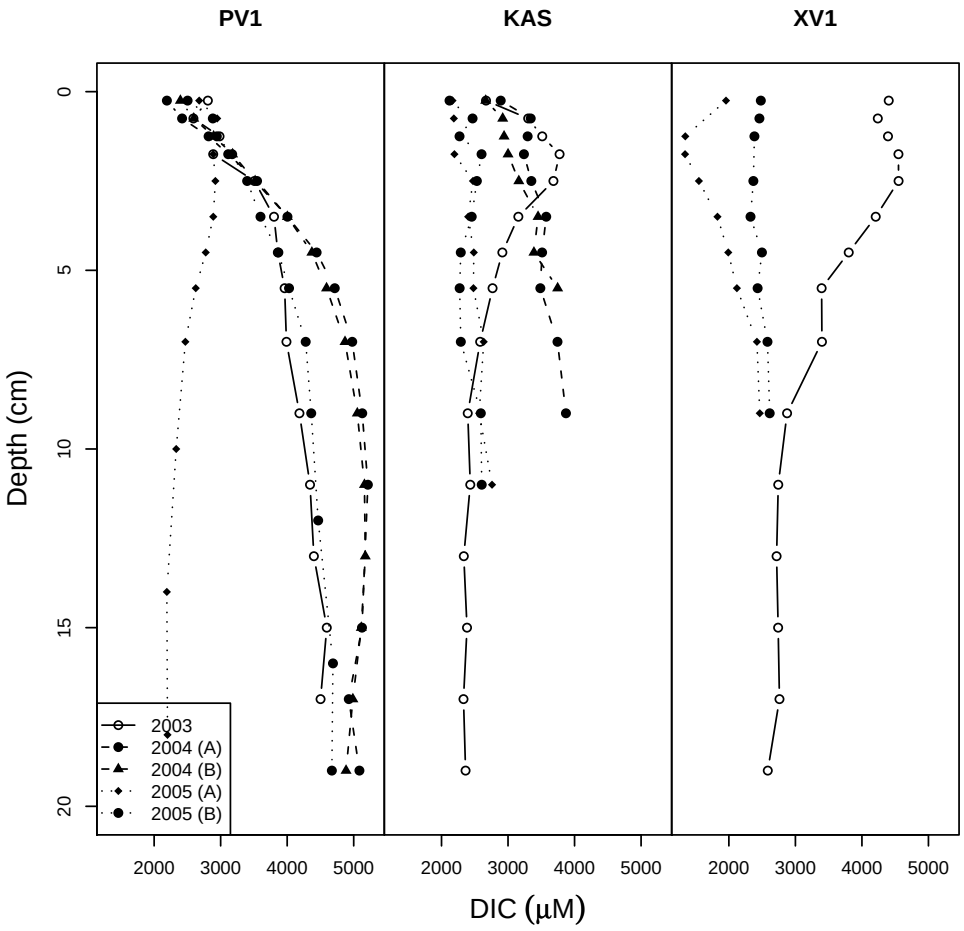

Figure 4.3: Pore water profiles of dissolved inorganic carbon in surface sediments of the three stations in the Gulf of Finland.

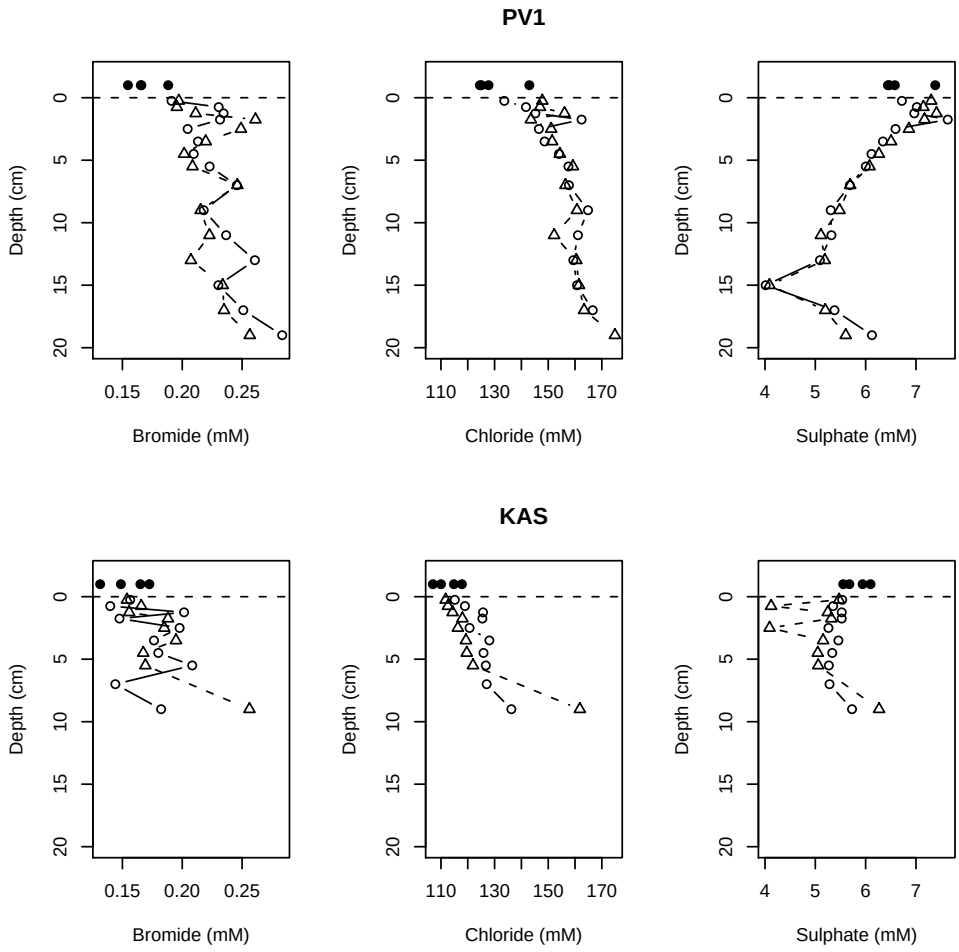

Figure 4.4: Pore water profiles of bromide, chloride and sulfate sampled in the 2004 cruise. Open symbols indicate replicate cores. Closed symbols indicate overlying water.

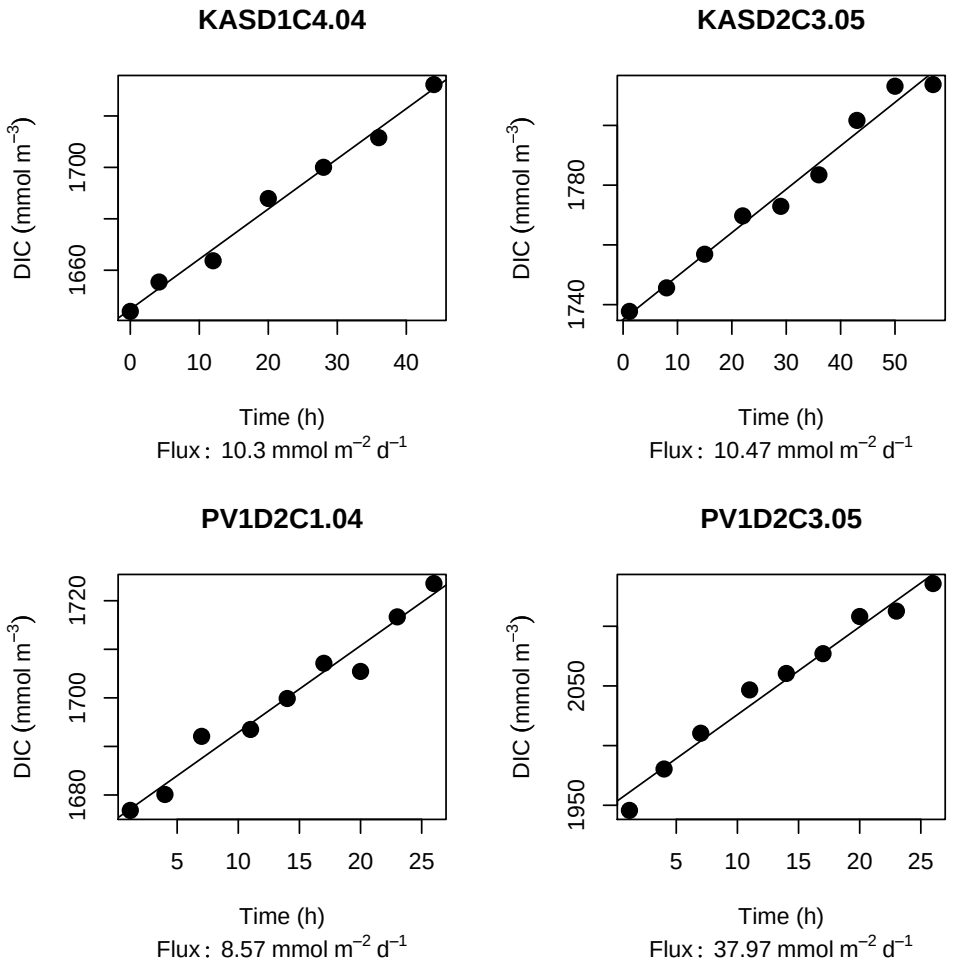

Figure 4.5: Examples of concentration changes of DIC, in benthic chamber incubations, at station PVI and KAS. Note the higher initial concentrations in 2005 compared to 2004, reflecting variations in bottom-water concentrations due to changing bottom water masses.

Table 4.2: Benthic fluxes of O_2 (mmol O_2 m^{-2} d^{-1}) into the sediment and dissolved inorganic carbon (mmol C m^{-2} d^{-1}) from the sediment. All fluxes are based on *in situ* chamber incubations. Respiration quotients (RQ) are calculated as DIC/O_2. Details about the lander deployments are found in Table 4.1.

Station	Year	Deployment	Chamber	DIC	O_2	RQ
PV1	2004	1	2	38.42	19.78	1.94
PV1	2004	1	3	48.91	13.38	3.66
PV1	2004	1	4	27.05	11.07	2.44
PV1	2004	1	5	31.93	15.96	2.00
PV1	2004	2	1	8.57		
PV1	2004	2	2	12.89	13.68	0.94
PV1	2004	2	3	12.17	11.10	1.10
PV1	2004	2	4	9.31	13.07	0.71
PV1	2005	1	1	34.27		
PV1	2005	1	2	33.09		
PV1	2005	1	3	35.24		
PV1	2005	1	4	37.43		
PV1	2005	2	1	46.15		
PV1	2005	2	2	39.37		
PV1	2005	2	3	37.97		
PV1	2005	2	4	30.29		
KAS	2003	1	3		14.31	
KAS	2003	1	4		10.18	
KAS	2003	1	5		12.77	
KAS	2003	2	3		9.12	
KAS	2003	2	4		8.91	
KAS	2003	2	5		8.76	
KAS	2004	1	1		7.32	
KAS	2004	1	2	9.47	7.06	1.34
KAS	2004	1	3	14.48	7.47	1.94
KAS	2004	1	4	10.30	9.29	1.11
KAS	2004	2	1	11.30	8.17	1.38
KAS	2004	2	2	16.09	12.21	1.32

Table 4.2: Continued...

KAS	2004	2	3	10.31	9.59	1.08
KAS	2004	2	4	15.33	12.10	1.27
KAS	2004	2	5	6.91		
KAS	2005	1	1	14.51	16.00	0.91
KAS	2005	1	2	17.71	15.27	1.16
KAS	2005	1	3	12.07	14.42	0.84
KAS	2005	1	4	13.80	15.70	0.88
KAS	2005	2	1	10.70	14.69	0.73
KAS	2005	2	2	10.26	13.96	0.73
KAS	2005	2	3	10.47	13.78	0.76
KAS	2005	2	4	12.21	13.84	0.88
XV1	2005	1	1		13.87	
XV1	2005	1	2	4.83	13.85	0.35
XV1	2005	1	3	4.84	13.48	0.36
XV1	2005	1	4	8.91	13.87	0.64
XV1	2005	2	1		14.84	
XV1	2005	2	2	14.18	14.67	0.97
XV1	2005	2	3		14.44	
XV1	2005	2	4		14.90	

Comparing oxygen consumption rates (Table 4.2) amongst the stations, no obvious difference could be found (ANOVA, $p=0.10$, $F_{2,35}=2.4$). Variations amongst individual chambers within one deployment were generally small and most variability was found between deployments. Oxygen consumption rates were similar or higher than rates previously reported for the Baltic Sea (Table 4.3).

Table 4.3: Published respiration rates in the Gulf of Finland (GoF) and other areas of the Baltic Sea. Site depths, bottom water concentrations of oxygen and sediment oxygen consumption rates obtained from (**1**) Conley et al. (1997), (**2**) Balzer (1984) and (**3**) Koop et al. (1990)

Area	Depth (m)	Season	O_2 consumption (mmol m^{-2} d^{-1})	Bw-O_2 (μM)	Ref.
GoF, Stn GF4	35	Summer	11.1	186	1
GoF, Stn GF6	44	Summer	12.3	214	1
GoF, Stn GF1	84	Summer	11.0	220	1
GoF, Stn GFF	85	Summer	12.7	266	1
Kiel bight	20	Spring	10.4	321	2
Kiel bight	20	Winter	4.13		2
Baltic proper	47	Summer	18.6	428	3
Baltic proper	82	Summer	15.3	196	3
Baltic proper	130	Summer	5.15	56	3

Benthic fluxes of DIC were significantly different (ANOVA, $p=10^{-8}$, $F_{2,39}=30.5$) between stations with a pattern similar to surface concentrations of organic carbon and were highest at station PV1, intermediate at KAS and lowest at XV1 (Fig. 4.6). To our knowledge, these fluxes of DIC are the first ones for the Gulf of Finland, thus no comparison with previous measurements can be made. However, the fluxes of DIC are comparable to other shelf areas such as the periodically hypoxic region of the Gulf of Mexico where Rowe et al. (2002) measured benthic DIC fluxes of 34±15 mmol m^{-2} d^{-1} (mean±st. dev. across eight stations).

Sediment surface values of δ^{13}C of sedimentary organic carbon at station PV1 and KAS were similar with values of -24.4 ‰ and -23.6 ‰, respectively. These values were used as the organic carbon isotopic end-member values. The isotopic values of DIC produced during incubations in the first and second deployment at PV1 were -12±6 ‰ and -19±3 ‰, respectively (Fig. 4.7). At station KAS the derived δ^{13}C-DIC value was better constrained with values of -20.9±1.9 ‰ and -20.3±-1.2 ‰, from the first and second deployment, similar to the value based on pore-water data

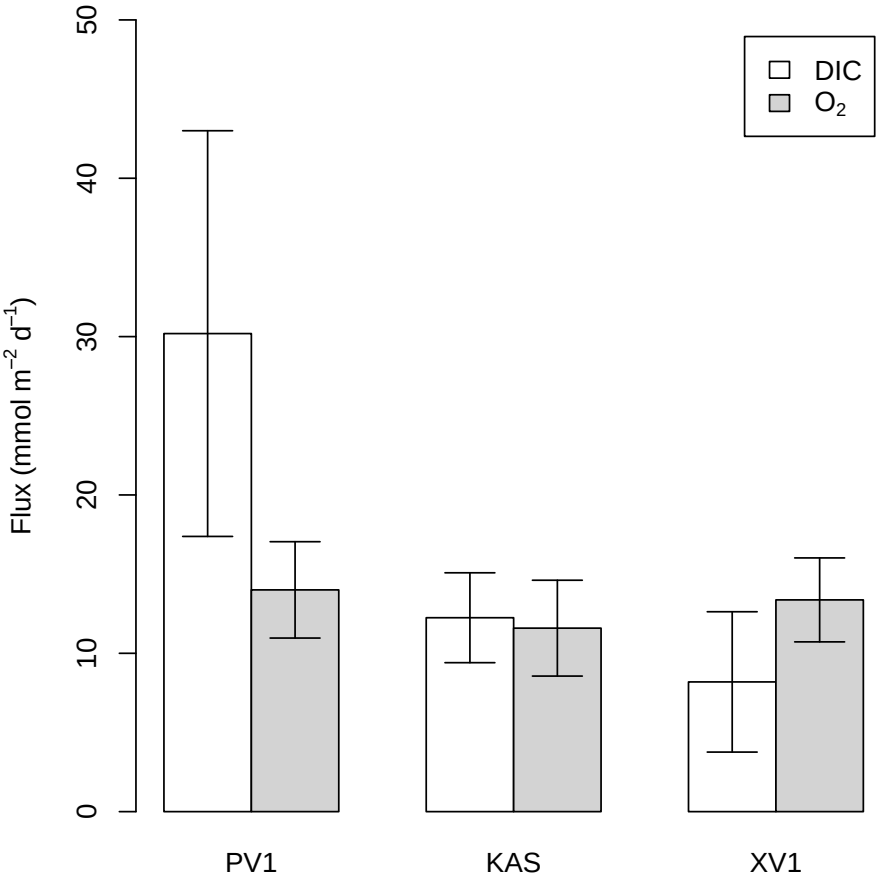

Figure 4.6: Benthic fluxes of DIC and O_2 at the three stations in the Gulf of Finland. Error bars indicate standard deviations.

Table 4.4: Relevant model parameters used in the calculations. Parameters were chosen in order to represent an accumulation bottom, such as station PV1. Biological activity such as bioturbation and irrigation was assumed to be absent. A detailed description of each parameter can be found in Soetaert et al. (1996b)

Parameter	Unit	Value	Description
ϕ_0	-	0.93	Porosity at surface
ϕ_∞	-	0.83	Porosity at depth
k_ϕ	cm	2.9	Porosity change length scale
w	cm yr^{-1}	0.1	Sediment accumulation rate
Cflux	mmol m^{-2} d^{-1}	20	Deposition of organic C
$\mathrm{Part_{Fdet}}$	-	0.7	Fraction of fast decaying C
$\mathrm{R_{Fdet}}$	d^{-1}	0.024	Decay rate of fast fraction
$\mathrm{R_{Sdet}}$	d^{-1}	0.00024	Decay rate of slow fraction
D_b	cm^2 d^{-1}	0	Bioturbation

from both these stations (Fig. 4.8). Unfortunately no data are available from station XV1 since the isotopic sampling was conducted only during the 2004 cruise. Using the end-member approach, carbonate dissolution contributed 15±3 % and 13.5±1 % to the total benthic DIC production at station KAS and PV1, respectively.

4.3.4 Model description and results

An extended version of the OMEXDIA-model (Soetaert et al., 1996b) was applied to study the effect of changing bottom water concentrations of O_2 and DIC.

For details of the model and parameter values, other than those listed in Table 4.4 see Soetaert et al. (1996b,a). In brief, OMEXDIA is a numerical, non-linear, coupled model, based on the 1-dimensional diagenetic equations as presented by Boudreau (1997). Solutes are transported by diffusion, whereas the solid phase is transported by advection and bioturbation. By describing aerobic carbon mineralization, nitrification, denitri-

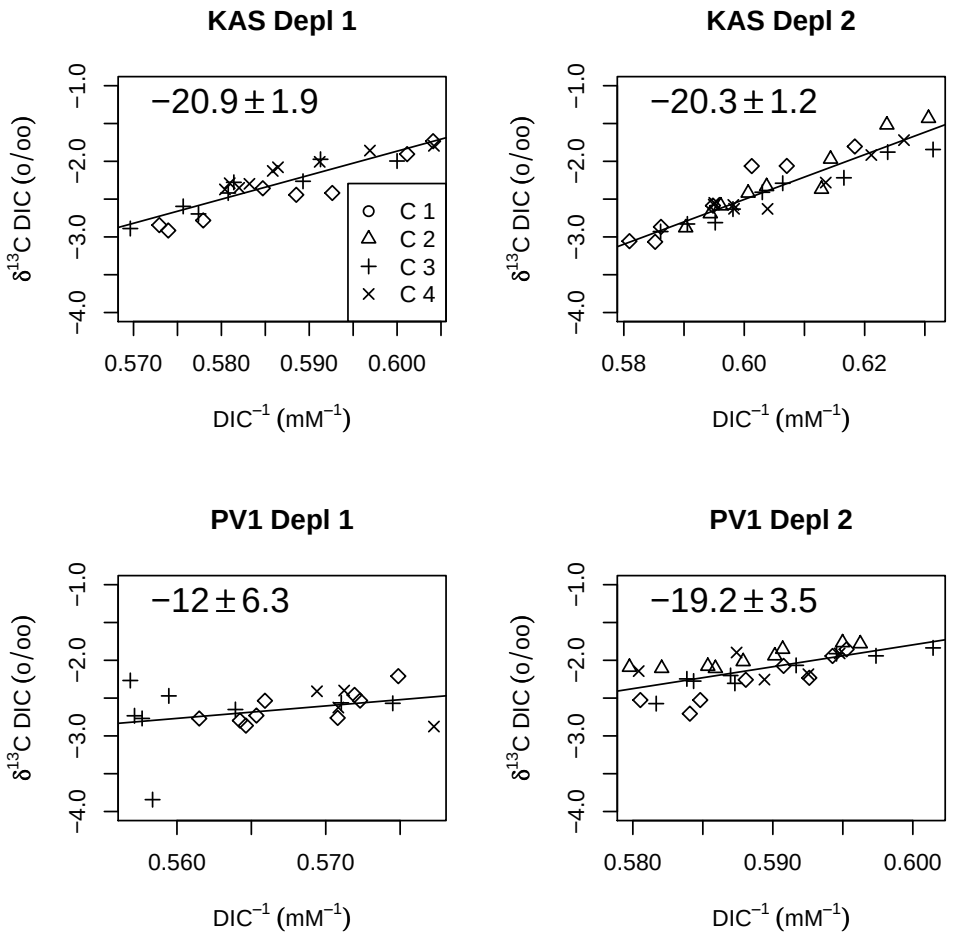

Figure 4.7: Keeling plots of chamber DIC. Numbers in the top-left corner of each subplot indicate estimated δ^{13}C of the DIC produced during incubation. Indicated errors are standard errors estimated by linear regression.

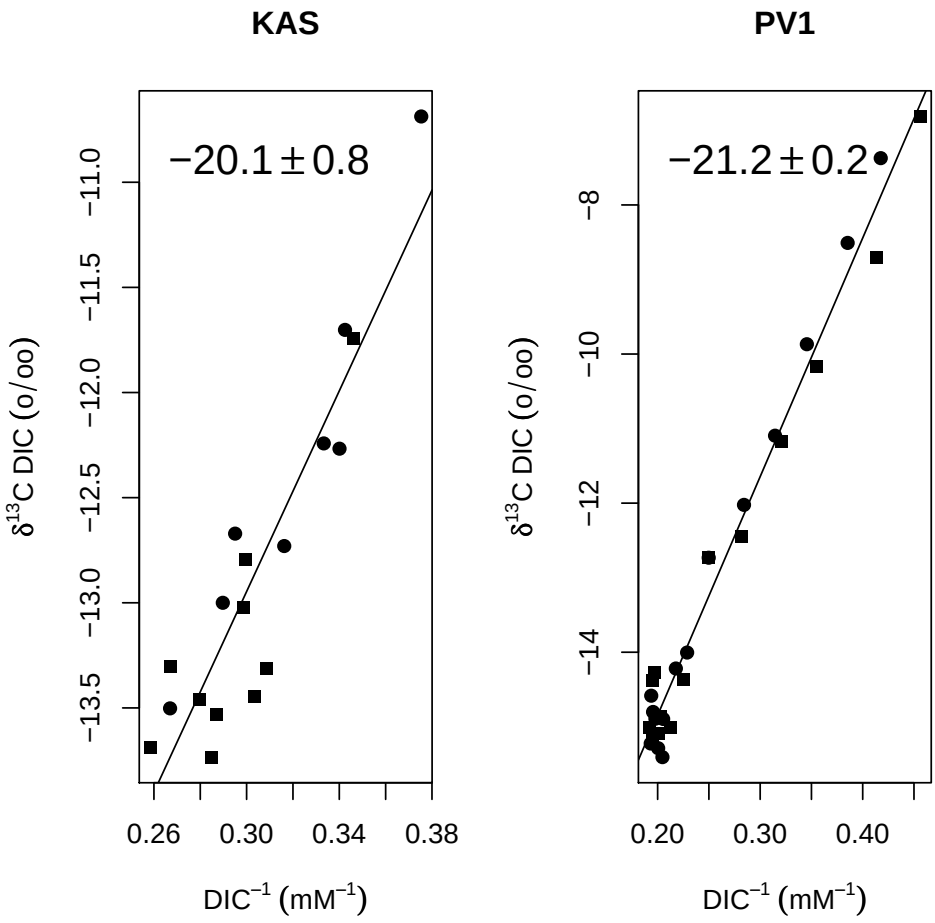

Figure 4.8: Keeling plot of pore water DIC. Numbers in the top-left corner of each subplot indicate estimated δ^{13}C of the DIC produced in the sediment. Indicated errors are standard errors estimated by linear regression.

fication, and lumping anaerobic mineralization processes, the model generates profiles of O_2, nitrate, ammonium, ODU (Oxygen Demand Units) and profiles of two carbon fractions with different first-order degradabilities and C/N ratios. The extension beyond the original OMEXDIA-model included the addition of DIC, modeled as a lumped species. The diffusion coefficient of HCO_3^-, used for DIC is based on values in Boudreau (1997). DIC is produced by degradation of the two organic carbon fractions and any possible carbonate dissolution or precipitation is ignored.

The purpose of this idealized model exercise was to quantitatively study the effect of a sudden change in the bottom water concentrations of O_2 and DIC, caused by e.g. an oscillating pycnocline, on the benthic fluxes of these species. The model was run dynamically and was initialized with steady-state distributions of all species. After a period of time, the bottom water concentrations, i.e. the boundary conditions, were changed to concentrations resembling those found below the halocline. Thus, O_2 was decreased from close to saturation to 10μM and DIC was increased from 1500 to 1900 μM. After ten days the original bottom water concentrations were restored.

The drop in the O_2 concentration (Fig. 4.9A) causes instantly a similar drop in the benthic flux of O_2 (Fig. 4.9C) because the transport of O_2 becomes limited by transport across the diffusive boundary layer. After the perturbation period, when the high O_2 concentration is restored, the flux increases slightly above the initial value for less than one day as a result of the re-oxidation of accumulated reduced substances, e.g. HS^-, in the sediment. The increase in the DIC concentration (Fig. 4.9B), causes a decrease in the flux of DIC (Fig. 4.9D), as a result of a less steep gradient across the sediment-water interface. The gradient is gradually restored and after one day attained at value of 90% of the steady-state flux. After ten days when the lower bottom water DIC concentration is restored, the reverse situation is found.

The conclusion of this model exercise is that DIC fluxes across the sediment-water interface, are a robust measure of benthic respiration in an environment such as the Gulf of Finland with large changes in the overlying water concentrations. Moreover, the flux of O_2 is more difficult to use directly as a measure of benthic respiration in a situation of low O_2 concentration, as the flux of O_2 across the sediment-water interface becomes limited by the diffusive boundary layer.

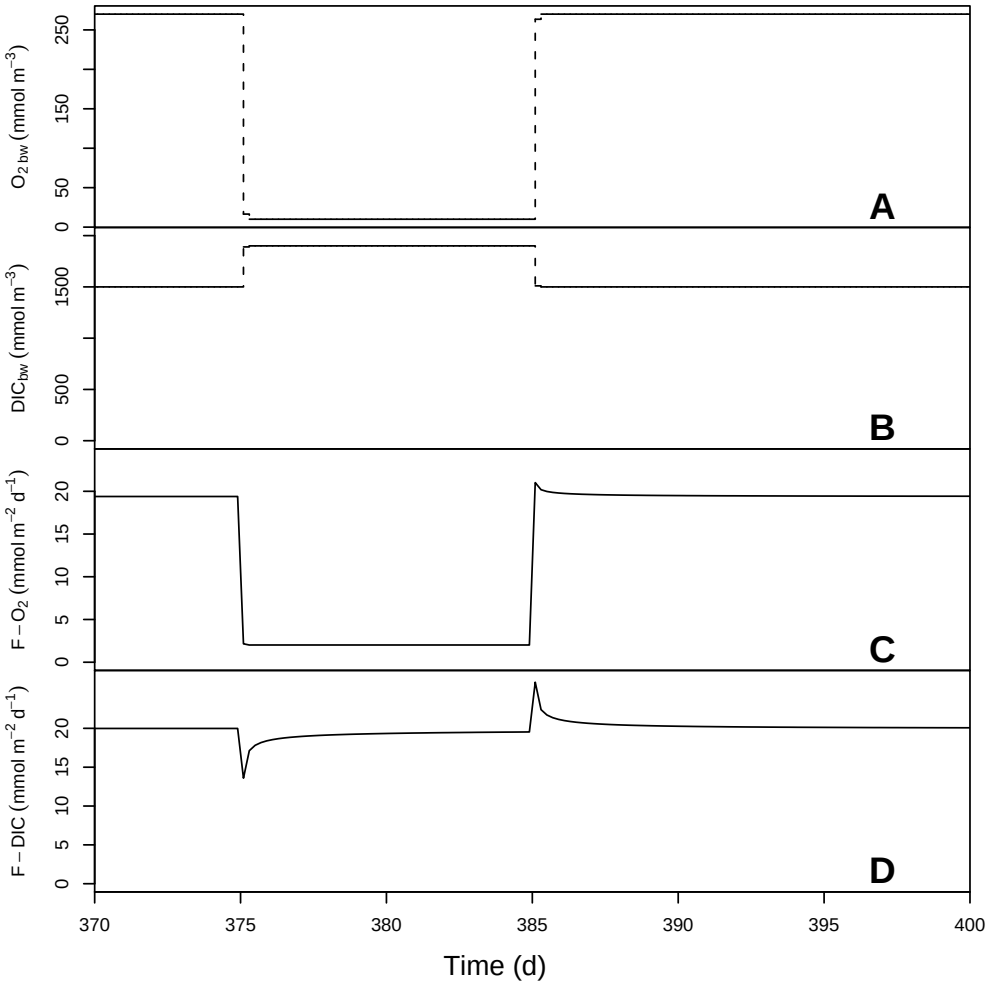

Figure 4.9: Varying bottom water concentrations of O_2 (**A**) and DIC (**B**) results in changes in benthic fluxes of O_2 (**C**) and DIC (**D**).

4.4 Discussion

4.4.1 Variations in overlying water masses

In a steady-state situation where the production of DIC and the overlying water concentration are constant, pore-water concentrations are expected to increase with increasing depth down in the sediment. At some depth the concentration will reach an asymptotic value where all labile carbon is consumed. This was not the case for many of the measured pore water profiles as shown in Figure 4.3. In several cases concentrations increased down to a certain depth but then decreased again. A plausible explanation for this is changing overlying water masses, with different concentrations of DIC. This idea was further supported by the concurrent variations with depth down into the sediment of the profiles of major anions such as bromide and chloride and to some extent sulfate, which are all affected by changes in salinity as their concentration in sea water is constant (Fig. 4.4).

4.4.2 Respiration rates in the Gulf of Finland

Oxygen consumption measurements have been used in numerous benthic studies of organic matter processing. Historically, the Winkler titration technique was used to accurately determine O_2 concentrations. At present, oxygen sensors such as optodes (Tengberg et al., 2006) are capable of continuously monitoring O_2 concentrations with a precision comparable to careful Winkler titration, but without any labor intensive titrations, thus being more cost-effective. Information on oxygen consumption has a value in its own to constrain the biogeochemical cycle of oxygen, but in most cases the ultimate focus is to estimate the respiration of organic carbon to carbon dioxide. If organic matter is respired solely with O_2, the coupling between these quantities depends mainly on the composition of organic matter and the amount of ammonium being nitrified (Anderson et al., 1986). However, aerobic respiration is only dominating respiration in oligotrophic deep-sea sediments, where the supply of organic carbon is limited. In other environments, such as continental shelf sediments respiration proceeds through the sequence of available electron acceptors with decreasing energy yield, O_2, nitrate, manganese and iron oxides, sulfate and carbon dioxide. In most sediments a large fraction of the products of anaerobic

respiration, diffuses upwards and becomes re-oxidized in the presence of oxygen. Thus, using oxygen consumption as a measure of benthic respiration requires the knowledge or assumptions about the other pathways of respiration. More specifically, it requires quantification of the amount of reduced substances, such as Mn^{2+}, Fe^{2+} or HS^-, that escape re-oxidation in the sediment either because they diffuse through the sediment-water interface or in the case of iron and sulfur become buried as pyrite (FeS_2) (van Cappellen and Wang, 1996; Wijsman et al., 2002). Organic matter mineralization through denitrification produces N_2 which escapes the benthic system in almost all sediments without being re-oxidized. This is thus not reflected in the oxygen consumption, but the relative importance of this pathway is usually less than 10% (Middelburg et al., 1996).

The most straightforward method to measure respiration rates of carbon is thus to measure the concentration change of DIC in a closed volume (Anderson et al., 1986). The only process other than respiration, interfering with this is dissolution/precipitation of carbonate minerals, and this term has to be independently assessed (see below).

Comparing benthic DIC and O_2 fluxes, a respiration quotient (RQ) was calculated as DIC/O_2 (Table 4.2). The RQ becomes unity if organic matter consists solely of carbohydrates, reduced substances are fully re-oxidized and the effects of nitrification and denitrification can be ignored or cancel each other. The higher RQ found at station PV1 and KAS (Fig. 4.10) is likely due to the limiting effect on the O_2 flux imposed by the occasionally hypoxic conditions causing an incomplete re-oxidation of reduced substances. Thus sediment oxygen consumption underestimates total benthic remineralization when a low O_2 concentration is limiting the flux across the sediment-water interface (Rowe et al., 2002).

4.4.3 Carbonate dissolution

In sediments, DIC is produced by two sources, carbonate dissolution and organic matter mineralization. By subtracting carbonate dissolution from the total production of DIC in sediments, the amount of organic matter mineralized in the sediments is obtained.

Three different approaches are used to measure dissolution of calcium carbonate from benthic chamber incubations or pore-water profiles. The first technique directly measures the concentration change in Ca^{2+} pro-

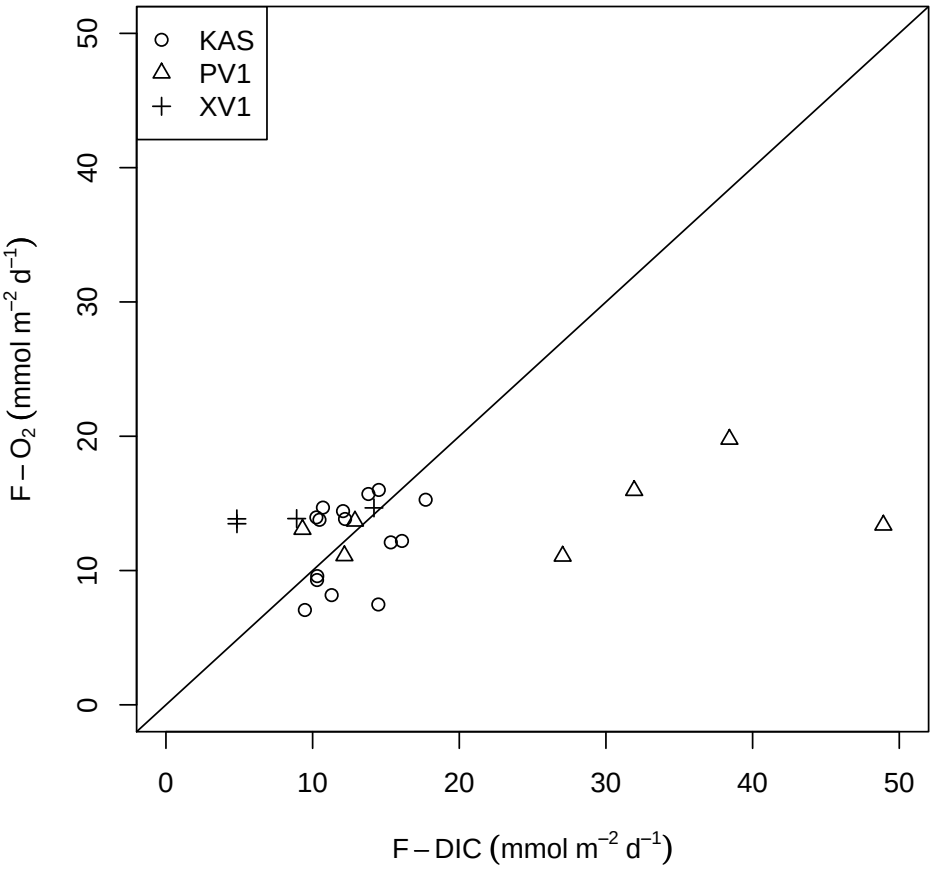

Figure 4.10: A comparison of all benthic DIC and all O_2 fluxes where oxygen was detectable initially in the chamber, at the three stations across the Gulf of Finland showing partial uncoupling due to variable concentrations of O_2 in the overlying water. The solid line shows a respiration quotient of 1, expected if organic matter consists of carbohydrates, anaerobically produced substances are fully re-oxidized and the effects of nitrification and denitrification can be ignored or cancel each other.

duced by $CaCO_3$ dissolution. This technique is hampered by the fact that Ca^{2+} is the third most important cation in sea water (after Na^+ and Mg^{2+}), i.e. it is present in millimolar concentrations. Thus for most sediments, concentration changes during incubations are practically undetectable (Stahl et al., 2004a).

The second technique uses the change in total alkalinity. Dissolution of carbonate minerals release CO_3^{2-} which increases total alkalinity by two alkalinity equivalents. However, numerous other processes occurring in continental shelf sediments also contribute to changes in total alkalinity, the most prominent one being sulfate reduction. Thus, estimating $CaCO_3$ dissolution in coastal sediments based on changes in total alkalinity involves independently estimating sulfate reduction and correcting for this term. As the contribution of sulfate reduction to total alkalinity fluxes can be of the same order of magnitude as carbonate dissolution, the errors inherent in this approach can be large as carbonate dissolution has to be calculated by the difference between two similar values, each with some uncertainty (Berelson et al., 1996).

The third approach, used in the present study, was to measure the change in the isotopic composition of DIC with time. It is based on an end-member approach, where organic carbon and calcium carbonate are the two end-members that contribute to the production of DIC, each with a distinct isotopic signal. Organic matter is depleted in ^{13}C compared to DIC in sea water because of the isotopic fractionation during primary production. Consequently, organic carbon has $\delta^{13}C$ ranging from -19 to -27 ‰, whereas carbonates typically have a much more constrained range of $\delta^{13}C$, close to 0 ‰. Thus, this approach involves the determination of the isotopic composition of both end-members and the isotopic composition of DIC produced in the sediment is then estimated from a Keeling plot (Mortazavi and Chanton, 2004).

However, as shown in Figure 4.11, a typical incubation in an environment with a benthic DIC flux of 10 mmol m^{-2} d^{-1} into a chamber with a overlying water height of 20 cm produces a change of 100 μM in the concentration of DIC, but only a change of 1.2 ‰ in the isotopic composition. This is in the case of no contribution from carbonate dissolution, where the change in $\delta^{13}C$ is maximal. It is thus difficult to constrain the contribution from carbonate dissolution, based on *in situ* incubations combined with an analytical precision of $\sim$ 0.1 ‰ as in our measurements where

small (6 mL) vials were used.

A possible confounding explanation for the production of isotopically heavy DIC relative to the sediment OM, is preferential mineralization of marine organic matter, as marine organic carbon is normally heavier than terrestrial carbon. This seems likely since it is well established that terrestrial OM is more resistant to degradation (Burdige, 2005). This would result in a lighter residue of undegraded organic carbon. At the steady accumulating station PV1, where a decrease from 6.5 % sedimentary organic carbon in the surface sediment to about 2.5% at 20 cm depth, the isotopic composition decreased from -23.9 ‰ at surface to -24.5 ‰ at depth. By using mass-balance calcuations we find that the mineralized organic carbon had an isotopic composition of -23.6, assuming that the isotopic composition of the deposited organic carbon has been constant. Thus, a slight shift towards presumably marine OM in the isotopic composition of the organic carbon endmember.

Continental shelf waters are generally not undersaturated with respect to carbonate minerals and carbonate dissolution in sediments is thus limited. No dissolution would take place without the oxidation of organic matter by O_2 and nitrate, taking place just below the sediment-water interface, which produces acidity and may lead to dissolution of calcium carbonate, termed metabolic dissolution (Mucci et al., 2000). The contributions of carbonate dissolution to the total production of DIC was 13.5% at station KAS and 15 % at PV1. These values are slightly higher than in the study of Berelson et al. (1996), where the contribution of calcium carbonate dissolution to the total DIC flux were 3–11 % at stations shallower than 100 meters situated on the Californian continental shelf.

4.4.4 Resuspension

In a shallow, non-tidal basin such as the Gulf of Finland, surface waves induce resuspension periodically (Kuhrts et al., 2004). Resuspension affects benthic organic matter cycling in two ways, on the one hand via direct effects such as changes in mineralization and oxidation of reduced compounds (Tengberg et al., 2003) and on the other hand via transport of sedimentary organic matter from erosion and transport bottoms to deeper situated accumulation bottoms. The observed distributions of organically enriched surface sediments at station PV1 might be the results of such re-

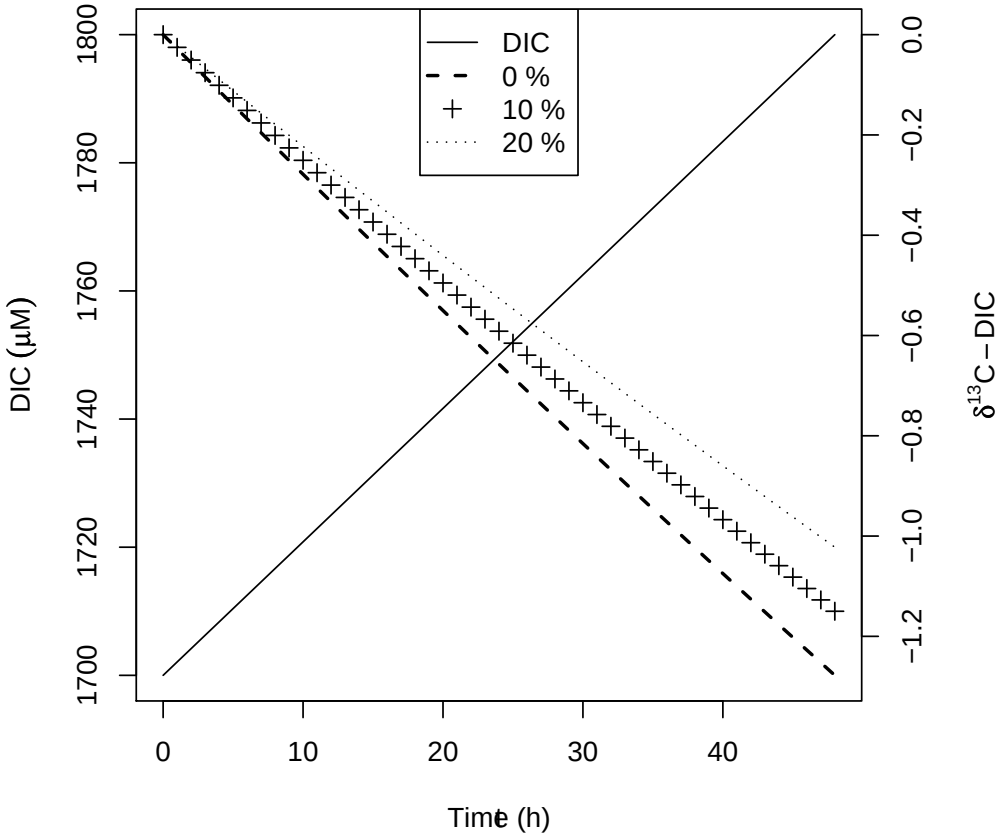

Figure 4.11: Concentration change of DIC together with the change in the isotopic composition during a hypothetical incubation, where carbonate dissolution is either not present or accounts for 10 or 20 % of the total DIC flux.

distribution of organic matter derived from erosion and transport bottoms such as at station XV1 and KAS. The increased input of organic matter also manifests itself in higher respiration at station PV1. Although the division of sediment bottom types mainly depends on the actual water depth, local topographical features may cause patches which deviate from the general classification, such as exhibiting transport characteristics in an accumulation area. This is a plausible explanation for the low respiration rates measured at one occasion at station PV1. The relevance of remobilization of organic matter, from shallower located bottoms to deeper bottoms, is the different impact it will have on the feedback to the pelagic ecosystem. If the organic matter is transported to bottoms located below the Baltic Sea permanent halocline, instead of being remineralized at the spot where it was initially deposited, the released nutrients will have a completely different temporal and spatial effect on the pelagic ecosystem, with an increased residence time due to the slow exchange across the halocline. The results of this study are in concordance with the results of Schneider et al. (2000), where carbon fluxes in the eastern Gotland Sea were investigated based on fluxes of POC across the halocline and changes in DIC below the halocline. In their study, local production contributed only 13–26 % of the total POC input with the remainder derived from lateral inputs.

4.5 Conclusions

Benthic respiration rates in the Gulf of Finland were quantified at three stations during three cruises, based on benthic chamber lander incubations. Sediment oxygen consumption rates were similar at all three stations, except at times when the overlying water was anoxic and no flux could be measured. Production of DIC was highest at station PV1, intermediate at station KAS and lower and more uncertain at station XV1. As these stations represent different bottom types, these results suggests an important role of the long-term effect of deposition, resuspension cycles where organic matter is transported laterally from shallower sediments to deeper ones. Such transfer will have a large impact on the organic matter and nutrient cycling in highly stratified systems such as the Baltic Sea.

5 Identifiability and uncertainty of bio-irrigation rates

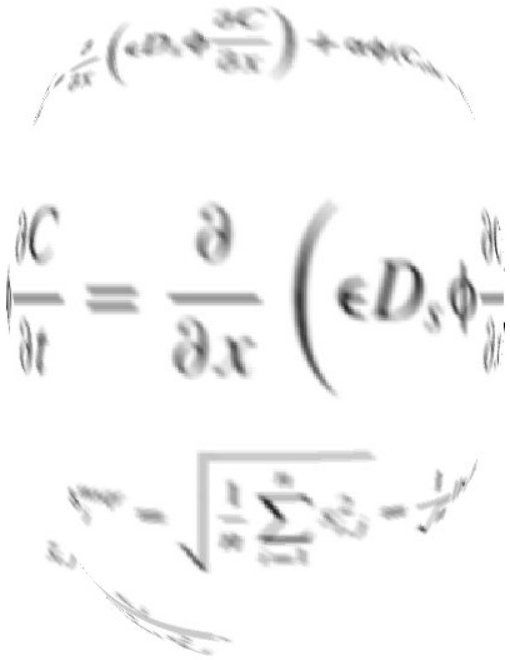

Johan Henrik Andersson, Jack J. Middelburg and Karline Soetaert, 2006, *Journal of Marine Research*, 64:407-429, doi:10.1357/002224006778189590

5.1 Introduction

Bio-irrigation, enhanced porewater exchange due to the presence of animal structures and burrow ventilation, is found in all sediments that are inhabited by benthic fauna. These animals ventilate their burrows to maintain their environment suitable to themselves. In absence of pumping the sediment would be dominated by microbes thriving without oxygen. As a result of these activities, profiles of all solutes in the sediment are impacted. This in turn affects the rates of most biogeochemical processes. Obtaining bio-irrigation rates not only allows assessing the activity of benthic organisms, but is also essential for the quantification of organic matter and nutrient cycling in sediments.

Estimating the rate of irrigation can be done in a number of different ways. The most common method is to compare fluxes measured by benthic chamber incubations, which take into account bio-irrigation, and fluxes based on modeled porewater profiles, assuming that these profiles are shaped only by molecular diffusion. Although most of the difference between these approaches can be attributed to irrigation, two confounding factors are the influence of sediment topography (Røy et al., 2002, 2005) and the respiration of the macrofauna itself (Herman et al., 1999). Wenzhöfer and Glud (2002) compiled oxygen consumption measurements from both chambers and porewater profiles and concluded that the ratio of total and diffusive oxygen uptake is 3–4 in shallow waters with the major fraction attributed to irrigation and not metazoan respiration.

A second approach uses naturally occurring tracers with predictable sources and sinks. One such tracer is ^{222}Rn which is produced by radioactive decay from ^{226}Ra. By measuring the production of ^{222}Rn in the absence of transport, e.g. in slurries, along with the *in situ* activity, transport parameters can be calculated. This approach has been used by e.g. Martin and Banta (1992) and Benoit et al. (1991). The half-life of ^{222}Rn is 3.8 d and this sets the maximum timescale to measure activity changes of this tracer to about three weeks.

A third approach is to deliberately inject an inert tracer, not naturally occurring in large amounts, to an enclosed body of overlying water. Tracers which have been used for this purpose are e.g. Br^- (Forster et al., 2003), T_2O (Emerson et al., 1984), D_2O (Bird et al., 1999; Berelson et al., 1999) and Cs (Berelson et al., 1998). The timescale of this type of tracer

is set by the experimental conditions (Martin and Banta, 1992) and is typically on the order of days. Irrigation rates can then be inferred either from the time-series of concentrations in the overlying water or from the profiles of the tracer in the sediment at the end of the experiment.

Most studies of bio-irrigation have been done on retrieved core incubations (e.g. Forster et al., 2003; Martin and Banta, 1992), but some have used benthic landers to eliminate the disturbance and change of environmental factors when retrieving cores (e.g. Rao and Jahnke, 2004; Sayles and Martin, 1995). Apart from the wish to obtain transport parameters, another reason to use the deliberate tracer technique is that it allows the estimation of the volume of the overlying water inside the chamber (Rao and Jahnke, 2004). This is a critical parameter, used in the calculation of benthic fluxes from concentration changes in the chamber. Therefore this information is essential for *in situ* studies when the sediment retrieving function of the benthic lander fails or is simply absent.

In order to interpret tracer results for these two different purposes, estimating irrigation rate and the volume of the overlying water, a mathematical model that includes bio-irrigation is fitted to the data. Although mechanistic multidimensional models of bio-irrigation exist for muddy (Aller, 1980) and permeable sandy sediments (Meysman et al., 2006), bio-irrigation is usually represented in a parameterized form as enhanced diffusion or as a non-local exchange process. In this paper, the term bio-irrigation refers to enhanced porewater exchange regardless of the transport mechanism, and not exclusively to non-local exchange (e.g. Boudreau, 1997).

The first mechanism of enhanced diffusion introduces an enhancement factor, which is multiplied with the diffusion coefficient, to account for solute mixing induced by meio- or macrofauna movement (Aller and Aller, 1992). Alternatively, non-local irrigation (Emerson et al., 1984; Boudreau, 1984) is governed by flushing of macrofauna burrows and includes a source minus sink term to account for water exchange at a certain depth in the sediment. The impact of these two processes on the solute profiles is rather different. Enhanced diffusion has the largest effect where the gradients are steep, which for most solutes is at the sediment-water interface. In contrast non-local exchange is most effective where the difference between the local concentration and the concentration of the overlying water is greatest, normally deeper in the sediment (Boudreau, 1997). By fitting

these models to tracer data, one can derive either the enhancement factor or the bio-irrigation rate, or both (Rao and Jahnke, 2004). However, there are more model parameters that are unknown or only partly known, e.g. the sediment porosity (gradient), the depth of burrow penetration, and in many cases the height of the incubation chamber. For a model to be able to estimate all these unknown parameters, the available data have to be of sufficient resolution. If this is not the case, optimization routines often fail to converge, parameter values may be highly correlated or the optimal parameter values are highly sensitive to random variations in the data. Thus, a common strategy in this case is either to fix some parameters at values based on literature or to simplify the model (i.e. reduce the number of parameters). In most cases whether or not a combination of parameters can be deduced from a certain data set has not been investigated.

In addition, a posteriori calculation of the uncertainty of the parameters is usually not done in the bio-irrigation literature. This is not because it is considered unimportant, but because it is more complex to calculate uncertainties for bio-irrigation models (which are non-linear), compared to the estimation of standard errors of the linear regression coefficients used for most benthic flux studies. Nevertheless, in order to allow comparison of differences in bio-irrigation between stations, seasons or among experimental treatments, it is necessary to know the uncertainty of the estimated parameters.

Recently it has been suggested by Rao and Jahnke (2004) that it is possible to distinguish between enhanced diffusive and non-local exchange, i.e. constrain several unknown parameters, using only time-series of tracer concentrations in the overlying water during incubations. Here we take a more statistically founded approach to the problem. First we investigate which combinations of parameters can be derived from a certain data set using the identifiability technique of Brun et al. (2001) (see details below). We do this for (1) a deep-sea and (2) a shallow-water muddy setting, and for typical data sets consisting of either a time-series of tracer in the overlying water, or a vertical profile of porewater concentration at the end of the incubation or both. Then we estimate the uncertainty of the estimated unknown parameters as arising from uncertain data and an imperfect model, by a numerical technique known as Bayesian inference (see details below). This technique is increasingly being used in the field of ecology and biogeochemistry (Harmon and Challenor, 1997; Dowd and

Meyer, 2003; Malve et al., 2005; van Oevelen et al., 2006), but it has not yet been applied to the field of early diagenesis.

5.2 Methods

5.2.1 Bio-irrigation model

The irrigation model describes transport of an inert tracer in a one-dimensional sediment column, with on top, a fully mixed water column with height as a variable parameter (Tab. 5.1). This allows modeling of both porewater profiles and concurrent changes in the overlying water inside the benthic chamber.

The concentration in the sediment per volume of liquid (C) of the tracer is described by,

$$\phi \frac{\partial C}{\partial t} = \frac{\partial}{\partial x}\left(\epsilon D_{\mathrm{s}} \phi \frac{\partial C}{\partial x}\right) + \alpha\phi(C_{\mathrm{olw}} - C) \;, \tag{5.1}$$

where D_{s} is the diffusion coefficient in porewater, ϕ is the porosity, t is time after injection of the tracer, x is distance below the sediment-water interface, ϵ is the enhancement of diffusion above molecular diffusion and α is the volume fraction per unit time that is exchanged between the porewater and the overlying water (C_{olw}), due to non-local exchange. Both ϵ and α decreases with depth below the irrigated zone (see details below). Grigg et al. (2005) and Meile et al. (2005) have discussed in detail the limitations to the use of a non-local exchange formulation in muddy, reactive sediments.

The upper boundary of the model is given by the concentration in the overlying water column C_{olw}. The flux across the sediment-water interface takes into account the diffusion at the interface and the integrated mass exchanged by burrow irrigation,

$$J = -\epsilon D_{\mathrm{s}} \phi \left.\frac{\partial C}{\partial x}\right|_{x=0} + \int_0^\infty \alpha\phi(C_{\mathrm{olw}} - C)\, dx \,. \tag{5.2}$$

The concentration in the overlying water is then altered by the flux across the sediment-water interface, and taking into account the height of

water inside the chamber (h),

$$\frac{\partial C_{\mathrm{olw}}}{\partial t} = -\frac{J}{h}\,. \tag{5.3}$$

Typically, irrigation is assumed constant with an enhanced diffusivity of ϵD_{s} or a non-local irrigation rate of α down to the mixed layer depth (L), decreasing exponentially with a e-folding depth of $k_{\epsilon,\alpha}$ below this depth,

$$\epsilon(x) = \begin{cases} \epsilon_{\mathrm{s}} & \text{if } x \leq L\,, \\ \epsilon_{\mathrm{s}} \cdot e^{-(x-L)/k_{\epsilon,\alpha}} & \text{if } x > L\,, \end{cases} \tag{5.4}$$

and analogous for α.

In some non-local irrigation models, the rate decreases exponentially, starting at the sediment-water interface (e.g. Martin and Banta, 1992). In these cases the exchange is most efficient close to the sediment-water interface where the gradients of chemical species are often large and the enhanced diffusion approach would also influence the porewater profiles in a similar way. Our model can be reduced to this approach by setting $L = 0$.

Porosity change with depth is described by,

$$\phi(x) = \phi_\infty + (\phi_{\mathrm{s}} - \phi_\infty)e^{-x/k_\phi}\,, \tag{5.5}$$

where ϕ_∞, ϕ_{s} and k_ϕ are regression parameters, representing respectively the porosity at infinite depth, the surface porosity and the length scale of porosity change.

Initial conditions of the model are ambient concentration in the porewater and ambient concentration of the overlying water homogeneously mixed with a known amount of tracer injected in the chamber.

When a sample is taken from the chamber during the incubation, an equivalent volume of ambient water with tracer concentration C_{bw}, is instantaneously mixed with the water in the chamber,

$$C_{\mathrm{olw},+} = (1 - \frac{V_{\mathrm{s}}}{hA})C_{\mathrm{olw},-} + \frac{V_{\mathrm{s}}}{hA}C_{\mathrm{bw}}\,, \tag{5.6}$$

where $C_{\mathrm{olw},+}$ are the concentration after and $C_{\mathrm{olw},-}$ the concentration before the sampling volume V_{s} is taken from the chamber with height h and surface area A.

Parameters (Tab. 5.1) were selected to represent muddy sediments and two different settings of the irrigation parameter representing the range found from continental shelf seas to the deep-sea (Soetaert et al., 1996b; Meile and Van Cappellen, 2003).

We use Br^- as the inert tracer. Diffusivity of Br^- (D_s) is corrected for tortuosity effects with a formulation representative for muddy sediments(Ullman and Aller, 1982; Soetaert et al., 1996b),

$$D_s = D\phi^2 \ , \tag{5.7}$$

where D is the molecular diffusivity in seawater, adjusted to *in situ* temperature following Boudreau (1997).

5.2.2 Sensitivity and identifiability

Sensitivity analysis is a commonly used method to understand the complex behavior of numerical models. Soetaert et al. (1998) used a Monte Carlo-type sensitivity analysis of a diagenetic model to constrain total mineralization, organic matter reactivity and bioturbation, based on a data-set of oxygen, nitrate, ammonium and particulate organic carbon. While total mineralization rates could be well constrained, this was not the case for organic reactivity and bioturbation because of their correlation. Berg et al. (2003b) used sensitivity analysis of a more elaborate diagenetic model to determine the relative importance of all parameters and found the non-local exchange rate to be the second most influential parameter only surpassed by organic matter reactivity. Bio-irrigation models have also been subjected to sensitivity analysis by e.g. Martin and Banta (1992) and Forster et al. (1999) to optimize incubation time or to identify the most influential parameters of their model. Sensitivity analysis can also be used in a test of near-linear dependence of parameters, where the aim is to find sets of parameters that can be constrained by the available data. This is referred to as identifiability analysis. The outcome of these analyses depends on the model formulations, the types of data available and the time or spatial resolution of this data. Identifiability analysis has been used by Omlin et al. (2001) to characterize a lake model and by Brun et al. (2002) for an activated sludge system, both highly complex models with many parameters.

Model sensitivity analysis was done following Brun et al. (2001). The main features of the technique are briefly repeated here. First sensitivity functions are calculated as,

$$s_{i,j} = \frac{\Delta\theta_j}{sc_i}\frac{\partial y_i}{\partial \theta_j}\,, \tag{5.8}$$

where $s_{i,j}$ is the sensitivity of parameter θ_j to model output corresponding to data point y_i, sc_i is a scaling parameter, which accounts for the case where the measured variables have different units and hence have widely differing values, $\Delta\theta_j$ is a typical value of the absolute uncertainty of the parameter and serves the purpose as a weighting factor and converts the uncertainties to relative numbers.

To rank the parameters according to their relative impact on the model output, a summarizing measure is defined,

$$\delta_j^{\mathrm{msqr}} = \sqrt{\frac{1}{n}\sum_{i=1}^{n} s_{i,j}^2} = \frac{1}{\sqrt{n}}||\mathbf{s}_j||\,. \tag{5.9}$$

To check whether two parameters have a similar sensitivity on the model output their sensitivity functions can be compared graphically and pairwise correlations calculated. If these functions appear different and correlations are low, the parameters are possibly identifiable. However when we are dealing with more than 2 parameters it is necessary to consider the possibility of compensation by linear combinations of parameter sets. Thus a multivariate approach becomes necessary. To test the identifiability, we first normalize the sensitivity functions,

$$\tilde{s}_{i,j} = \frac{s_{i,j}}{\sqrt{\sum_{k=1}^{n} s_{k,j}^2}}, \tag{5.10}$$

and then compute the collinearity index, as defined by Brun et al. (2001),

$$\gamma(\theta) = \frac{1}{\sqrt{\min\left(\mathrm{EV}\left[\tilde{\mathbf{S}}^t\tilde{\mathbf{S}}\right]\right)}}\,, \tag{5.11}$$

where $\tilde{\mathbf{S}}$ is the matrix of normalized sensitivity functions of the parameters in the set and $\tilde{\mathbf{S}}^t$ it's transpose and EV are the eigenvalues.

The collinearity index can be interpreted like this: a value of 1 means that all parameters in the set have a completely different effect on the modeled output corresponding to the data points, whilst a value of 20 means that the change in model results caused by the change of one parameter can be compensated to 95% with a change in other parameters. According to Omlin et al. (2001) serious identifiability problems occur at a value between 10 and 15. We have chosen 10 as reference value above which we will reject a certain sampling design as suitable for estimating all parameters in the parameter set.

Three different sampling layouts will be presented:

- (C) Samples taken from the chamber at 15 time-points, evenly spread over a 72 hour period. Other strategies with fewer time-points were tested, but results were similar and are therefore not presented.
- (P) Samples from 15 depth intervals of the porewater at the end of the experiment, with a thickness of 0.5 cm down to 2 cm depth, 1 cm to 6 cm depth and 2 cm down to a total depth of 20 cm.
- (C+P) A combination of both the chamber and porewater samples.

This was done with the two different irrigation settings, representative for deep sea (**D**) and shallow (**S**) sediments resulting in six numerical experiments in total.

Uncertainties ($\Delta\theta_j$) of all parameters were set to 10% in the absence of more detailed information. Note that the choice of absolute uncertainties $\Delta\theta_j$ only affects the magnitude of the relative sensitivities and hence the ranking of the parameters, but does not affect the collinearity index, $\gamma(\theta)$, because of the normalization of the matrix of sensitivity functions (Brun et al., 2001). Nevertheless, if this technique is applied to a site-specific study, it is useful to incorporate previous knowledge about the uncertainties of each parameter to derive a correct ranking of parameter influence. Scaling factors of the observed data (sc_i) are set to unity.

5.2.3 Bayesian inference

Bayesian techniques (Gelman et al., 2003) are well-suited to calculate parameter uncertainty for nonlinear models such as the bio-irrigation model

used here. Bayesian inference differs from classical statistical techniques such as Maximum Likelihood Estimation, which includes the least-squares technique as a special case, in that both parameters and observed values are treated as random variables and probability distributions can be calculated for all of them. The probabilities of the parameters, given observed data and prior knowledge are found from Bayes' rule,

$$p(\theta|y_{\text{obs}}) = \frac{p(\theta)p(y_{\text{obs}}|\theta)}{p(y_{\text{obs}})}\,, \tag{5.12}$$

where θ is the parameter vector, $p(\theta)$ is the *prior* distribution of the model parameters, y_{obs} are observed data, $p(y_{\text{obs}}|\theta)$ is the likelihood of the observed values, given the model and the parameter vector θ, and $p(\theta|y_{\text{obs}})$ is the *posterior* distribution of the parameters, i.e. the probability of the parameter vector given the data.

A Bayesian analysis is always an updating of existing knowledge with new data. Thus, prior knowledge about the parameter values is incorporated in the prior distribution ($p(\theta)$), whilst the uncertainty in the data is represented by the distribution ($p(y_{\text{obs}})$), either as standard deviations for each data point, or as a variance-covariance matrix, which takes into account the co-variation of data variables. In the case where little information is available for parameters, a uniform distribution can be used where only the lower and upper limits are given. We have chosen uniform distributions for parameters to only restrict the parameters to physically meaningful values without giving any particular value in this range a higher probability.

To calculate the posterior distribution of parameters ($p(\theta|y_{\text{obs}})$), a computational technique known as Markov Chain Monte Carlo (MCMC) was used (Gilks et al., 1996). MCMC simulates values from the posterior parameter distribution. The result of this simulation can be directly evaluated with histograms or density plots, or statistical properties such as median and standard deviations can be calculated to quantify the uncertainty in estimated parameter values. However, one must ensure that the simulation has been run long enough to reach a stationary distribution covering the posterior with a chosen accuracy. To check that simulations were run long enough we used the criteria given by Raftery and Lewis (1996) implemented in the R package `coda` (Plummer et al., 2006).

For the Bayesian inference two different data-sets were used. Forster et al. (2003), measured porewater concentrations at the end of a bio-irrigation experiment using Br^- as an inert tracer. The data-set selected from this paper is the one that was collected in August, 1989 in the German Bight, southern North Sea, where five replicate cores were sliced in 18 intervals with a thickness of 0.5 cm down to 3 cm depth, 1 cm down to 10 cm and 2 cm down to a total depth of 20 cm. The duration of the experiment was 95 hours. The variance-covariance structure of the data-points at each depth interval was calculated from the five replicate cores and used in the calculation of the model likelihood (Eq. (5.12)) . This data-set will be referred to as Porewater.

A second data-set was obtained from an *in situ* experiment using the Göteborg lander, at station PV1 (59°35.14′N,23°28.23′E) in the Gulf of Finland, Baltic Sea. The operation of this lander is described in Stahl et al. (2004b). Br^- was again used as an inert tracer, and sampled from the chamber at nine different times during the incubation lasting 30 hours. Sample extraction volumes were 60 mL at each time since samples were taken not only for bromide but also for several other solutes. Samples were filtered through 0.45 μm filters before storage. The samples were subsequently measured by anion-chromatography with electro-chemical detection (DIONEX P850, ED40). A standard deviation of 30 mmol m^{-3} was estimated from the analytical precision (RSD <2 %). This data-set will be referred to as Chamber.

The parameters used for both applications are found in Table 5.4. Parameters ϵ, α and h in the second case, were assigned prior distributions. All other parameters were assumed to be known.

5.2.4 Implementation

The partial differential equation (5.1) is solved numerically (Soetaert et al., 1996b) where the sediment is subdivided into 100 layers with a thickness of the top-layer of 0.05 cm and each layer increasing in thickness with 3 %, reaching a total depth of 30 cm. To maintain a sufficient numerical precision the integration was done by the Bulirsch-Stoer (Stoer and Bulirsch, 1983) routine, an implicit integration routine that is well adapted to solve stiff differential equations.

The model, sensitivity analysis and Bayesian inference were all imple-

Table 5.1: Parameters of the tracer model

		Value		
θ_j	Unit	Shallow	Deep	Description
Unknown parameters				
ϕ_s	-	0.9	0.9	Porosity at surface
ϕ_∞	-	0.7	0.7	Porosity at depth
k_ϕ	cm	0.5	0.5	Porosity attenuation
ϵ_s	-	6.0	1.1	Diffusion enhancement
α_s	h^{-1}	0.05	0.001	Non local exchange
L	cm	10	10	Mixed layer depth
$k_{\epsilon,\alpha}$	cm	1	1	Enhancement attenuation
h	m	0.2	0.2	Height of chamber
Known parameters				
Add	mmol	24	24	Amount of tracer added
T	°C	15	4	Temperature
A	m^2	0.04	0.04	Surface area of chamber
C_{bw}	mmol m^{-3}	0	0	Ambient concentration

mented in Fortran using the FEMME environment (Soetaert et al., 2002) with the output visualization facilitated by the R package (R Development Core Team, 2007). Both the model and the visualization tools are available from the authors on request.

5.3 Results and discussion

5.3.1 Sensitivity functions

In order to uniquely estimate several parameters from a given data-set, they should have a different impact or sensitivity on the model results. The meaning of a sensitivity function is exemplified in Figure 5.1, where the model has been run with and without irrigation (A,B) and with two different heights of the benthic chamber (C,D). The differences between these model outputs, emphasized by the arrows in the figure, are examples of sensitivity functions. When the model is run with irrigation, and compared to a run without irrigation, there is no change in the initial concentration since this value is only determined by the physical dimensions and the amount of tracer. After some time however, the concentration in the overlying water is lower than without irrigation since more tracer is displaced into the porewater (Fig. 5.1A). Thus, an increase in the irrigation leads to a decrease in the concentration, hence the negative sign on the sensitivity function (Fig. 5.1B). It is also apparent that the influence of irrigation increases with time, at least until the time is reached when the tracer is distributed homogeneously across the entire depth of the core. An increase in the height of the overlying water increases the volume and with a fixed amount of tracer the added concentration becomes lower, i.e. again a negative sign on the sensitivity (Fig. 5.1C,D). A lower concentration in the overlying water also implies a smaller gradient between overlying water and porewater, resulting in a slightly smaller tracer flux. This causes the small change over time in the sensitivity (Fig. 5.1D). It is also important to look at the magnitude of the sensitivity functions. A 10 % change in the height has a much larger influence than a similar change in the irrigation rate.

Sensitivity functions for all parameters and for deep-sea settings are shown for a time series of tracer concentration in the chamber in Figure 5.2

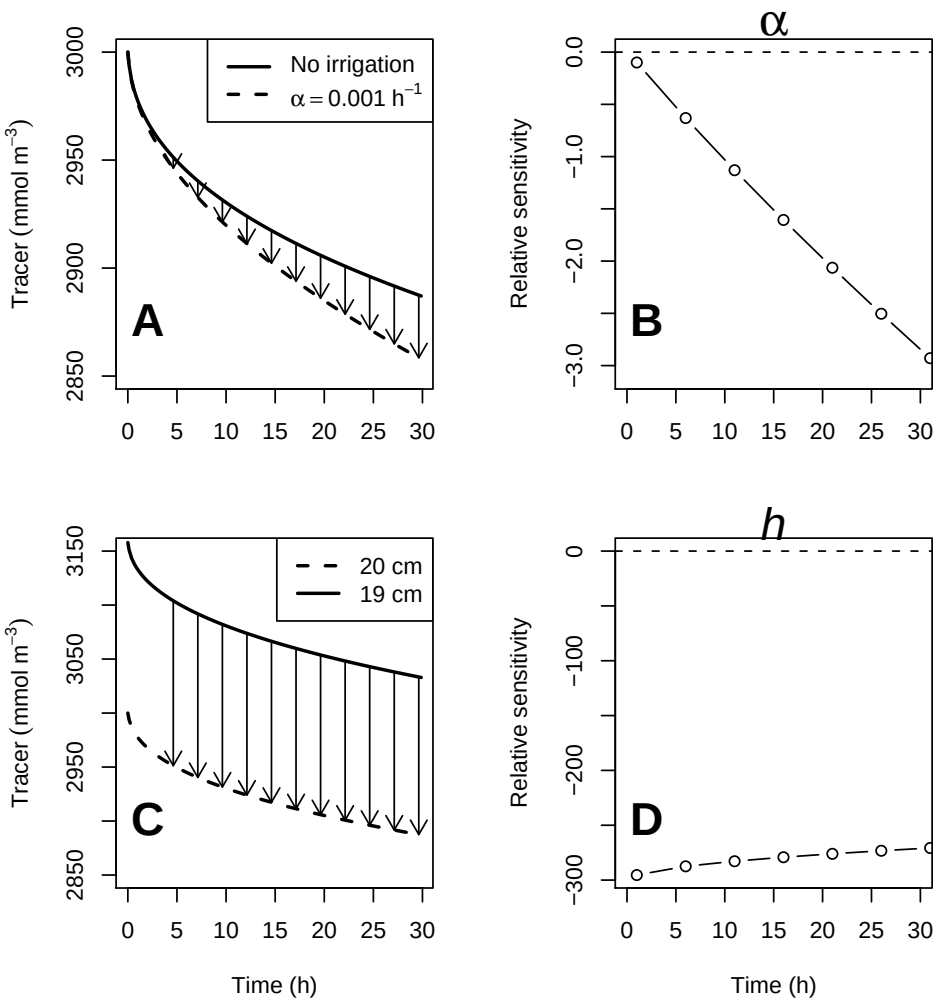

Figure 5.1: The sensitivity of a parameter is the change in the model output caused by a small change in the parameter. This is exemplified by comparing the modeled tracer concentration in the benthic chamber without irrigation and with $\alpha = 0.001$ h^{-1} (**A**) and the corresponding sensitivity function (s_α)(**B**) or by changing the height of the overlying water (**C**) and the corresponding sensitivity (s_h)(**D**).

and for a vertical profile in the sediment in Figure 5.3. The sensitivity of all parameters on the tracer concentration in the chamber is negative, meaning that an increase in the parameter value, yields a decrease in the concentration. The absolute sensitivity of all parameters except the height over the overlying water in the chamber (h) increases over time, whereas the absolute sensitivity of h decreases slightly over the course of incubation (Fig.5.2). This suggests that it will be difficult to estimate several parameters since the sensitivities are so similar.

The sensitivities of the various parameters on the tracer concentration in the sediment are much more dissimilar and show patterns that are more or less intuitive (Fig.5.3). Porosity at the surface, ϕ_s has a positive sensitivity in the surface layers and no impact at the lower part, whereas ϕ_∞ has a negative sensitivity at the top, positive at intermediate and zero in the lower part. A higher porosity means increased transport due to a larger exchange surface and a less tortuous path. Thus a higher surface porosity increases the flux from the chamber to the surface sediment, elevating the concentration in the top sediment layers and lowering it in the chamber. A higher porosity at infinite depth increases the flux from the surface layers to deeper layer, thereby decreasing the concentration in the surface layers and increasing it deeper down. The sensitivity of the mixed layer depth, L, is most prominent at the depth of L and decreases rapidly with distance. Chamber height, h, has a negative sensitivity at the top, mirroring the tracer concentration profile.

The two most interesting parameters in the context of bio-irrigation are ϵ and α, and because of their different mechanistic nature the sensitivities of these parameters on the tracer concentration in the porewater are different in two ways. The sensitivity of ϵ is always positive and is limited to the top layers in contrast to α which is negative in the top layer and has a positive sensitivity in deeper layers. The magnitude and depth range of these sensitivity functions also depends on the time when the experiment is terminated (Fig. 5.4), as a result of deeper penetration of the tracer into the sediment. Nevertheless, the influence of the two bio-irrigation parameters on the tracer concentration profile in the sediment remains different. These results show that the sensitivity of these parameters are not strongly linearly dependent and indicates the potential ability to constrain both of them based on observed porewater profiles. However, as there are more unknown parameters, this can be deceiving, and we need

to test the possibility of a linear combination of several parameters affecting the model in a similar way. First we discuss the overall or average impact of all parameters.

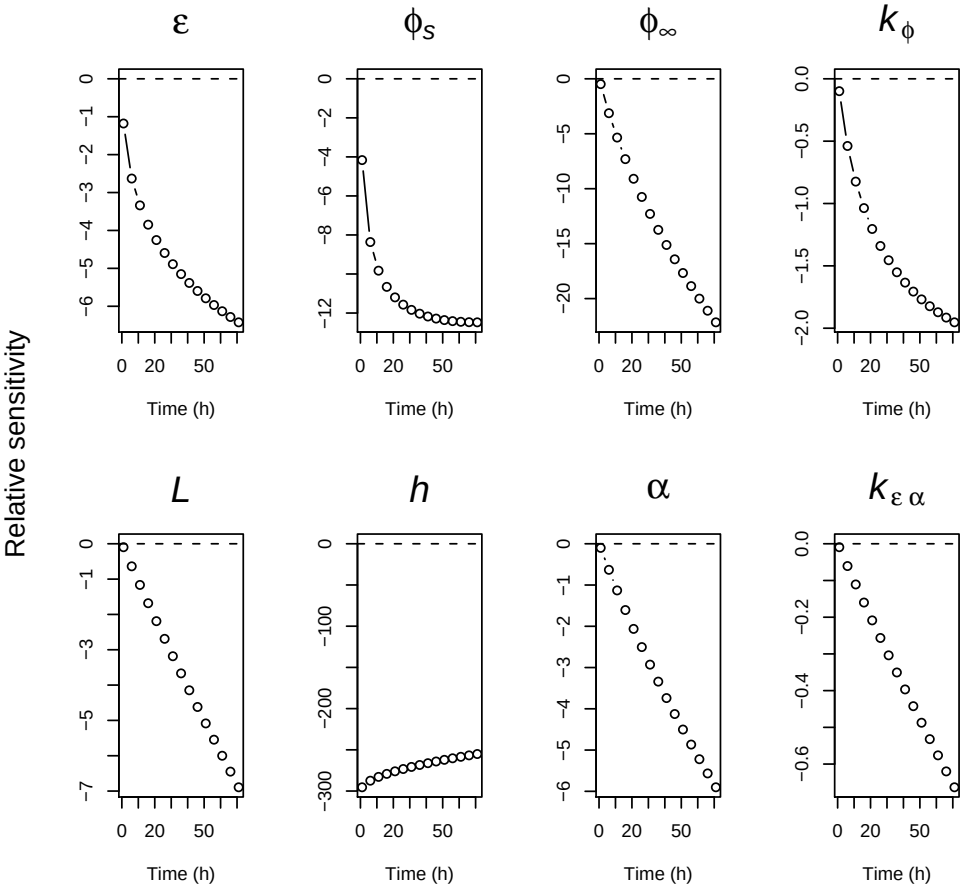

Figure 5.2: Sensitivity functions of model output of the tracer concentration in the overlying water with parameters in deep sea settings (sampling layout **D** C). A negative relative sensitivity implies that an increase in the parameter value lowers the tracer concentration. Parameter names and values are found in Table 5.1

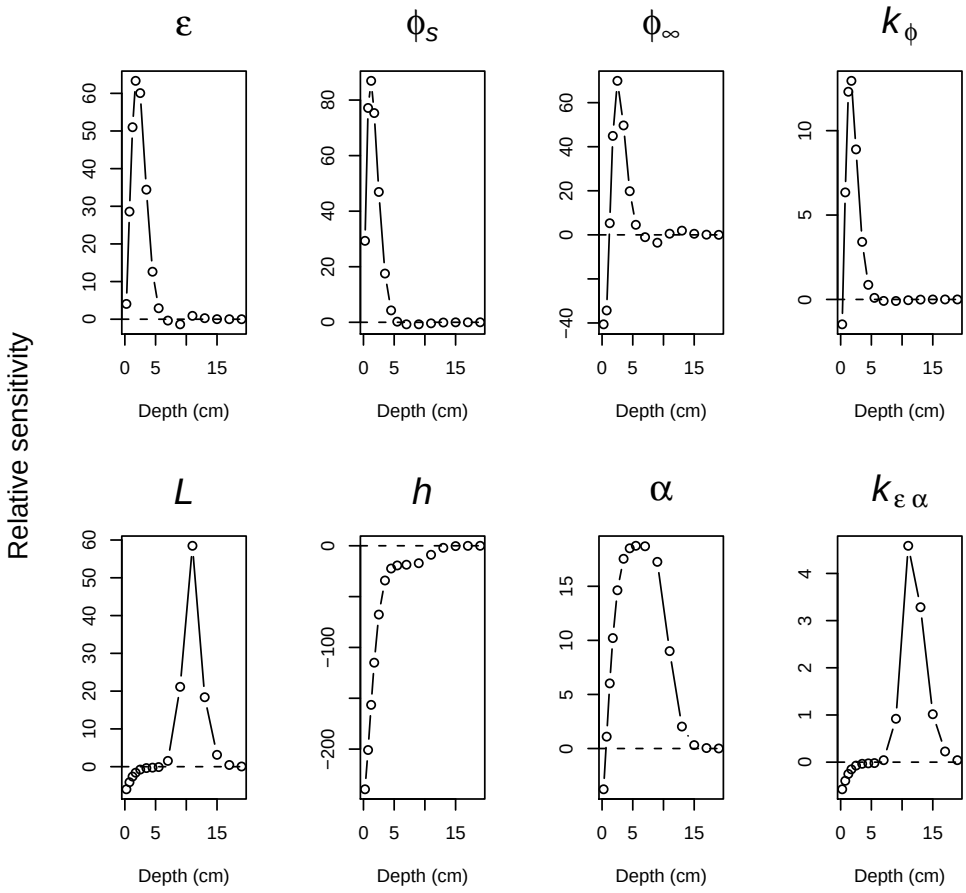

Figure 5.3: Sensitivity functions of model output of the tracer concentration in the sediment after 72 hours of the experiment with parameters in deep sea settings (sampling layout **D** P). A negative relative sensitivity implies that an increase in the parameter value lowers the tracer concentration. Parameter names and values are found in Table 5.1.

5.3.2 Sensitivity ranking

The total impact of each parameter (defined in Table 5.1) is estimated by the sensitivity measure defined in equation (5.9).

The parameter with the largest impact in all model experiments is h, the height of the overlying water. As a fixed amount of tracer is injected in the chamber the height directly determines the initial concentration in the chamber. Therefore this parameter affects the output from the start, as can be seen in Figure 5.2: the sensitivity function immediately has a very negative value which decreases slightly in importance afterwards. The next most important parameters, are ϕ_s or ϕ_∞. Of intermediate importance are the irrigation parameters, ϵ, α and L. Two parameters with very limited influence are $k_{\epsilon,\alpha}$ and k_ϕ, the parameters that represent the depth attenuation of ϵ, α and ϕ respectively. $k_{\epsilon,\alpha}$ has the least impact of all parameters in all model experiments. This limited sensitivity of bio-irrigation models to $k_{\epsilon,\alpha}$ indicates that detailed knowledge of the depth distribution of irrigation is difficult to derive using only one tracer.

Table 5.2: Sensitivity ranking based on δ_j^{msqr} (Eq. 5.9) of the model parameters. **D** and **S** refer to shallow and deep parameter settings (Tab. 5.1) and C, P and C+P are different sampling strategies, with either data from chamber, porewater or a combination.

Parameter	**D** C	**D** P	**D** C+P	**S** C	**S** P	**S** C+P
h	271	97.6	203.4	268	101	203
ϕ_∞	14.5	29.1	22.9	16.3	31.3	25.0
ϕ_s	11.3	38.8	28.6	11.7	36.7	27.2
ϵ	4.98	28.8	20.6	5.50	28.9	20.8
L	4.17	16.9	12.3	4.13	16.2	11.8
α	3.67	11.9	8.87	3.58	11.4	8.46
k_ϕ	1.48	5.50	4.02	1.63	5.61	4.13
$k_{\epsilon,\alpha}$	0.40	1.51	1.11	0.40	1.64	1.07

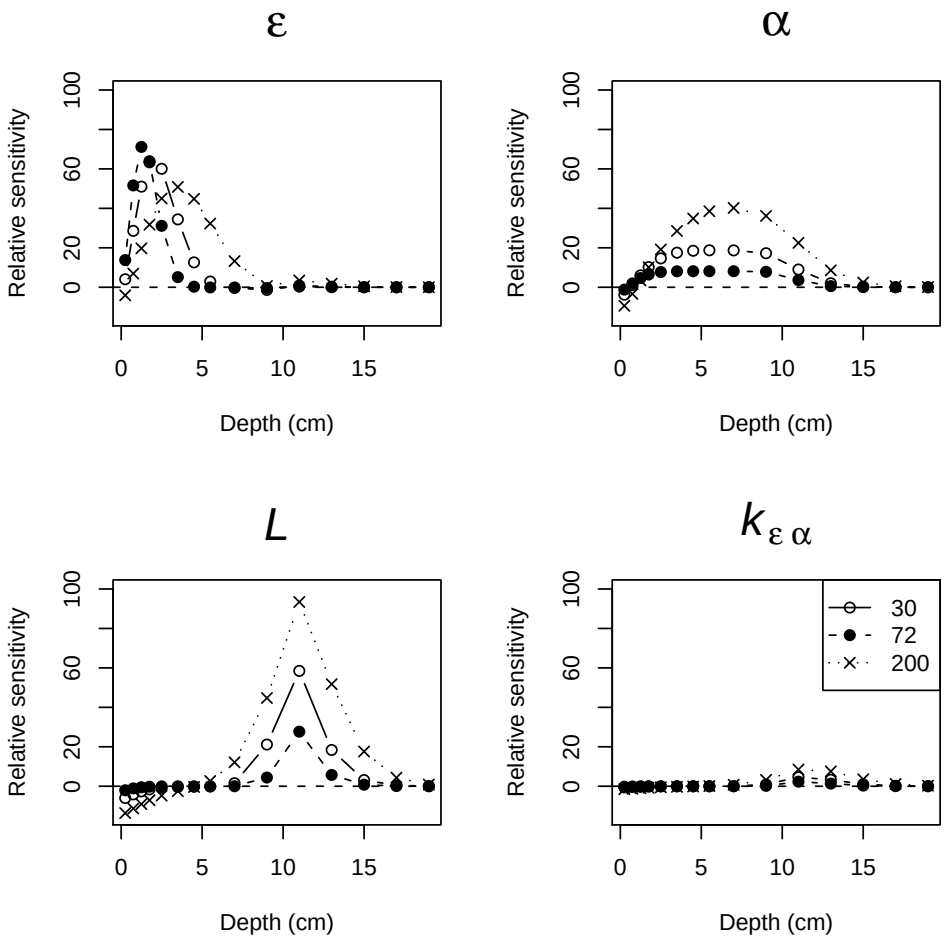

Figure 5.4: Influence of incubation time and sediment depth on sensitivity functions of parameters, directly related to bio-irrigation, after 30, 72 and 200 hours using parameters in deep sea settings (sampling layout **D** P). A positive relative sensitivity implies that an increase in the parameter value increases the tracer concentration. Parameter names and values are found in Table 5.1.

5.3.3 Identifiability

Table 5.3: Collinearity indices of six different sampling layouts. **D** and **S** refer to shallow and deep parameter setttings (Tab. 5.1) and C, P and C+P are different sampling strategies, with either data from chamber, porewater or a combination. Bold numbers indicate a non-identifiable combination of parameters, i.e. a collinearity index above 10.

No.	Parameters	**D** C+P	**D** C	**D** P	**S** C+P	**S** C	**S** P
2	ϵ ϕ_s	3.10	**10.7**	3.11	2.90	9.67	2.90
2	ϵ ϕ_∞	1.69	7.42	1.69	1.76	7.86	1.76
2	ϵ L	1.01	5.43	1.03	1.01	5.46	1.03
2	ϵ h	1.03	4.22	1.70	1.03	4.19	1.67
2	ϵ α	1.49	6.00	1.46	1.57	6.11	1.53
2	ϕ_s ϕ_∞	1.23	4.41	1.16	1.24	4.35	1.16
2	ϕ_s L	1.01	3.63	1.05	1.01	3.52	1.06
2	ϕ_s h	1.01	6.12	2.64	1.01	6.40	2.66
2	ϕ_s α	1.28	3.88	1.23	1.29	3.77	1.24
2	ϕ_∞ L	1.07	**18.8**	1.01	1.08	**16.6**	1.01
2	ϕ_∞ h	1.28	2.80	1.05	1.29	2.83	1.04
2	ϕ_∞ α	1.60	**29.3**	1.50	1.69	**25.7**	1.59
2	L h	1.13	2.52	1.04	1.14	2.52	1.05
2	L α	1.25	**51.6**	1.20	1.27	**46.7**	1.23
2	h α	1.09	2.62	1.16	1.09	2.62	1.16
3	ϵ ϕ_s ϕ_∞	5.37	**431**	**23.3**	5.00	**412**	**20.6**
3	ϵ ϕ_s L	3.10	**94.6**	3.12	2.90	**78.0**	2.91
3	ϵ ϕ_s h	3.11	**19.2**	4.81	2.91	**17.9**	4.55
3	ϵ ϕ_s α	3.44	**140**	3.62	3.33	**116**	3.50
3	ϵ ϕ_∞ L	1.73	**54.8**	1.70	1.80	**50.3**	1.78
3	ϵ ϕ_∞ h	2.17	**19.4**	5.53	2.31	**21.2**	5.89
3	ϵ ϕ_∞ α	1.71	**87.8**	1.69	1.79	**79.4**	1.77
3	ϵ L h	1.13	**13.4**	1.70	1.14	**13.5**	1.67
3	ϵ L α	1.72	**126**	1.67	1.86	**114**	1.80
3	ϵ h α	1.56	**15.0**	1.92	1.64	**15.4**	1.97
3	ϕ_s ϕ_∞ L	1.26	**49.0**	1.18	1.28	**43.5**	1.19

Table 5.3: *(continued)*

No.	Parameters	**D** C+P	**D** C	**D** P	**S** C+P	**S** C	**S** P
3	ϕ_s ϕ_∞ h	1.45	**11.7**	3.53	1.47	**11.9**	3.52
3	ϕ_s ϕ_∞ α	1.61	**81.2**	1.52	1.69	**71.7**	1.61
3	ϕ_s L h	1.13	**10.1**	2.64	1.14	**10.2**	2.66
3	ϕ_s L α	1.47	**114**	1.42	1.52	**102**	1.47
3	ϕ_s h α	1.32	**10.6**	2.68	1.33	**10.7**	2.71
3	ϕ_∞ L h	1.29	**29.4**	1.06	1.31	**26.4**	1.06
3	ϕ_∞ L α	1.70	**403**	1.63	1.82	**327**	1.76
3	ϕ_∞ h α	1.72	**46.7**	1.70	1.83	**41.5**	1.78
3	L h α	1.25	**77.0**	1.34	1.28	**69.6**	1.37
4	ϵ ϕ_s ϕ_∞ L	5.48	**635**	**23.3**	5.11	**657**	**20.7**
4	ϵ ϕ_s ϕ_∞ h	**13.4**	**435**	**150**	**12.7**	**421**	**132**
4	ϵ ϕ_s ϕ_∞ α	5.38	**584**	**24.7**	5.01	**593**	**21.9**
4	ϵ ϕ_s L h	3.12	**137**	4.83	2.92	**118**	4.57
4	ϵ ϕ_s L α	3.53	**1750**	3.66	3.47	**1250**	3.59
4	ϵ ϕ_s h α	3.53	**196**	5.62	3.42	**173**	5.34
4	ϵ ϕ_∞ L h	2.17	**110**	5.54	2.31	**107**	5.90
4	ϵ ϕ_∞ L α	1.73	**569**	1.71	1.86	**481**	1.81
4	ϵ ϕ_∞ h α	2.19	**192**	5.95	2.33	**183**	6.30
4	ϵ L h α	1.74	**193**	1.99	1.88	**175**	2.10
4	ϕ_s ϕ_∞ L h	1.45	**82.5**	3.54	1.47	**74.6**	3.53
4	ϕ_s ϕ_∞ L α	1.74	**581**	1.69	1.87	**491**	1.84
4	ϕ_s ϕ_∞ h α	1.72	**150**	3.85	1.83	**135**	3.83
4	ϕ_s L h α	1.47	**160**	2.69	1.52	**141**	2.74
4	ϕ_∞ L h α	1.88	**464**	1.91	2.05	**386**	2.07
5	ϵ ϕ_s ϕ_∞ L h	**13.4**	**5050**	**154**	**12.7**	**4650**	**136**
5	ϵ ϕ_s ϕ_∞ L α	5.51	**1890**	**24.7**	5.18	**1930**	**22.0**
5	ϵ ϕ_s ϕ_∞ h α	**13.4**	**2450**	**155.2**	**12.7**	**2280**	**133**
5	ϵ ϕ_s L h α	3.60	**1760**	5.69	3.54	**1450**	5.46
5	ϵ ϕ_∞ L h α	2.19	**1090**	5.98	2.34	**952**	6.35
5	ϕ_s ϕ_∞ L h α	1.88	**1100**	3.88	2.06	**951**	3.88
6	ϵ ϕ_s ϕ_∞ L h α	**13.4**	**40300**	**165**	**12.8**	**36300**	**140**

The collinearity indices for various parameter combinations (Tab. 5.3) differ dramatically between the sampling layouts C on the one hand and C+P and P on the other hand, but not between deep-sea and shallow-water sediments, irrespective of their contrasting parameter settings. On the basis of a collinearity criterion of 10, chamber time-series data alone can be used to constrain at most two parameters. The difference between C+P and P is not so large. These sampling strategies allow the estimation of up to five of the six desirable parameters. However both irrigation and porosity parameters can be estimated when the combination of chamber time-series and a sediment profile are available, but not based on sediment data alone. The reason for this is that the loss of tracer in the overlying water is necessarily recovered by the total inventory in the sediment. Thus, by comparison with the profile, the porosity can be estimated irrespective of the amount of irrigation. Note that, as porosity is normally obtained from independent measurements and imposed via equation (5.5) rather than estimated from the tracer data, both sampling strategies (P or C+P) provide the necessary information. Moreover, as the water column height in all core incubations and some chamber deployments is known this will also decrease the number of unknown parameters.

5.3.4 Application to measured data

Additional to the identifiability problem, there is measurement error, and this can be rather large compared to the concentration change in the chamber during the incubation, or vertically in the sediment. This error is incorporated in the Bayesian analysis which besides providing the parameters values that best fit the observed data, also provides error margins on all estimated parameters.

The model fit to the Chamber data-set is shown in Figure 5.5 together with the posterior parameter distribution of ϵ, α and h. The fit of the model to the observed data is reasonable and representative of previous experiments found in the bio-irrigation literature (e.g Forster et al., 1999; Rao and Jahnke, 2004). The jagged look of the model output is due to the sampling at discrete times, which reduces the concentration of the tracer in the chamber. Note that this reduction is of similar magnitude as the infiltration of the tracer in the sediment.

The posterior parameter distributions are summarized in Table 5.5.

Except for the chamber height, the posterior parameter estimates have skewed distributions with long tails toward higher values. Thus, the irrigations values (ϵ,α) with highest probability are low, implying that transport is dominated by molecular diffusion. This was expected for this sediment where no macrofauna is present. However the uncertainties in these bio-irrigation parameters are quite high for any useful interpretation. The prime reason for injecting the tracer in this case, was to determine the water height and this can be estimated with reasonable precision (28±1 cm). A reliable estimate of chamber height is desirable as any uncertainty in h directly translates to uncertainties in the fluxes of all chemical species measured with the chamber technique.

The model fit to the Porewater data-set shown in Figure 5.6 constrains the posterior distribution of the bio-irrigation parameters to a much larger extent (Tab. 5.5). With an enhancement factor in the order of 8±2 there is no doubt that transport is enhanced above molecular diffusion. The magnitude of non-local irrigation is rather low ($2.3{\cdot}10^{-4}\,\mathrm{h}^{-1}$), which is equivalent to replacing the porewater in the irrigated zone about twice a year. Based on this set of profiles, we are thus able to constrain both the magnitude of diffusion enhancement (ϵ) and non-local irrigation (α). The posterior parameter distributions of the bio-irrigation parameters can then be fed into a more general diagenetic model to calculate the uncertainties in the rates of all other biogeochemical processes. Note that, if transport is dominated by non-local exchange it may not be sufficient to use the estimated value of α for all chemical species, since the non-local exchange model only approximates a three-dimensional model, when reaction kinetics are very simple. It has been shown recently by Grigg et al. (2005) and also by Meile et al. (2005) that α may differ among chemical species. On the one hand there are components such as silicate, which are, once produced, relatively inert in the sediment and then the non-local approach (Emerson et al., 1984) applies. On the other hand there are reactive components such as aqueous Fe^{2+}, which are both produced and consumed and for which more complex mechanistic approaches are required.

5.3.5 Experimental considerations

Conducting experiments in general and bio-irrigation experiments in particular always involves compromises. Working *in situ* is generally considered to be superior to retrieving cores for measuring benthic fluxes as it avoids decompression artifacts which are known to be important at depths > 1000 m (Epping et al., 2002). However for bio-irrigation measurements, it is necessary to sample the porewater at the end of the experiment and this may be difficult under *in situ* conditions. If the lander is unable to retrieve the incubated sediment undisturbed, the *in situ* approach is not very satisfactory. A general advantage of benthic landers is however that the surface area usually is large enough to accommodate the benthic inhabitants in a more natural way than in cores.

One of the crucial parameters in our model was the height of the incubation chamber. To eliminate the problem of estimating the height of a core sufficiently accurate we emphasize the approach used by Berg et al. (2001), where cores are submerged in a big tank and where the tracer is added to the tank. The decrease in tracer concentration of overlying water will then be negligible and the height will not have the same importance as in a traditional incubation. Keeping the concentration at a constant level will also maximize the signal in the porewater.

Sampling the porewater at the end of the incubation improves the parameter estimation considerably. It is likely that the estimate from the chamber-only data would improve with longer incubation times (if oxygen is kept at ambient concentration). However, to optimally constrain all parameters it is not sufficient to sample the porewater only at the end, but it is also necessary to sacrifice cores at multiple times since the maximal sensitivity is reached at different times for the various relevant parameters. This is illustrated in Figure 5.7. The summarized sensitivity on the concentration in the porewater (Eq. (5.9)) of the bio-irrigation parameters α, ϵ, peak at 400–600 and 30–50 hours respectively while L and $k_{\epsilon\ \alpha}$ never reach an optimum during 1000 hours of incubation using the two parameter settings in Table 5.1. Thus while the duration of the experiment can be optimized with respect to the expected rates, multiple time-points of porewater profiles are required to identify and constrain the mechanism of bio-irrigation.

Table 5.4: Fixed parameters of the tracer model for the two bayesian applications, Chamber refer to where data were only available from the benthic chamber (Andersson, unpublished) and Porewater where the data from Forster et al. (2003) were used.

	Unit	Porewater	Chamber	Description
ϕ_s	-	0.52	0.93	Porosity at surface
ϕ_∞	-	0.44	0.83	Porosity at depth
k_ϕ	cm	0.3	2.9	Porosity decay coefficient
L	cm	10	10	Mixed layer depth
$k_{\epsilon,\alpha}$	cm	7	7	Enhancement decay coefficient
h	cm	10	-	Height of chamber
Add	mmol	14	17.1	Amount of tracer added
T	°C	16	2.5	Temperature
A	cm^2	78.5	400	Surface area of chamber
C_{bw}	μM	0	260	Ambient concentration

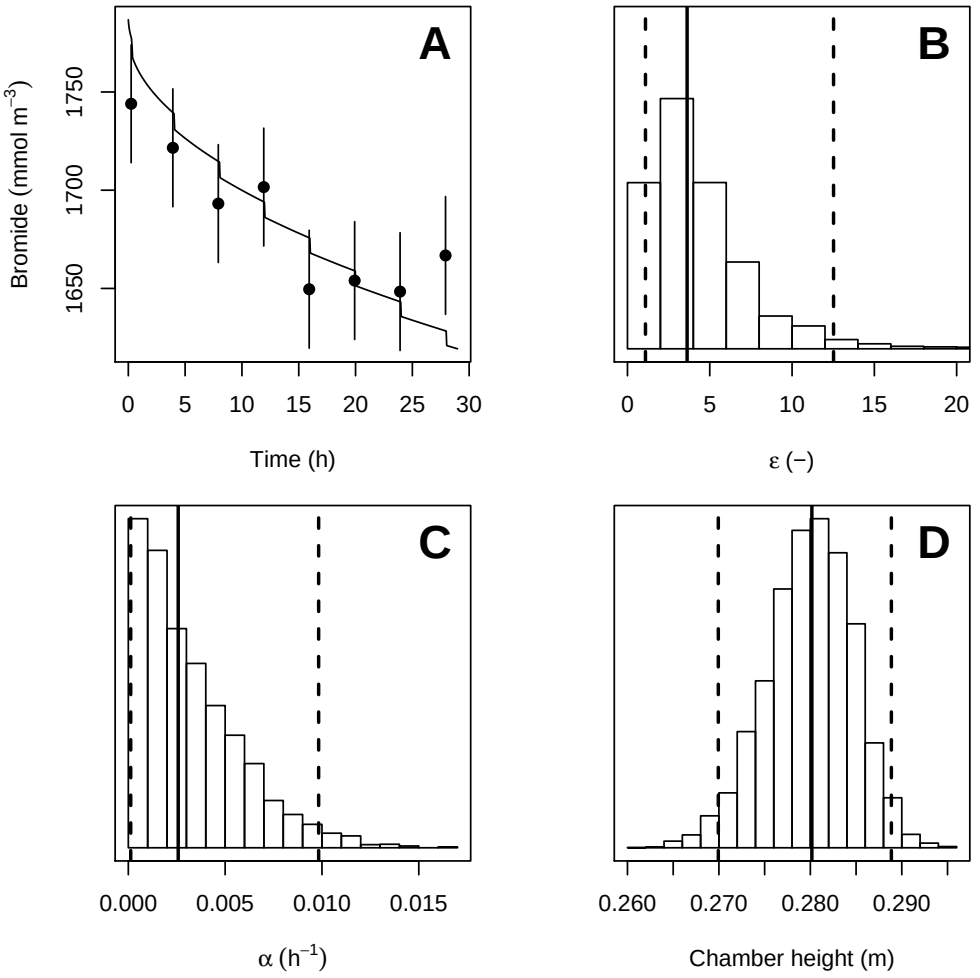

Figure 5.5: Observed values from an *in situ* chamber incubation (Andersson *et al*, unpublished data) where the line shows modeled results (**A**). Panel **B-D** show histograms and lines indicating the median and lower and higher end of the 95% credible interval of parameters ϵ, α and h, respectively.

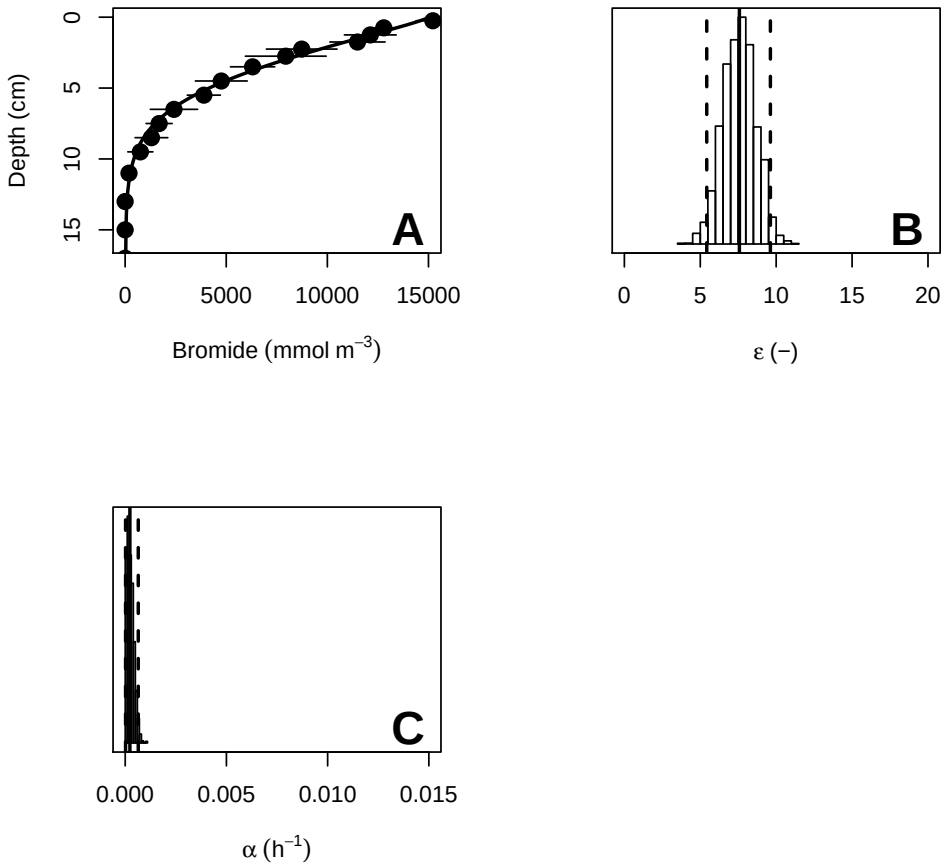

Figure 5.6: Observed porewater data from a retrieved core incubation (Forster et al., 2003), where the lines shows modeled results (**A**). Panel **B-C** show histograms and lines indicating the median and lower and higher end of the 95% credible interval of parameters ϵ and α, respectively. Note that the same scale of the parameter distributions has been used as in Figure 5.5.

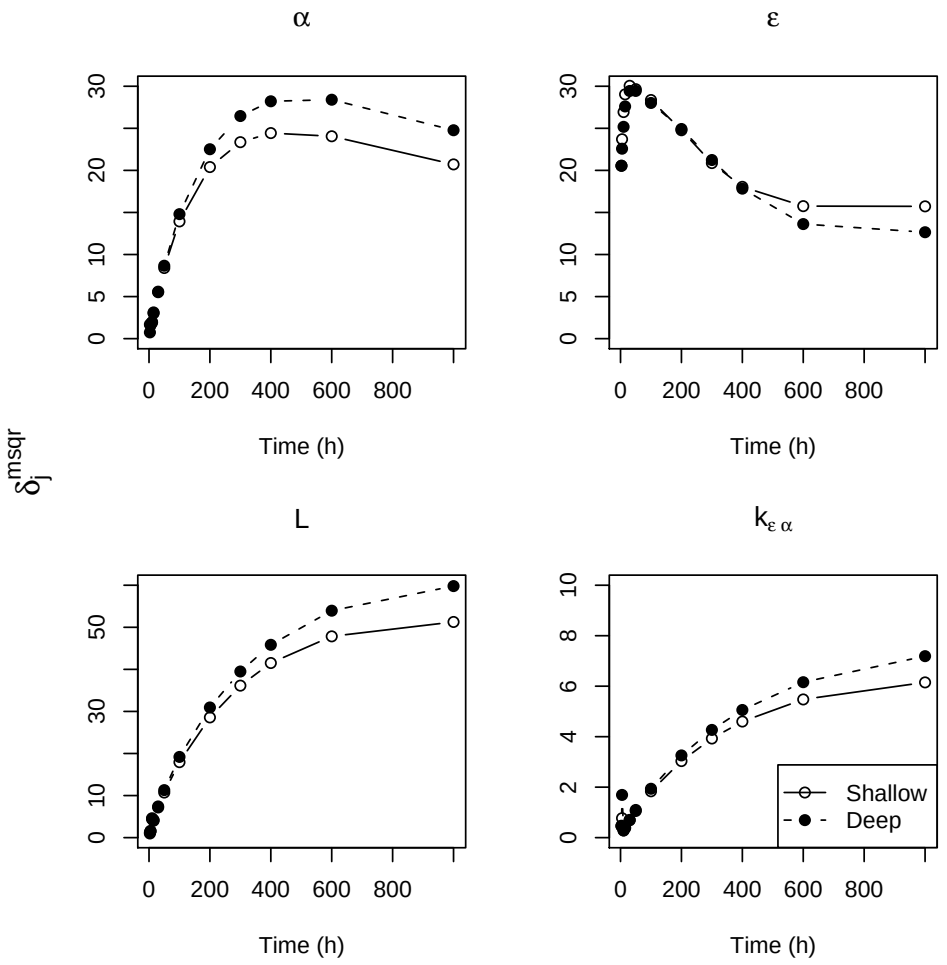

Figure 5.7: The summarized sensitivity based on δ_j^{msqr} (Eq. 5.9) on the modeled tracer concentration in the porewater reaches optimal values at different times. Shallow and deep refer to the two parameter sets in Table 5.1. All functions start at 3 hours, which is considered to be a minimum time to integrate irregular animal behavior (Forster et al., 1999).

Table 5.5: Prior and posterior distributions of parameter values. Prior distributions are uniform distribution. Reported values of the posterior distributions are median and the limits of the 95% credible interval, calculated as quantiles from the MCMC simulated values.

	Prior		Posterior		
Parameter	Min	Max	Median	Lower	Upper
Chamber data					
ϵ	1	100	3.5	1.1	12
α	0	0.1	$2.5{\cdot}10^{-3}$	$1.2{\cdot}10^{-4}$	$9.8{\cdot}10^{-3}$
h	0.15	0.4	0.28	0.27	0.29
Porewater data					
ϵ	1	100	7.6	5.4	9.6
α	0	0.1	$2.3{\cdot}10^{-4}$	$1.7{\cdot}10^{-5}$	$6.4{\cdot}10^{-4}$

5.4 Conclusions

We have demonstrated the usefulness of identifiability analysis and Bayesian uncertainty analysis, previously not used in the field of diagenetic modeling. On the one hand, identifiability analysis may prove its worth during the experimental design stage of research, before models are used for the interpretation of the data. It allows testing whether a certain data set is sufficiently accurate for the estimation of the unknowns. On the other hand, Bayesian uncertainty analysis aids in the interpretation of measured data and allows derivation of realistic uncertainties. This analysis could also serve to estimate the precision of the measurements that would give a pre-defined accuracy of parameters.

Besides introducing techniques new to this field, we have also obtained specific results about bio-irrigation models. The most influential parameters of such models are the height of the overlying water, followed by the porosity and then by the parameters of irrigation. In order to constrain the rate and mechanism by which bio-irrigation occurs, it is necessary to perform incubations where the sediment can be sampled at the end. The identifiability analysis revealed that tracer concentration changes in the overlying water during the incubation do not provide enough information on the mode of bio-irrigation but provide sufficient information to tightly constrain the height of the overlying water.

6 Evaluation of a life time based optode to measure oxygen in aquatic systems

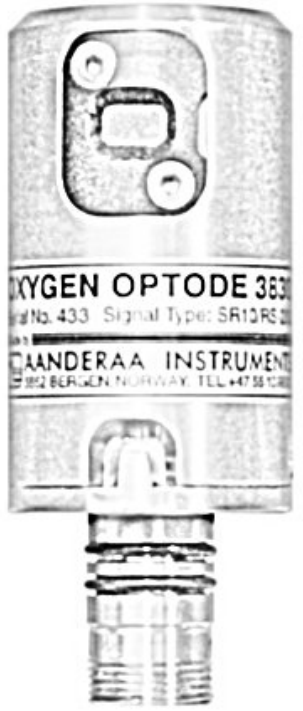

Anders Tengberg, Jostein Hovdenes, **Johan Henrik Andersson**, Olivier Brocandel, Robert Diaz, David Hebert, Tony Arnerich, Christian Huber, Arne Körtzinger, Alexis Khripounoff, Francisco Rey, Christer Rönning, Jens Schimanski, Stefan Sommer and Achim Stangelmayer, 2006, *Limnology and Oceanography: Methods*, 4:7-17

6.1 Introduction

Most chemical and biological processes are influenced by changes in dissolved oxygen concentrations. Oxygen is therefore a prime parameter to measure in a variety of applications ranging from industrial processes to environmental studies.

The standard method to analyze oxygen content in water is a two-step wet chemistry precipitation of the dissolved oxygen followed by a titration. The method was first described by Winkler (1888) and has since then remained the overall standard. Winkler titration is a method which is almost always performed in the laboratory on collected water samples. The collection and handling of water samples can induce errors and the analytical work is time consuming and demands meticulous care. It is therefore not a suitable method to obtain *in situ* data with high spatial and temporal resolution.

For *in situ* measurements of oxygen, electrochemical sensors, often called Clark type sensors after a US patent are the most common (Clark, 1959; Kanwisher, 1959). Electrochemical sensors have been developed and used in a wide range of applications and therefore vary in size and design from micrometer sized glass electrodes to more robust macro electrodes with sensing tips of several centimeters (for a review see Glud et al. (2000) and references therein). Performance studies of different types of electrochemical sensors have been presented in e.g. Briggs and Viney (1964); Atwood et al. (1977); Hitchman (1978); Gneigner and Forstner (1983); Short and Shell (1984); Berntsson et al. (1997); Gundersen et al. (1998); Glud et al. (2000). Regardless of the design, these studies have shown that the Clark sensor requires frequent (at least monthly) calibration to obtain accurate measurements of dissolved oxygen. Other shortcomings that has been demonstrated for these type of sensors are irreversible pressure effects (hysteresis), cross sensitivity (Berntsson et al., 1997) and contamination by hydrogen sulfide (H_2S).

Optodes (also called optrodes) may provide a more suitable method than electrochemical sensors for direct measurement of dissolved oxygen. Optode technology has been known for years (e.g. Kautsky, 1939) but it is relatively new to the aquatic research (e.g. Klimant et al., 1995; Glud et al., 1999a; Wenzhöfer et al., 2001). The fundamental principle is based on the ability of selected substances to act as dynamic luminescence quenchers.

In the case of oxygen, if a ruthenium-complex is illuminated with a blue light it will be excited and emit a red luminescent light with an intensity, or lifetime, that depends on the ambient oxygen concentration. It is important to distinguish between three different principles in detecting the red luminescence: Intensity (how strong the luminescence is), life-time (how quickly the luminescence dies out) and phase shift (in principle also a life time based measurement, see below Measurement Principle). Intensity based measurements are technically easier to do, but they can drift over time. The different signal detection techniques are summarized by Wolfbeis (1991),Demas et al. (1999) and Glud et al. (2000) along with a wide range of applications. Klimant et al. (1995) and Stokes and Romero (1999) described intensity based oxygen optodes and their use. The function and use of lifetime based optodes were described by Holst et al. (1995) and Klimant et al. (1997).

Optode technology has an advantage over conventional sensors in that it can also be used to assess oxygen distributions in two dimensions (e.g. Holst et al., 1997, 1998; Glud et al., 1999b, 2001, 2005) as well as for detection of other substances (e.g. Klimant et al., 2000; Huber et al., 2000, 2001a,b; Hulth et al., 2002; von Bultzingslowen et al., 2002).

In this paper we evaluate a commercially available lifetime-based oxygen optode and compare its performance with different electrochemical sensors and oxygen concentrations obtained by Winkler titration. A novelty with this sensor, compared to the optodes used in other studies, is that it combines the benefits of using a platinum porphyrine luminescence dye with digital signal processing electronics (DSP). The construction and working principles of this sensor is described briefly and its accuracy and precision evaluated in the laboratory. The influence of simultaneous changes in oxygen, salinity, temperature, stirring, pressure and pH was tested by using multivariate statistical methods. Data from extended evaluations of pressure behavior as well as response time are presented and discussed. Finally a range of field application examples are given to demonstrate the performance of oxygen optodes in different field settings.

6.2 Materials and procedures

6.2.1 Measurement principle

The particular type of sensor that has been used in this evaluation is commercially available from Aanderaa Data Instruments, Norway (Oxygen Optode model 3830 and model 3930, Tengberg et al., 2003). The sensor is based on oxygen luminescence quenching of a platinum porphyrine complex. The lifetime and hence the oxygen measurement is made by a so called phase shift detection of the returning, oxygen quenched red luminescence. The relationship between oxygen concentration and the luminescent decay time can be described by the Stern-Volmer equation:

$$[O_2] = \frac{1}{K_{SV}} \left(\frac{\tau_0}{\tau} - 1 \right) \quad , \tag{6.1}$$

where τ = decay time, τ_0 = decay time in the absence of oxygen and K_{SV} = Stern-Volmer constant (the quenching efficiency). The foil is excited with a blue-green light modulated at 5 kHz. The decay time is a direct function of the phase of the received red luminescent light which is used directly for oxygen detection, without calculating the decay time. The basic working principles of dynamic luminescence quenching, lifetime-based optodes and phase shift detection can be found in e.g. Klimant et al. (1997); Demas et al. (1999); Glud et al. (2000).

The sensor housing is made of Titanium, rated to 600 bar pressure, with a diameter of 36 mm and a total length of 86 mm. This housing includes an optical part, a temperature sensor (Fig. 6.1) and the necessary electronics (a microprocessor with digital signal processing capacity) to process signals and output absolute temperature compensated oxygen readings (in μM or % saturation). An advantage of using digital signal processing, over analog technology, is enhanced possibilities of signal filtering and less risk of drift in the electronics with changes in temperature and over time.

The sensing foil is composed of an oxygen sensitive luminescent substance (luminophore) that is embedded in a polymer layer which is coated onto a thin film of polyester support (Fig. 6.1). The most commonly used oxygen lumniphores have been ruthenium complexes (e.g. Klimant et al., 1997; Stokes and Romero, 1999) but for this sensor an oxygen-sensitive

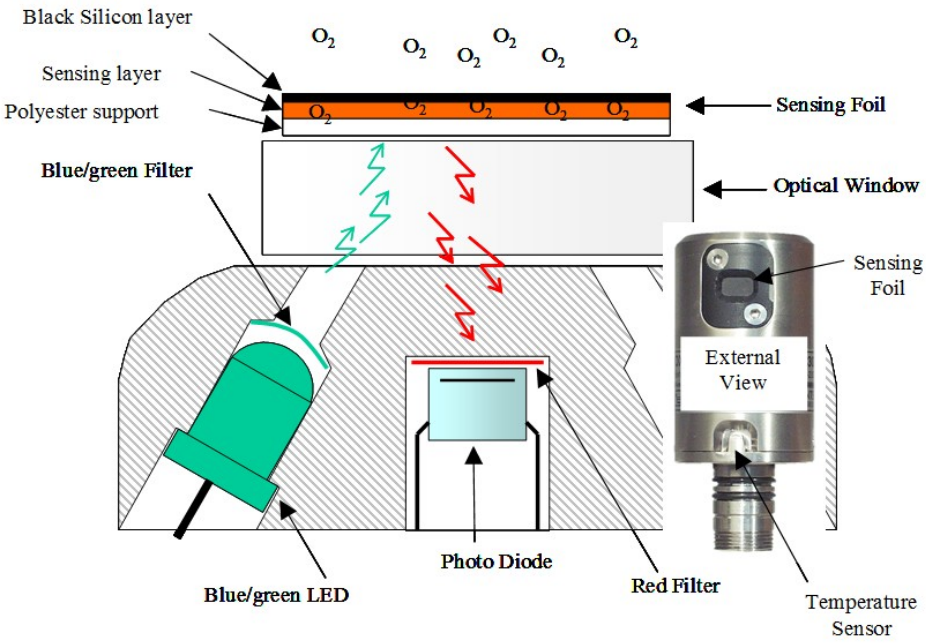

Figure 6.1: Optical design and an outside view of the evaluated optode-based oxygen sensor

luminophore based on a platinum porphyrine complex, commercial available from PreSens GmbH (Regensburg, Germany) was used mainly due to its longer lifetime (about a factor 5 longer than for ruthenium). A longer lifetime makes it easier to detect the signal and to obtain stable readings. Another advantage with platinum porphyrine is that it is less sensitive to photobleaching.

We tested two types of foils, with and without, a gas permeable protective black silicon layer (Fig. 6.1). The silicon layer also acts as an optical isolation layer to avoid potential influence from fluorescent/luminescent material in the surrounding water and/or direct incoming sunlight, when measuring in the photic zone. The disadvantage of this layer is that the sensor response time becomes longer.

6.2.2 Calibration performance

The response of an optode is such that it yields the highest sensitivity at low oxygen concentrations, it follows the Stern-Volmer equation (e.g. Demas et al., 1999). The response is also affected by temperature, which requires compensation in calibrations/measurements. To evaluate the effect of different calibration strategies on sensor accuracy two different procedures were tested (Table 6.1). The first was a 30-point calibration (5 different temperatures and 6 different oxygen concentrations) of a batch of foils (normally produced in batches of 100) to obtain foil-specific calibration constants. These are stored in the sensor processor when the foil is mounted. Then a two point calibration is performed at 0 % and 100 % air-saturation, taking into account the prevailing air pressure. The batch constants and the two-point calibration are used together to fit the Stern-Volmer equation to the particularities of the foil and the sensor. This is the calibration procedure that is presently used when these sensors are produced.

A second set of calibrations were performed on 20 different sensors to assess if and by how much the accuracy could be improved by making an individual sensor specific 30-point calibration with the foil mounted from the start. This method is more time consuming, since every sensor has to go through an elaborate calibration procedure, but it is likely to better account for individualities of sensors and foils.

Table 6.1: Description of different tests and their major conclusions

Test # (number of sensors used)	Test (test period)	Location; Equipment	Main physical settings* O=O_2;T=Temp pH=pH;P=Pres Sa=Salinity St=Stirring	Major conclusions	Data in Fig. #
1 (∼20)	Accuracy of calibration methods (5 days)	Lab; Mass flow controllers, thermobath	O:0-500;T:2-40 pH:7;P:1 Sa:0 St:from gas mix	Batch: Accuracy ±5μM Individual: Accuracy ±2μM Precision±1μM	Not shown
2 (3)	Multivariate calibration (10 days)	Lab; Incubation device, press. chamb.	O:0,115,230;T:6,13,20 pH:5,6.5,8;P:1,250,500 Sa:0,17,34 St:0,25,50 RPM	Sal influence, corrected with standard equations; Press effect 4%/100 bar, linear; No sensor is individual	Fig.2 Fig.3A Fig3.B
3 (3)	Pressure Cycling (1 day)	Lab; Incubation device, press. chamb.	O:380;T:7 pH:7,P:3-405 Sa:0 St:0 RPM	Press effect 4%/100 bar, linear, no remaining pressure effects (hysteresis) No sensor is individual	Fig.2 Fig.4
4 (3)	Response time of isolated & non isolated (1 day)	Lab; Air & N_2 bubbled water	O:0,284;T:20 pH:7,P:1 Sa:0 St:from bubbling	Isolation:t_{67}=23s,t_{90}=47s, t_{99}=95s No isolation:t_{67}=6s,t_{90}=10s, t_{99}=18s	Not shown
5 (1)	Long term stability I (580 days)	Off Canada in Labrador Current; Argo float	O:295;T:3 pH:ND;P:180 Sa:0 St:nat. circulation	No drift detected Average conc.=295μM Standarddev.=0.7μM values=80 samples	Fig.5
6 (1)	River fouling sensitivity (20 days)	Orge River (France); Monitoring station	O:170-300;T:15-22 pH:ND;P:1 Sa:0 St:nat. circulation	Electrochemical sensor affected by fouling after 2 days; Naked Optode no influence of fouling within 20 days	Fig.6
7 (2)	Waste water fouling sensitivity (90 days)	Various waste water treatment plants	O:0-150:T10-25 pH:ND;P:1 Sa:0 St:nat. circulation	Naked Optode stable 14 days; Copper plate has no effect; With water jet optode stable more than 90 days	Not
8 (1)	Slurry of livestock waste (2 hours)	Bioreactor	O:0-90;T:35 pH:ND;P:2 Sa:0 St:no	Above 6% Total Solids the mixing in the slurry not sufficient achieve good readings	Not shown
9 (1)	On-line ship system accuracy (35 days)	R/V Meteor expedition Brasil-Africa; Flowtrough	O:190-215;T:26-30 pH:ND;P:2 Sa:31-36 St:troughflow	50400 values, no spikes Average difference 0.9 μM, Standard dev. 1.1 μM Winkler values=72	Fig.7
10 (1)	Profiling on CTD accuracy (10 hours)	Off Guinea; Optode logger on CTD with bottles	O:17-233;T:2-28 pH:ND;P:1-550 Sa:26-33 St:nat. circulation	High correlation Average difference 2.1μM Standard dev.=5.1μM Winkler values=14	Fig.8

* Oxygen concentration given in μmol/L; Temperature in °C;Pressure in bar; Salinity in ppt

6.2.3 Cross sensitivity, pressure hysteresis and response time

The solubility of oxygen in water is dependent on salinity and temperature (e.g. Weiss, 1970; Garcia and Gordon, 1992). This means that in absolute concentration a seawater sample will contain less oxygen than a freshwater sample at the same temperature although the partial pressure is the same (e.g. 100 % saturation). In theory both electrochemical sensors and optodes measure partial pressure which implies that salinity and temperature corrections have to be done to obtain absolute values. To validate if such relatively simple corrections are sufficient to get an accurate response or if also other factors can have an effect multivariate statistical methods can be used (e.g. Francois et al., 2002; Bourget et al., 2003; Haus et al., 2003). In Berntsson et al. (1997) one type of electrochemical oxygen sensor was tested with such methods for simultaneous changes in oxygen concentration, temperature, salinity, pressure, stirring and pH in 19 different experiments.

In this study we used the same methods as described in Berntsson et al. (1997) but with higher pressure levels of 1, 250 and 500 bar (Table 6.1). To be able to perform these tests under controlled conditions, an experimental chamber that can be placed inside a pressure tank was constructed (Fig. 6.2).

A set of separate pressure tests were performed on the optodes, using the same equipment as described in Figure 6.2, to evaluate the effects of high pressure and rapid pressure cycling. The pressure was varied in cycles from 3 to 405 bar. Pressurizing from 3 to 405 bar took approximately 4 minutes. The return to 3 bar was done by opening the valve of the pressure chamber and took less than 1 minute.

The response time was assessed with two different foils one which was optically isolated and the other without optical isolation. It should be noted that there is no standard way of testing the response time and the results obtained are to a large extent dependent on how the tests are done. In our case we choose to simply move the sensors, without wiping the water off, between two containers one which was air saturated and the other depleted in oxygen, through stripping with N_2 gas.

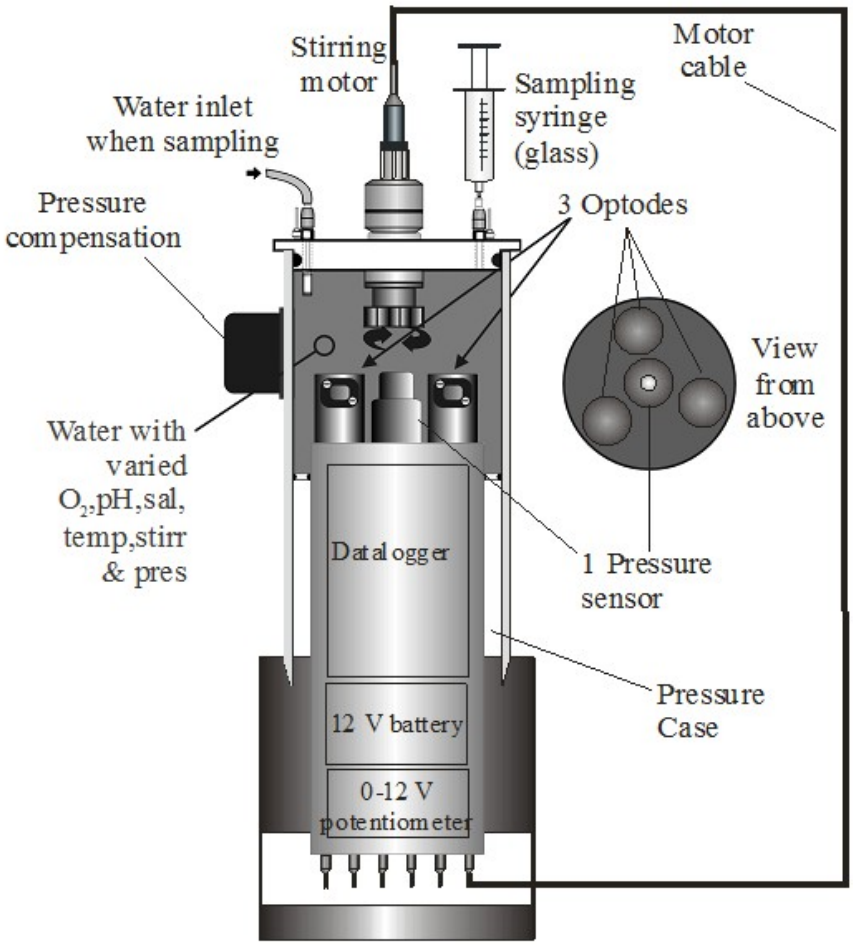

Figure 6.2: Set-up that was used for multivariate calibration and for pressure testing of three optodes in parallel. Temperature is measured by the optodes and pressure by a separate pressure sensor placed in the center of the top plate.

6.2.4 Long-term stability

The amplitude of the red luminescent signal (see Fig. 6.1) should not be of importance if a life time based detection method is used. So if the foil is bleached/degraded over time, which it will be, or the optical properties of the system change, for example with changes in temperature the response should not be affected. To evaluate the long-term stability several laboratory and field evaluations were performed. One such evaluation that lasted for 580 days was collected by an optode that was mounted on a profiling Argo[1] float. These floats are autonomous and freely drifting in the oceans. Today there are about 1900 units in operation. The floats can change their buoyancy and hence move up and down in the water column while collecting data (salinity, temperature and more recently also oxygen). When the float is at the surface they transmit data back via satellite. For more information about these floats and their use with focus on oxygen measurements see Körtzinger et al. (2004, 2005).

6.2.5 Sensitivity to biofouling

Biofouling and bacterial growth is a major obstacle to long-term monitoring in the aquatic environment. The types of fouling that occur vary greatly from one environment to another and so do the effects of fouling. In order to test this, three different evaluations were done (Table 6.1).

A network of environmental on-line monitoring stations has been operational in rivers around Paris (river L'Orge) for many years. One of the most important parameters to monitor at these stations is oxygen, which is measured with electrochemical sensors. Oxygen has also been the most labor-demanding parameter since drifting slime blocks the membrane of the sensors and rarely allows them to be operational for more than one week. Therefore weekly service intervals are conducted. During service the oxygen sensors are taken up, cleaned and a recalibrated (in two points). With the aim of prolonging the time between services an oxygen optode was tested for three weeks in parallel with one of the electrochemical sensors. The electrochemical sensor was submitted to its regular weekly service and calibration intervals while the optode was left untouched for a 20 days test period.

[1] `http://www-argo.ucsd.edu`

City waste waters have a high content of organic material, the microbiological activity is elevated and the oxygen concentration is a critical element for proper processing. An accurate monitoring of oxygen in waste water treatment plants is necessary to optimize the relation between cleaning efficiency and energy used for water aeration. Several comparative tests (Table 6.1) were made with optodes in two different waste water treatment plants (in Västerås, Sweden and at the Attleboro waste water treatment plant, Providence, USA). In the aeration basins, the residence time is relatively short (hours) and the bubbling ensures mixing of the water. The fouling consists of high organic content slime. Unprotected optodes were placed in parallel with special process-adapted electrochemical sensor systems with continuous cleaning.

A third and extreme test of the operational ability of the sensor to measure in high content of reactive organic matter (5-12% weight) was performed in a bioreactor for livestock waste (e.g. Skjelhaugen, 1999). An optode was used in several studies measuring both in the headspace above the waste slurries and directly within them.

6.2.6 Other field applications

We selected two additional examples of data that were collected in the marine environment with the aim of covering a wide range of measuring situations from shallow depth to the deep sea (5500 m), from tropical surface waters with temperatures approaching 30°C to cold abyssal surroundings with temperatures around 2°C and with oxygen levels ranging from 20 to 230 μM. In both cases the data registered by the optodes were compared with independent measurements of oxygen obtained on collected water samples that were analyzed by Winkler titration.

One data set was collected from a shipboard underway seawater pumping system during a 35-day expedition to the tropical Atlantic Ocean. The other was obtained with a cable operated profiling CTD (Conductivity, Temperature and Depth) instrument that was lowered to 5500 m off Guinea in the Equatorial Atlantic.

6.3 Assessment

6.4 Calibration performance

The individual 30 point sensor calibrations enhanced the accuracy (±2 μM) by a factor of approximately 3 compared to a batch calibration with a subsequent two point calibration (Table 6.1). The reason for the better performance is still unclear and awaits further investigation. The obtained accuracy (±5 μM) using a batch-calibrated sensor should be sufficient for most applications, especially in the coastal environment were variations in dissolved oxygen are often large. The absolute precision (resolution) of the sensors was the same regardless of the calibration method. As expected the sensor performance was better (± 0.5 μM) at lower oxygen concentrations. At the higher end (300-500 μM) precision was approximately ± 1 μM.

6.4.1 Cross sensitivity and pressure hysteresis

The outcome of the multivariate calibration was that stirring had no effect, which was expected from earlier work by Klimant et al. (1995) and since the sensor is not consuming any oxygen. Pressure had an influence (about 4 % lower response per 100 bar of pressure) but was fully reversible and predictable (i.e. all sensors had the same response). Temperature also has an influence on the optical measurements but since the optodes described here are equipped with temperature sensors this effect is automatically compensated for by the internal processor and no remaining influence of temperature could be distinguished, which also indicates that the temperature compensation was done correctly. Figure 6.3A gives raw data from the three different sensors that were run in parallel during the multivariate evaluations. Figure 6.3B shows the data after a general salinity and pressure compensation (Garcia and Gordon, 1992).

Repeated pressure cycling between 3 and 405 bar confirmed the above described pressure effect of 4 % lower response per 100 bar and also demonstrated that rapid pressure cycling did not leave any remaining pressure effects (hysteresis) on the sensors (Fig. 6.4).

Potentially other substances present in natural waters could interfere with the oxygen measurements. Contamination by hydrogen sulfide (H_2S)

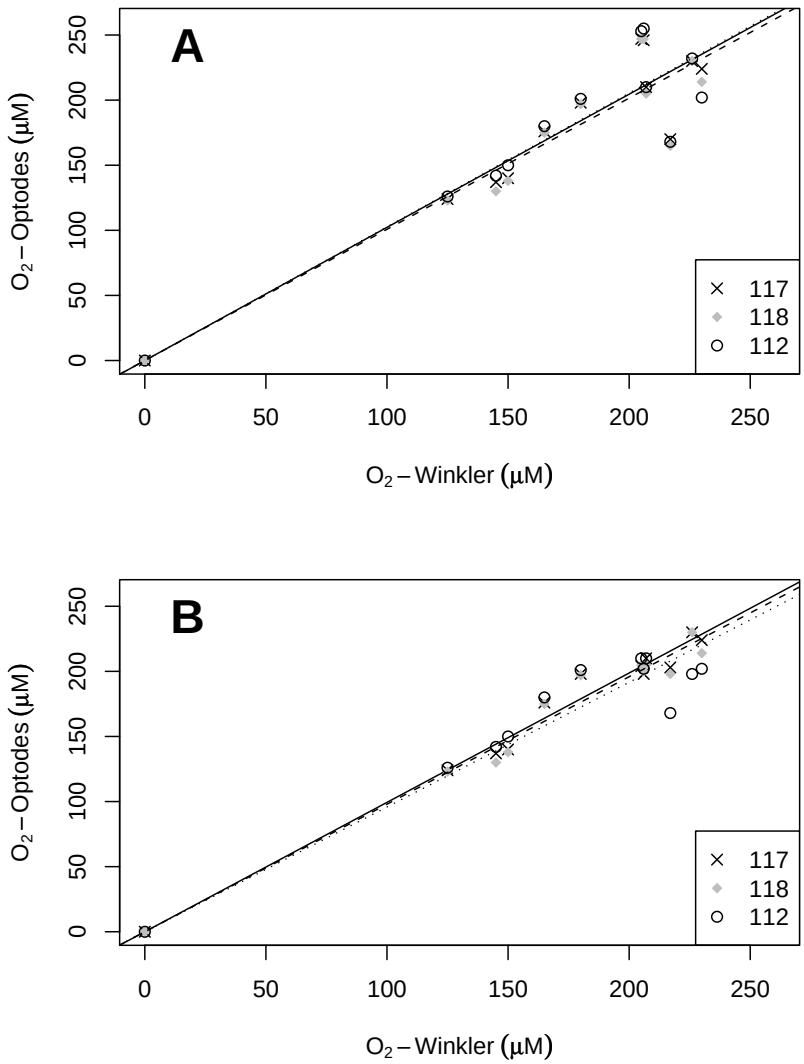

Figure 6.3: Results from multivariate calibration experiments. Oxygen readings obtained with three parallel optodes plotted against oxygen readings obtained by Winkler titrations. Figure 3A shows the raw data and figure 3B the data after pressure (4 % per 100 bar) and salinity compensation, according to Garcia and Gordon (1992).

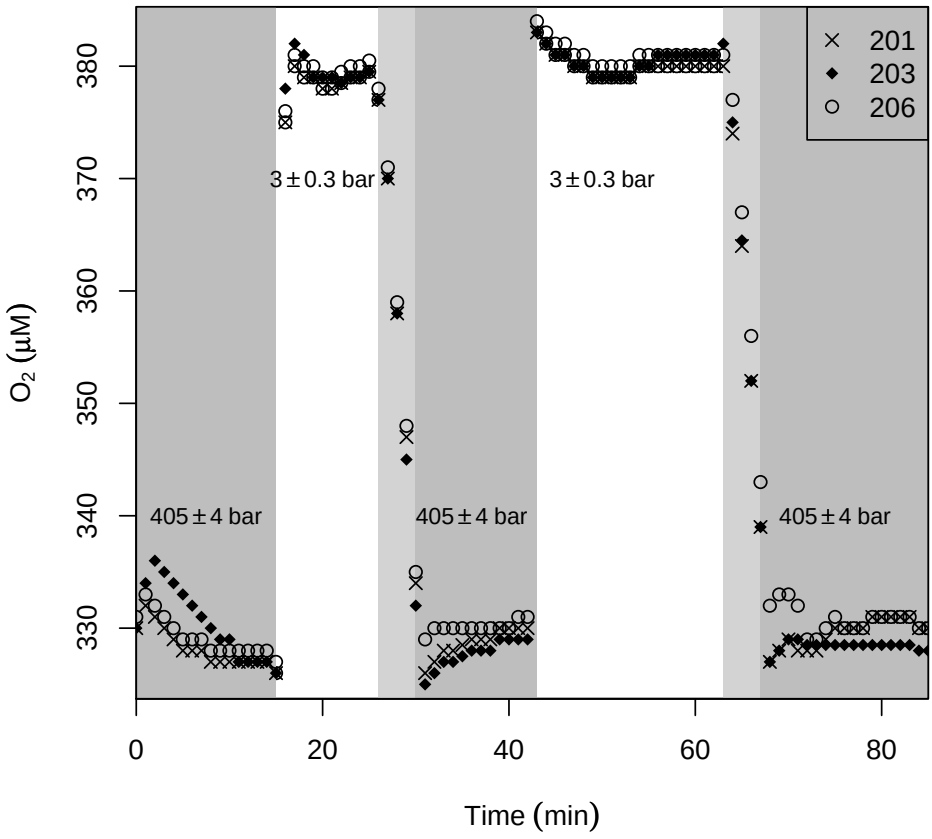

Figure 6.4: Oxygen readings from three optodes during pressure cycling between 3 and 405 bar. The pressurization (from 3-405 bar) took approximately 4 minutes. The depressurization lasted approximately 1 minute.

is a major concern when using electrochemical sensors in oxygen depleted environments. H_2S has no influence on the response of the optodes and it will not damage them in any way (Klimant et al., 1995). The only interferences (cross-sensitivity) are found with gaseous sulfur dioxide (SO_2) and gaseous chlorine (Cl_2).

The 90 % response time of the sensors were approximately 45 s with the optically isolated foils (t90 = 45 s) and 10 s for the foil without optical isolation.

6.4.2 Long-term stability

Figure 6.5 presents 580 days of oxygen and density data from one of the Argo floats that was drifting off the east coast of Canada, most of the time in the Labrador Current. The presented data are collected every time the float is passing at 1800 m depth. At this depth and in this region previous investigations have demonstrated that the density and oxygen conditions should be constant. This is confirmed by the collected data which gave relatively constant density and oxygen (295.0 ± 0.7 μmol L^{-1}) readings. No drift in the oxygen readings could be detected it is only at the end of the deployment (after about 400 days) when the float has moved out of the Labrador Current that there is a small and expected shift in oxygen and density values.

Other data sets from continuous field measurements for periods of 10-20 months (e.g.Rafos floats[2]) have also indicated no drift (not presented here) which give reason to believe that the stability of these sensors is at least 600 days and probably longer.

6.4.3 Sensitivity to biofouling

A direct side by side comparison of an electrochemical sensor with an optode at a river monitoring station demonstrated that in spite of becoming covered with slime only after 2-3 days the optode was stable for the whole twenty days test period. In general the electrochemical sensor started to drift towards lower values after 2-3 days. After cleaning and recalibration it returned to readings which were similar to the optode recordings

[2] `http://www.po.gso.uri.edu/rafos/`

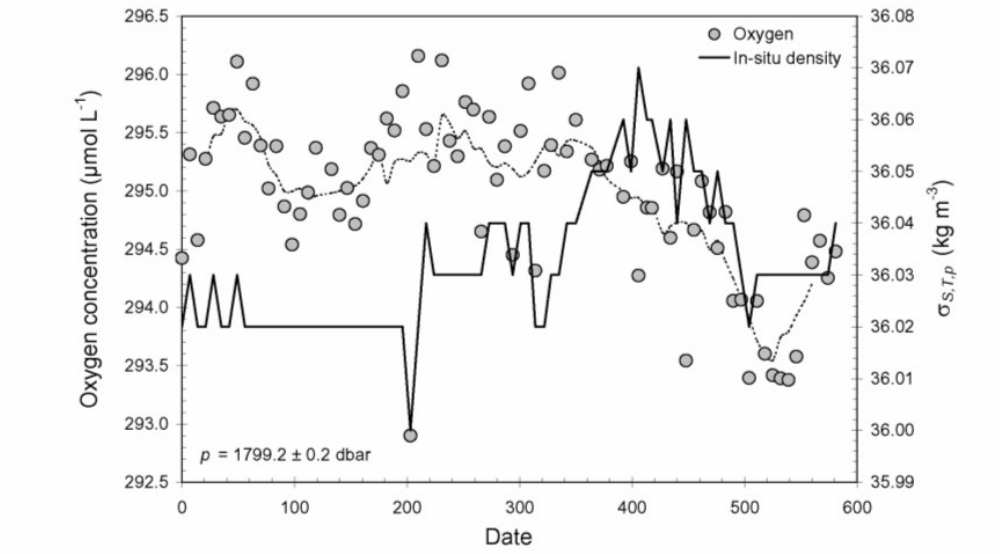

Figure 6.5: Five hundred and eighty days of oxygen and density data collected from a free drifting Argo float off the east coast of Canada in the Labrador Current. The presented data shows oxygen readings as the float passes at 1800 m depth. As long as the float was in the Labrador Current (the first 400 days) it is considered that salinity, temperature and oxygen readings at this depth should be constant. The data demonstrates no drift over the given time period but as the float moves out of the Labrador Current the oxygen and density readings shift slightly. The average oxygen readings during the whole period were 295.0 ± 0.7 μmol L^{-1}. The dotted line is a seven point centered running mean of the measured oxygen concentrations.

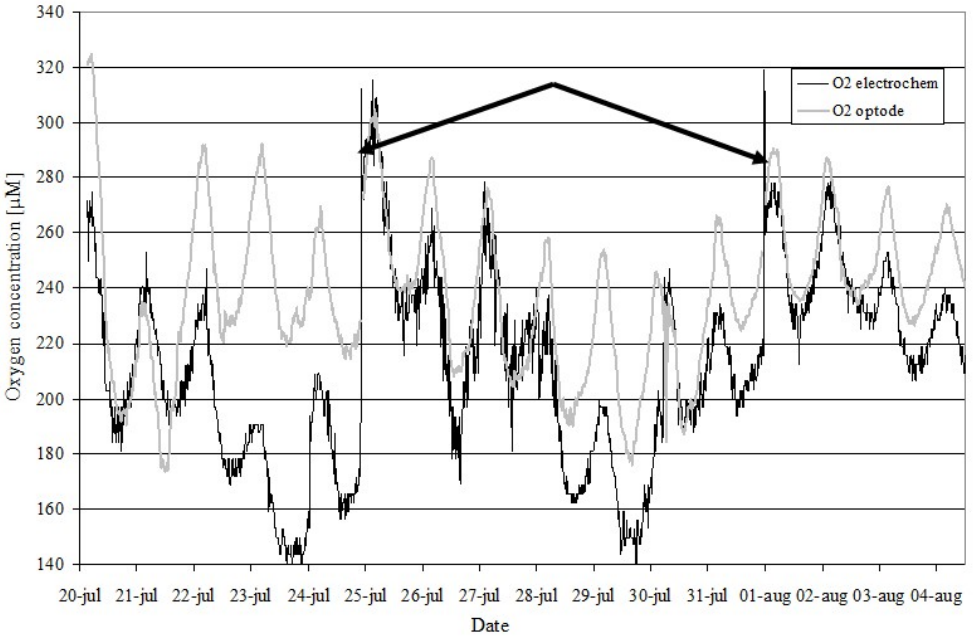

Figure 6.6: Oxygen data from a comparison between an optode and an electrochemical sensor at a monitoring station in the River l'Orge (France). Two occasions when the electrochemical sensor was taken up, cleaned and recalibrated are marked with arrows in the figure. The optode was never cleaned during this experiment.

(Fig. 6.6). Measured oxygen concentrations in the river follow the daily variations in temperature. When the water becomes colder during night the oxygen solubility increases leading to higher concentrations. During daytime the temperature increases and the oxygen level drops. In this particular case fouling did not have any detectable influence on the optode. There are, however, other river examples (data not shown here) in which the slime possibly contained more active microorganisms and the fouling started to affect the naked optode after 14 days (see also example from waste water treatment plants below).

In the aeration tanks of city waste water unprotected optodes were

placed in parallel with special process-adapted electrochemical sensor systems with continuous cleaning. Unprotected optodes gave correct readings on average for 14 days. After that the microbiological oxygen consumption of the organic material that had accumulated in the small depression in front of the foil (see Fig. 6.1) resulted in signal drift. The use of a protective copper plate had no effect, on the contrary the mounting of the plate made the particles accumulate faster. To solve this problem a spray nozzle (normally used to clean cars) was fitted and directed towards the sensor foil. The nozzle was connected to a freshwater garden hose. By turning on the water the sensor was sprayed/cleaned once every 1-2 days and it was continuously operated in this mode for 90 days (data not shown) without any visible fouling effects and without any drift.

The result from an evaluation of using an optode in a bioreactor containing slurries of livestock waste concluded that in organic waste concentrations below 6 % (weight) the sensor was functioning well for time periods of up to one week. When introduced into the slurries with concentrations above 6 % the response rapidly dropped to readings close to 0 and stayed at these levels in-spite of high levels of aeration. We believe that the reason for this artifact is caused by an improper mixing of the slurry in the depression just in front of the sensor.

6.4.4 Other field applications

Figure 6.7 presents a subset of optode data that were collected from a shipboard underway seawater pumping system during a 35-day expedition to the tropical Atlantic Ocean. The two meridional sections along ∼26.5°W (southbound) and ∼24 °W (northbound) shows similar oxygen concentrations at 5 m depth in the surface mixed layer. The corresponding saturation level is 101.5-104.5 %. The observed variability is mainly due to small-scale patchiness of phytoplankton (confirmed by separate samples) but also exhibits some diel cyclicity. Oxygen concentration from Winkler titration of samples taken regularly from 5 m depth hydro casts along the two transects are in good agreement with the optode data (offset = 0.9 μM, rms = 1.1 μM). Winkler samples were also taken regularly from the underway pumping system but these discrete samples show frequent contamination by small air-bubbles and are therefore of inferior quality (data not shown).

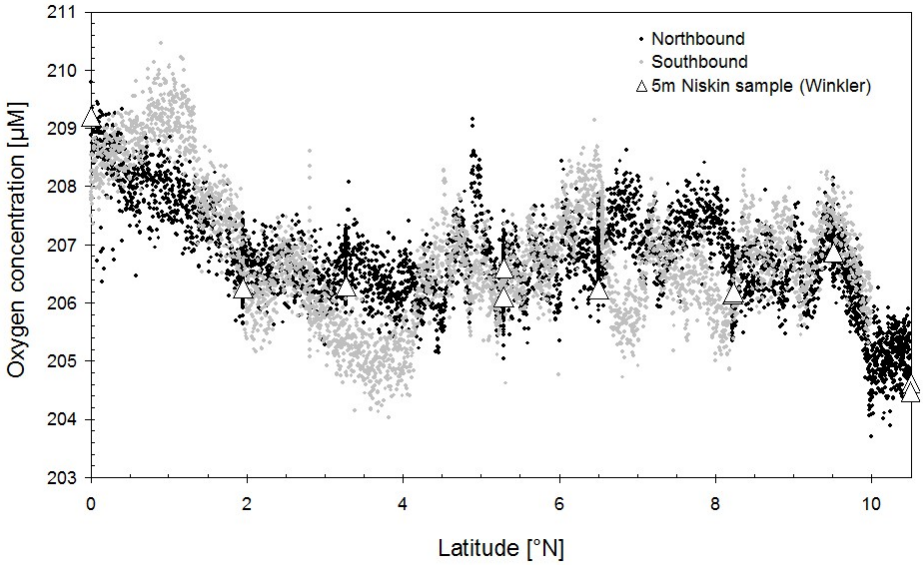

Figure 6.7: Tropical surface ocean oxygen data collected during a cruise to the tropical Atlantic Ocean. Optode measurements were made on seawater provided by an underway pumping system whereas Winkler titrations were made on water samples taken with Niskin bottles from regular hydrocasts from the same depth as the water intake of the pumping system.

Examples of data from the up cast of one CTD mounted optode, along with Winkler analyzed data from discrete samples, are presented in Figure 6.8. The average difference between the Winkler values and the optode readings was 2.1 ± 5.1 μM. No indications of remaining pressure effects (hysteresis) were discovered and the sensor was reading 252 μM in the air before the deployment and 253 μM after. Absence of pressure hysteresis was better demonstrated in the pressure cycling test presented above (Fig. 4) and has also been confirmed through numerous other field deployments on profiling CTD instruments (data not shown).

6.5 Discussion, comments and recommendations

The data presented above strongly suggest that the lifetime-based methodology and the oxygen optode sensors evaluated here are well-suited for measurements of dissolved oxygen in the aquatic environment. The performance of this method in general and of this type of sensor in particular has been demonstrated through numerous laboratory and field examples. When comparing to the general behavior of electrochemical sensors it seems that the lifetime-based optical technology is superior in all aspect, except for the fast response time that has been demonstrated by electrochemical microelectrodes.

A fast response time is desirable for sensors that are used on profiling CTD instruments (typical descent/ascent rates of 0.5 m/s), on towed vehicles (often towed at 2-5 m/s) and when high frequency sampling is required to resolve rapid oxygen fluctuations for example close to the bottom (e.g. Berg et al., 2003a). Electrochemical microelectrodes (e.g. Revsbech, 1989) are unmatched with regard to fast response time and a well-designed sensor can have a 90 % response time (t_{90}) of around 0.1 s (Glud et al., 2000). These sensor are however not rugged and difficult to handle and they suffer from the typical limitations of electrochemical sensors (except possibly stirring sensitivity since the oxygen consumption is low). Microoptodes are easier to make and more robust than the electrochemical microelectrodes and these have shown response times (t_{90}) of around 2 s. Larger electrodes are more rugged but the response times are generally

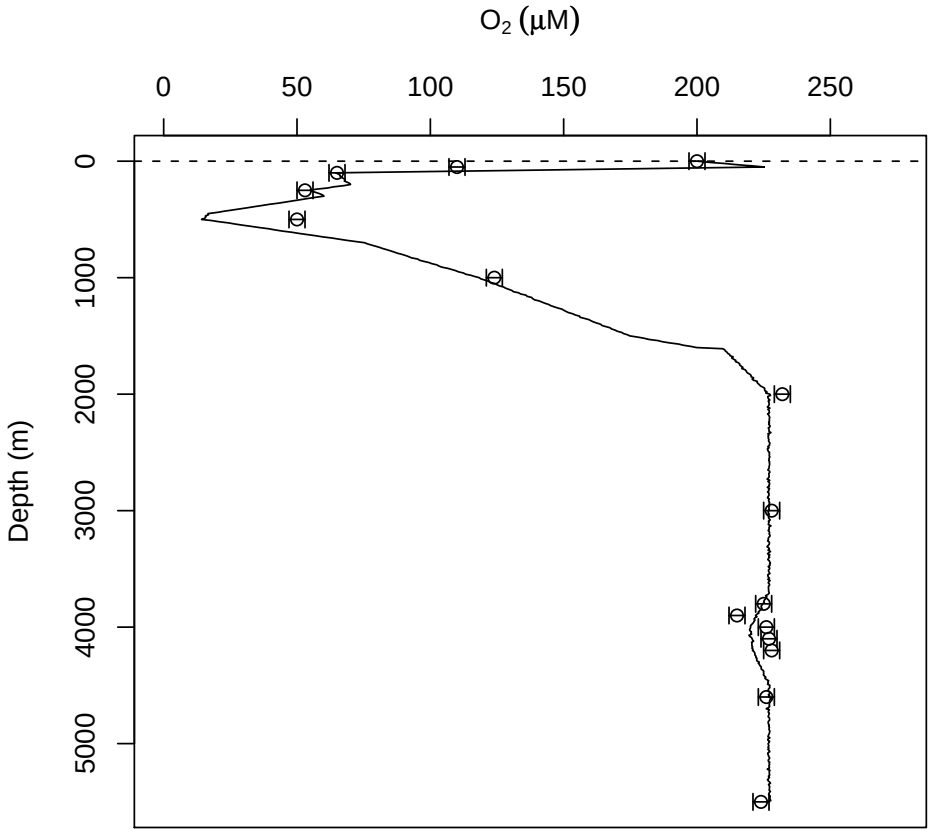

Figure 6.8: Optode (continuous line) and Winkler data (dots) from CTD deployment to 5500 m depth in the equatorial Atlantic off Guinea.

longer. A typical electrochemical macro-sensor has a t_{90} of 30-120 s but this can be improved by using thinner membranes (which also makes the sensor more stirring sensitive and noisy). With future development there is potential to improve the response time of the optode foils / sensors but most likely not to the level achievable with microelectrodes (t_{90} = 0.1 s).

In the coastal marine environment the fouling is often a major impediment to monitoring. Unlike the cases described above (rivers and waste water) the fouling often consists of plants (e.g. algae, seaweed etc.) and/or animals (e.g. shell building barnacles). Several trials were done to prevent the effects of fouling on the here described sensors. The most efficient method developed so far has been to wrap a beryllium-copper alloy net (used for domestic cleaning) around the sensor. In environments with heavy fouling (shallow coastal waters in Chesapeake Bay and in the Gulf of Mexico) this method prolonged the service interval from approximately 7-10 days to 40-60 days. It is important to prevent the beryllium-copper net to enter into contact with the metal of the sensor since this will create a galvanic element which makes the mesh disappear faster. It also makes it significantly less efficient in preventing fouling. Electronic isolation was obtained by wrapping tape around the sensor before adding the alloy net. Other solutions such as a fixing a fine meshed copper plate in front of the foil has proven inefficient in most situations since the mesh was quickly clogged and prevented a proper water exchange.

It should be noted that all the above presented long-term (1-2 years) stability data were collected in environments with low fouling. When fouling is affecting the sensor such long stabilities can not be expected.

The active chemical compound used on this sensor is a platinum porphyrine complex which has the advantage to yield a longer and more easily detectable lifetimes than the more commonly used ruthenium complexes (e.g. Klimant et al., 1997; Stokes and Romero, 1999). Ruthenium-based sensors are likely to generally perform similar to the sensors tested here but the accuracy and precision is expected to be lower, due to the shorter lifetimes of Ruthenium. The pressure-behavior might also be different.

A crucial point for the long-term stability of this type of sensors is how strongly the sensing compounds are bound to the support layer and how rapidly they bleach with time (number of excitations). If the sensing substance dissolves with time or if it bleaches rapidly the long-term stability will be compromised. The technology presented here appears to be stable

for years (not yet fully demonstrated) but this is chemistry dependent and the same stability can not automatically be assumed for other chemistries (e.g. ruthenium complexes or platinum porphyrine complexes with different ligands). Also the design of the electronic, mechanical and optical systems differs between sensor makes and differences in performance should be expected.

Use of this sensor in waste water treatment plants and in live stock waste has demonstrated that this design, with the foil placed in a shallow depression, is not optimal for these types of applications. Organic material accumulates in the depression, the response time becomes longer and the bacteria change the local oxygen conditions. A leveled mounting of the foil would most likely improve the ability of the sensor in this type of environments since the accumulation of organic material would become lower.

The oxygen response of an optode is exponential, yielding highest sensitivity at low concentrations. A high sensitivity at low concentrations is important in environments such as ocean oxygen minimum zones, found in e.g. the Pacific Ocean and Arabian Sea. A slight change in the ambient oxygen level can make a drastic change in the benthic community, due too different tolerance levels of hypoxia (Levin, 2003).

Appendix - Salinity compensation

Salinity compensation of oxygen readings from optode and calculation of saturation at a given salinity and temperature (Garcia and Gordon, 1992).

Input variables:

1. O_2 = O_2 concentration in μM, from the optode

2. T = Temperature in °C, from the optode temperature sensor

3. S = Salinity from a parallel salinity measurement

Empirical constants:

$A_0 = 2.00856$
$A_1 = 3.22400$
$A_2 = 3.99063$
$A_3 = 4.80299$
$A_4 = 9.78188 \cdot 10^{-1}$
$A_5 = 1.71069$
$\beta_0 = -6.24097 \cdot 10^{-3}$
$\beta_1 = -6.93498 \cdot 10^{-3}$
$\beta_2 = -6.90358 \cdot 10^{-3}$
$\beta_3 = -4.29155 \cdot 10^{-3}$
$C_0 = -3.11680 \cdot 10^{-7}$

Intermediate calculations:

$$T_s = \ln\left(\frac{298.15 - T}{273.15 - T}\right) \tag{6.2}$$

$$\alpha = S(\beta_0 + \beta_1 T_s + \beta_2 T_s^2 + \beta_3 T_s^3) + C_0 S^2 \tag{6.3}$$

$$\beta = A_0 + A_1 T_s + A_2 T_s^2 + A_3 T_s^3 + A_4 T_s^4 + A_5 T_s^5 \tag{6.4}$$

Final results:

Salinity compensated oxygen concentration,

$$O_{2,S} = O_2 e^{\alpha} \tag{6.5}$$

Oxygen concentration at saturation with air at a pressure of 1013 mbar,

$$O_{2,\mathrm{sat}} = e^{\beta+\alpha}/2.2414 \tag{6.6}$$

Percent saturation in the given water,

$$O_{2,\%sat} = 100 \cdot \frac{O_{2,S}}{O_{2,\mathrm{sat}}} \tag{6.7}$$

Summary

As stated in the introduction to this thesis, the aim was to advance the knowledge on respiration in ocean margin sediments and the assessments of tools needed for this purpose. Knowledge has been gained in several areas relating to respiration in both sediments and the water column, such as (1) a reassessment of the efficiency of the biological pump, (2) uptake and respiration of phytodetritus and (3) respiration in differing coastal sediment types. Tools that have been implemented and evaluated are (1) model uncertainty analysis techniques and (2) an optical sensor for the measurement of oxygen in the aquatic environment.

Chapter 2 is a study of the biological pump and global respiration patterns in the deep ocean (> 200m) using an empirical model based on sediment oxygen consumption data. The biological pump fuels most heterotrophic activity in the deep ocean by exporting particulate organic carbon below the euphotic zone. The concurrent consumption of CO_2 in surface waters drives a flux of CO_2 from the atmosphere to the ocean. This flux affects atmospheric CO_2 levels and the biological pump, thus, has a large impact on present-day, as well as, past and future climate. The efficiency of this pump depends on the rate of carbon fixation, export out of the euphotic zone and the depth of respiration. In this thesis the depth dependence of respiration patterns was modelled using a compiled data set of sediment oxygen consumption rates. We showed that the depth relationship can best be described by a double exponential model. For the upper part of the ocean, our resulting equation is similar to previous flux-depth relationships but predicted fluxes are significantly larger in deeper waters. The sediment oxygen consumption is fuelled mainly by POC, thus sediment respiration data were used to infer the amount of POC settling through the water column at a given depth. By assuming a uniform flux laterally across the global ocean the depth attenuation of POC could be derived. The results from this study imply a more efficient biological pump. Total oceanic respiration below the shelf break (200 m) is estimated

to be 827 Tmol O_2 yr^{-1}.

Chapter 3 is a study of the short-term fate of phytodetritus, which was investigated across the Pakistan margin of the Arabian Sea. Stations ranged in water depths from 140 to 1850 m, encompassing the oxygen minimum zone ($\sim$ 100–1100 m). Phytodetritus sedimentation events were simulated by adding ^{13}C-labelled algal material to surface sediments in retrieved cores as well as *in situ* using a benthic chamber lander. Retrieved cores were incubated at *in situ* temperature and oxygen concentrations. Overlying waters from cores and the lander chamber were sampled periodically. The incubations were terminated and sampled (for organisms and sediments) after durations of two and five days. The labelled carbon was subsequently traced into bacterial lipids as a proxy of bacterial biomass, foraminiferan and macrofaunal biomass as well as into dissolved organic and inorganic pools. The major part of the label was left unprocessed in the sediment, mainly at the surface. The largest pool of processed carbon was found in dissolved inorganic carbon, attributed to respiration. Both temperature and oxygen were environmental factors found to influence the rate of respiration. Macrofaunal influence was most pronounced at the lower part of the oxygen minimum zone, where just enough oxygen exists in connection with relatively abundant food supply. Thus, at this depth macrofauna were able to dominate the processing of phytodetritus in contrast to the remaining stations were bacteria and foraminifera thrived.

Chapter 4 is a study of benthic respiration rates in the Gulf of Finland. Rates were based on *in situ* incubations using benthic chamber landers. Three contrasting stations with different sediment accumulation regimes were visited during three cruises in 2003, 2004 and 2005. Results show a variable overlying water mass with changing salinity and other conservative species such as bromide and chloride. Connected with these changes are changes in the concentrations of O_2 and dissolved inorganic carbon. The effect of changes in water masses on the benthic fluxes was investigated with a dynamic diagenetic model. Fluxes of dissolved inorganic carbon were highest at the station with accumulation bottom, intermediate at the station with transport bottom and lowest at the station with erosion sediments.

Chapter 5 is primarily a theoretical investigation of how well a certain model parameter can be constrained based on a certain dataset. Bio-

irrigation is often quantified through incubations where an inert tracer such as bromide is added to the overlying water of a core or a benthic chamber. The tracer distribution in the overlying water or the porewater is subsequently followed. The interpretation of the tracer distribution is based on fitting observed data with a model containing several parameters, where some parameters such as the enhancement over molecular diffusion or non-local exchange are *a priori* unknown. In this chapter, it was tested under what conditions the results obtained through this fitting are robust. First identifiability analysis was used to investigate the minimum data requirements for two contrasting types of sediment, representative for deep-sea and shallow-water settings. Then two different representative datasets were used to estimate uncertainties of the fitted parameters, based on a Bayesian technique, the Markov Chain Monte Carlo. The results from this study imply that using *only* the concentration change in the overlying water, it is not possible to constrain both the rate and the mechanism of bio-irrigation, thus, sampling the porewaters at the end of the incubation is a necessity.

Chapter 6 is an evaluation of the performance of a commercially available lifetime-based optode. The availability of an oxygen sensor with a high accuracy and low detection limit is very useful in characterizing low-oxygen environments accurately, where large shifts in benthic communities occur with very small shifts in oxygen concentration. (cf. Chapter 3). Respiration measurements, such as sediment oxygen consumption (cf. Chapter 2 & 4) are also improved by a sensor with high precision and no additional consumption. The performance of the sensor was evaluated and compared with data obtained by other methods. A set of 10 different tests was performed, including targeted laboratory evaluations and field studies, covering a wide range of situations from shallow coastal waters and wastewater treatment plants to autonomous lander deployments at abyssal depths. The principal conclusion is that, owing to high accuracy ($\pm$ 2 μM), long-term stability (more than 20 months), lack of pressure hysteresis and limited cross-sensitivity, this method is overall more suitable for oxygen monitoring in the aquatic environment than other methods.

Outlook

The research presented in this thesis could potentially be extended in several directions. The global respiration estimates in chapter 2 does not include continental shelves. A similar type of analysis based on sediment respiration could be used while taking into account some of the features where shelf sediments differ from slope and deep-sea sediments, i.e. (1) light reaching the bottom in many places resulting in sediments being not only a sink for organic matter but also a source through benthic photosynthesis and, (2) higher-permeability, coarse-grained sediments where hydrodynamic interaction enhances transport through the surface sediment (Jahnke, 2005).

In chapter 3 a positive correlation between depth and length of the time lag of label appearance in the DIC pool was found. The increase in station depth corresponded with a decrease in temperature. Thus, a possible mechanism to explain this result is the difference in response to temperature between the bacterial groups performing the hydrolysis of organic matter and the respiration (Weston and Joye, 2005). This could be investigated more closely by adding labeled algae devoid of DOC and measuring the appearance into DOC and DIC at different temperatures.

In chapter 4, sediment accumulation rate was found to be an important factor influencing the benthic respiration rate in the Baltic Sea. This information could be used in improving existing ecosystem models of the Baltic Sea by a refined parameterization of resuspension and lateral transport of sediment including organic matter.

The usefulness of identifiability analysis and Bayesian uncertainty analysis, previously not used in the field of diagenetic modeling was demonstrated in chapter 5. Both techniques could be applied in connection with a more complex diagenetic model, such as the one used in chapter 4. This analysis would then aid an optimization of the field sampling as well as provide estimates of reaction rates along with uncertainties. Reaction rates including uncertainties of processes such as denitrification could then be compared with rate measurements (e.g. N_2/Ar technique) in order to validate the model results or to identify discrepancies in the current knowledge on diagenetic modelling.

Samenvatting

Zoals beschreven in de introductie van dit proefschrift, is het doel van dit proefschrift het vergroten van de kennis van respiratiesnelheden in oceaanbodems. Deze kennis is vergroot middels (1) een vernieuwde kwantificering van de biologische pomp, (2) consumptie en respiratie van phytodetritus en (3) meting van de respiratie in verschillende typen kustsedimenten. Technieken die zijn geïmplementeerd en geëvalueerd omvatten (1) analyse van modelonzekerheid en (2) optische sensoren voor de meting van zuurstofprofielen in aquatische sedimenten.

Hoofdstuk 2 is een studie van de biologische pomp en respiratiesnelheden in de diepe oceaan ($>$ 200m) door middel van een empirisch model en data van zuurstof consumptiesnelheden. De biologische pomp transporteert particulair organisch koolstof (POC) beneden de photische zone en voedt daarmee het gros van heterotrofe aktiviteit in de diepe oceaan. In het oppervlaktewater wordt CO_2 opgenomen vanuit de atmosfeer om het transport van (organisch) koolstof door de biologische pomp te compenseren. Deze opname van CO_2 beïnvloedt het CO_2 gehalte in de atmosfeer en daarom heeft de biologische pomp een grote invloed op het hedendaagse klimaat. De efficiëntie van de pomp hangt af van de snelheid van koolstoffixatie, export uit de photische zone en diepte waarop de respiratie plaatsvindt. De diepte-afhankelijkheid van de respiratie is in dit proefschrift beschreven door het modelleren van een dataset van zuurstofopnamesnelheden in sedimenten. We tonen aan dat de data het best worden beschreven door een model met twee exponentiele functies. De parameters in het model voor het ondiepe gedeelte van de oceaan zijn vergelijkbaar met eerder gepubliceerde modelresultaten. De voorspelde respiratiesnelheden zijn echter significant hoger in de diepe oceaan. Omdat zuurstofopname voornamelijk wordt veroorzaakt door de afbraak van POC, kan de depositie van POC op een bepaalde diepte in de oceaan worden afgeleid uit de gemeten respiratiesnelheden. Wanneer we een uniforme depositie over de oceanen veronderstellen, kunnen we de afbraak van POC

over de diepte berekenen. Hieruit blijkt dat de biologische pomp efficiënter werkt dan voorheen gedacht. De totale respiratie in de oceaan beneden de 200 m wordt hiermee geschat op 827 Tmol O_2 jaar^{-1}.

Hoofdstuk 3 is een studie naar de korte termijn afbraak van phytodetritus in sedimenten van de Arabische Zee. De stations waar het onderzoek is uitgevoerd lagen op een diepte van 140 tot 1850 m en daarmee liggen meerdere stations in de zuurstofarme zone die loopt van $\sim$ 100 – 1100 m. De depositie van phytodetritus werd gesimuleerd door het toevoegen van ^{13}C verrijkte algen aan kernen met sediment aan boord van het schip en *in situ* door middel van een lander. Incubaties vonden plaats onder *in situ* temperatuur en *in situ* zuurstofconcentratie. Bodemwater uit de kernen en de lander werden gedurende het experiment bemonsterd. De incubaties werden beëindigd na 2 en 5 dagen. Het toegevoegde ^{13}C werd vervolgens gemeten in bacteriële vetzuren (als maat voor bacteriële biomassa), foraminifera en macrofauna biomassa, alsmede in opgelost organisch en anorganisch koolstof. Het grootste gedeelte van het toegevoegde phytodetritus werd niet verwerkt gedurende het experiment en werd teruggevonden in de bovenste laag van het sediment. Het grootste gedeelte van verwerkt koolstof werd gerespireerd en werd daarom teruggevonden als opgelost anorganisch koolstof. De omgevingstemperatuur en zuurstofconcentratie bleken van invloed op de respiratiesnelheid. De opname door macrofauna was het hoogst aan de diepe rand van de zuurstofarme zoneovergang, omdat er juist voldoende zuurstof is in combinatie met een relatief hoog voedselaanbod. Op dit station neemt macrofauna het meeste phytodetritus op, terwijl bacteriën en foraminifera domineren op de andere stations.

Hoofdstuk 4 is een studie naar de respiratiesnelheid in sedimenten van de Finse Golf. Respiratiesnelheden werden gemeten door *in situ* incubaties met een lander. Drie stations met verschillende sedimentatiesnelheden werden bezocht tijdens expedities gedurende 2003, 2004 en 2005. De watermassa's bleken variabel zoals bleek uit veranderlijke saliniteit en concentratie van chloride en bromide. De verschillende watermassa's werden ook gekarakteriseerd door andere zuurstof- en opgelost koolstofconcentraties. De effecten van veranderende watermassa's op fluxen tussen sediment en water zijn onderzocht met behulp van een diagenetisch model. De fluxen van opgelost anorganisch koolstof bleken het hoogst op het station waar de bodem accumuleerde en het laagst op het station met eroderende

sedimenten.

Hoofdstuk 5 is een theoretische analyse naar de mogelijkheid om bepaalde model parameters te schatten met behulp van een bepaalde dataset. Bioirrigatie wordt veelal gekwantificeerd door middel van het toevoegen van een inerte stof, zoals bromide, aan het bovenstaande water in een sedimentkern. De concentratie van de inerte stof wordt opgevolgd in de tijd. Deze data worden gefit met een model waarvan enkele parameterwaarden, zoals het belang van moleculaire diffusie ten opzichte van biologische uitwisseling, onbekend zijn. In dit hoofdstuk wordt onderzocht welke data nodig zijn om tot een robuuste schatting van parameterwaarden te komen. Ten eerste werd een identificeerbaarheids analyse gebruikt om uit te zoeken wat de minimale eisen aan een dataset zijn. Ten tweede werd een onzekerheidsanalyse uitgevoerd op datasets die representatief zijn voor twee duidelijk verschillende soorten sediment; een diepzeesediment en een kustsediment. De onzekerheidsanalyse is een statistische Bayesiaanse techniek, gebaseerd op Monte Carlo Markov Chain. De resultaten van deze studie laten duidelijk zien dat *alleen* het concentratieverloop van de inerste stof in het bovenstaande water onvoldoende is om de snelheid en het mechanisme van bioirrigatie te bepalen. Aanvullende bemonstering is nodig in de vorm van het meten van een diepteprofiel van de concentratie in het poriewater van het sediment.

Hoofdstuk 6 is een evaluatie van een commercieel beschikbare optode. Een nauwkeurige zuurstofsensor met een lage detectielimiet is zeer geschikt om gebieden te karakteriseren met een lage zuurstofconcentratie. In dergelijke gebieden kunnen kleine veranderingen in zuurstofconcentratie leiden tot grote verschuivingen in de bentische gemeenschap (cf. Hoofdstuk 3). Ook respiratiemetingen, zoals zuurstofconsumptie door het sediment (cf. Hoofdstuk 2 & 4), worden nauwkeuriger wanneer gebruik gemaakt kan worden van een sensor die precies is en geen zuurstof verbruikt. De optode werd getest en vergeleken met andere methoden om zuurstofconcentratie te meten. Tien verschillende testen werden uitgevoerd, o.a. een laboratorium- en veldtest, in ondiepe kustsedimenten, nabij zuiveringsinstallaties voor afvalwater en in diepzeesedimenten. Geconcludeerd kan worden dat door de hoge nauwkeurigheid ($\pm$ 2 μM), stabiliteit over lange periode ($>$ 20 maanden), ongevoeligheid voor drukverschillen de optodetechniek beter geschikt is om zuurstofconcentraties in aquatische sedimenten te meten dan andere methoden.

Perspectieven

Het onderzoek zoals beschreven in dit proefschrift kan in meerdere richtingen worden uitgebreid. De totale respiratie in de diepzee zoals geschat in hoofdstuk 2 bevat niet de respiratie in het continentale plat. Een vergelijkbare analyse gebaseerd op gemeten respiratiesnelheden zou kunnen worden gedaan, mits er rekening wordt gehouden met de volgende eigenschappen van deze sedimenten: (1) doordat licht deze sedimenten kan bereiken kunnen deze ook een bron van organisch koolstof zijn en (2) verhoogd transport door het sediment als gevolg van een hogere permeabiliteit van deze grove sedimenten (Jahnke, 2005).

In hoofdstuk 3 werd een positieve correlatie gevonden tussen sedimentdiepte en vertraging waarmee ^{13}C werd gerespireerd. Stationdiepte correleerde sterk met temperatuur. Een mogelijk mechanisme waaraan de vertraagde respiratie kan worden toegeschreven is, dat de hydrolyserende en respirerende bacteriën verschillend reageren op temperatuur (Weston and Joye, 2005). Dit mechanisme kan worden onderzocht door ^{13}C verrijkte algen, zonder DOC (i.e. opgelost organisch koolstof), toe te voegen en de hydrolyse en respiratie te meten onder verschillende temperaturen.

In hoofdstuk 4 bleek de sedimentatiesnelheid van het sediment van invloed op de respiratiesnelheid in de Baltische Zee. Deze relatie kan worden gebruikt om bestaande ecosysteemmodellen van de Baltische Zee uit te breiden met een beschrijving van resuspensie en lateraal transport van sediment en organisch materiaal.

Identificeerbaarheidsanalyse en Bayesiaanse onzekerheidsanalyse werden nog niet eerder in diagenetische modellen gebruikt, maar het nut van beide technieken is aangetoond in hoofdstuk 5. Beide technieken kunnen ook op complexere diagenetische modellen (zie bijvoorbeeld hoofdstuk 4) worden toegepast om de strategie van veldmetingen te optimaliseren en een onzekerheidsschatting van gemodelleerde reaktiesnelheden te bepalen. De reaktiesnelheid en onzekerheid van bijvoorbeeld denitrificatie kan met gemeten snelheden (met bijvoorbeeld de N_2/Ar technieken) worden vergeleken om de modelresultaten te valideren of om tekortkomingen van de huidige modellen te vinden.

Acknowledgments

First and foremost I want to thank my supervisors, Jack, Karline and Carlo for giving me the opportunity to work at NIOO and supporting me during four years in my work with ideas, valuable knowledge and all other assistance in order to being able to perform the research which finally ended up in this thesis. Jack, you were always very supportive with both modeling and experimental work. I appreciate your fast, yet thorough response in connection with reviewing manuscripts and this thesis. Karline, you taught me a lot about modeling, both concepts and techniques. Without your guidance in biogeochemical modeling I would not be where I am today.

I would like to thank the members of the reading committee for accepting the task to read and approve my thesis, Ronnie Glud, Greg Cowie, Per Hall, Philippe van Capellen and Gert de Lange.

I'm grateful to Greg Cowie, Lisa Levin and all others involved in the Arabian Sea project for putting together this project, where my PhD project could be part of. Being on sea for eight weeks is very special, certainly both interesting and exciting, but sometimes also hard when you have to leave your beloved one at home, or simply when you are out of fresh fruit or decent wine and have to settle with beer brewed in the Seychelles.

In connection with planning the work for the Arabian Sea, performing the chemical analyses at home and in the end interpreting the results, I would like to thank Leon Moodley for always helping out.

I also would like to thank the people working in the department of Marine Chemistry at Göteborg University, Per, Anders and Elin for being able to continue our work together despite me moving to the Netherlands. There where many moments of joy and some of seasickness on or on the way to the Gulf of Finland. I hope that our collaboration will continue also in the future.

Els, you took care of all us disoriented newcomers at NIOO, it was very

nice to have you around. The soup, the chats during coffee breaks, more important to me than can be described in words ...

The staff downstairs in the labs also deserves a lot of credit after analysing thousands of samples!! Thank you Joop, Marco, Cobie, Jan, Yvonne, Peter and Pieter.

I want to direct a special thanks to Dick for helping me out in all sorts of situations, ranging from model development to assistance with calling stubborn Dutch electricity companies. And of course for supporting me as "paranimf" during my thesis defense. I also enjoyed you as a dive buddy and coming to your home and being served food based on recipes from countries I barely knew existed.

I liked the the international atmosphere at the NIOO, something I doubt I will experience again. If you were curios how things worked in Belgium, Spain, France, Germany, Italy, Ukraine, Thailand, China, Portugal and of course the Netherlands, there were always someone to ask.

Karel, you shared office with me for a long time, even though I was hidden behind my big computer screen, it was always nice to have you around to discuss with, about all silly emails, about isotopes, R, LaTeX and many other things. Thank you for supporting me on my defense as my "paranimf". I also enjoyed the ski holidays, and I was happy to see you down the black slope. I am of course also quite amused to see you going headfirst down it. This is a moment that will stay in my memory for long ... since I have it on tape ;-)

From the first day at the NIOO until today and hopefully longer, Britta, you were always there when me and Maria needed help with moving, painting or cat-sitting. I hope you will visit us now and then, despite the fact that you have returned to the Danish backwaters.

Those among us skilled in mathematics can quickly calculate that four years is a significant part of a lifetime. My time in the Netherlands was not only dedicated to work. I also took the opportunity, as suggested by my supervisors, to have a look around. I visited a lot places in France, the Belgian Ardennes (love the beer!) and the Netherlands and certainly around Zeeland. I am happy to have seen and experienced many new things, like paddling gently through the wetlands in the Biesbosch to sea kayaking in fierce waves in the North Sea (thank you people in Kanoclub Zeeland). I am also very glad to have made some new friends, you know you are always welcome to Sweden!

Curriculum Vitae

Henrik Andersson was on born on the 15th of December in Sölvesborg, Sweden. At Göteborg University he studied mainly chemistry biology and specialized in marine chemistry with the study of biogeochemistry in marine sediments of the Hanö Bay under the supervision of Prof. Per Hall. After completion of his MSc degree (in swedish *Fil. Mag.*) he continued to work for some time in the group of Prof. Per Hall. From February 2002 until May 2006, he worked as a PhD student at the Netherlands Institute of Ecology (NIOO-KNAW), Center for Estuarine and Marine Ecology in Yerseke. The research performed during this period is presented in this thesis. In June 2006 he joined the Danish Meteorological Institute, Centre for Ocean and Ice in Copenhagen, Denmark working as an ecological modeller with 3D-models of the North Sea/Baltic Sea.

Publications

2007

J.H. Andersson C. Woulds, M. Schwartz, G. L. Cowie, L. A. Levin, K. Soetaert, J.J. Middelburg, Short-term fate of phytodetritus across the Arabian Sea Oxygen Minimum Zone, *Biogeosciences Discussion*, 4:2493–2523

C. Woulds, G.L. Cowie, L.A. Levin, **J.H. Andersson**, J.J. Middelburg, S. Vandewiele, P.A. Lamont, K.E. Larkin, A.J. Gooday, S. Schumacher, C. Whitcraft, R.M. Jeffreys, M. Schwartz, Oxygen as a control on sea floor biological communities and their roles in sedimentary carbon cycling, *Limnology and Oceanography*, 52(4):1698-1709

2006

J.H. Andersson, J.J. Middelburg och K. Soetaert, Identifiability and uncertainty of bio-irrigation rates, *Journal of Marine Research* 64:3 407–429

A. Tengberg, J. Hovdenes, **J.H. Andersson** and 12 other authors, Evaluation of a Life Time based Optode to measure Oxygen in Aquatic Systems, *Limnology and Oceangraphy: Methods* 4:7–17

2004

A. Tengberg, H. Ståhl, G. Gust, P.O.J. Hall, V. Müller, U. Arning, **H. Andersson**, Intercalibration of benthic flux chambers I. Accuracy of flux measurements and influence of chamber hydrodynamics, *Progress in Oceanography* 60:1–28

J.H. Andersson, J. W. M. Wijsman, P. M. J. Herman, J. J. Middelburg, K. Soetaert, and C. Heip, Respiration patterns in the deep ocean, *Geophysical Research Letters*, 31, L03304, doi:10.1029/2003GL018756

2001

H. Andersson, Sedimentary carbon dynamics in the Hanö Bay, Baltic Sea : Diagenetic modelling of field data, *MSc Thesis*

In press

C. Woulds, **J. H. Andersson**, G. L. Cowie, J. J. Middelburg and L. A. Levin, ^{13}C tracer studies on the short-term fate of organic carbon in marine sediments: comparing the Pakistan margin to other regions, *Deep-Sea Research II*

In preparation

J. H. Andersson, A. Tengberg, H. Stahl, J. J. Middelburg, K. Soetaert and P. O. J. Hall, Respiration of organic carbon in sediments of the Gulf of Finland, Baltic Sea

Bibliography

Number(s) following each reference points to the page(s) were they referred to.

Aller, R. C. (1980). Quantifying solute distributions in the bioturbated zone of marine sediments by defining an average microenvironment. *Geochimica et Cosmochimica Acta*, 44(12):1955–1965. 81

Aller, R. C. (1994). The sedimentary Mn cycle in Long-Island Sound - its role as intermediate oxidant and the influence of bioturbation, O_2, and C_{ORG} flux on diagenetic reaction balances. *Journal of Marine Research*, 52(2):259–295. 27

Aller, R. C. and Aller, J. Y. (1992). Meiofauna and solute transport in marine muds. *Limnology and Oceanography*, 37(5):1018–1033. 81

Anderson, L. G., Hall, P. O. J., Iverfeldt, A., Rutgers van der Loeff, M. M., Sundby, B., and Westerlund, S. F. G. (1986). Benthic respiration measured by total carbonate production. *Limnology and Oceanography*, 31(2):319–329. 51, 71, 72

Andersson, J. H., Middelburg, J. J., and Soetaert, K. (2006). Identifiability and uncertainty analysis of bio-irrigation rates. *Journal of Marine Research*, 64(3):407–429. 54

Andersson, J. H., Wijsman, J. W. M., Herman, P. M. J., Middelburg, J. J., K, S., and C, H. (2004). Respiration in the deep ocean. *Geophysical Research Letters*, 31:L03304. doi:10.1029/2003GL018756. 44

Antia, A. N., Koeve, W., Fischer, G., Blanz, T., Schulz-Bull, D., Scholten, J., Neuer, S., Kremling, K., Kuss, J., Peinert, R., Hebbeln, D., Bathmann, U., Conte, M., Fehner, U., and Zeitschel, B. (2001). Basin-wide particulate carbon flux in the Atlantic Ocean: regional export patterns

and potential for atmospheric CO_2 sequesteration. *Global Biogeochemical Cycles*, 15(4):845–862. 14, 19

Archer, D. and Devol, A. (1992). Benthic oxygen fluxes on the Washington shelf and slope - a comparison of in situ microelectrode and chamber flux measurements. *Limnology and Oceanography*, 37(3):614–629. 7, 16

Aristegui, J., Agusti, S., and Duarte, C. M. (2003). Respiration in the dark ocean. *Geophysical Research Letters*, 30(2):1041. doi:10.1029/2002GL016227. 19, 21, 22, 23

Armstrong, R. A., Lee, C., Hedges, J. I., Honjo, S., and Wakeham, S. G. (2002). A new, mechanistic model for organic carbon fluxes in the ocean based on the quantitative association poc with ballast minerals. *Deep Sea Research Part II: Topical Studies in Oceanography*, 49:219–236. 20

Atwood, D. K., Kinard, W. F., Barcelona, M. J., and Johnson, E. C. (1977). Comparison of polarographic electrode and winkler titration determinations of dissolved-oxygen in oceanographic samples. *Deep-Sea Research*, 24(3):311–313. 112

Balzer, W. (1984). Organic-matter degradation and biogenic element cycling in a nearshore sediment (Kiel-bight). *Limnology and Oceanography*, 29(6):1231–1246. 50, 64

Barnett, P. R. O., Watson, J., and Connelly, D. (1984). A multiple corer for taking virtually undisturbed samples from shelf, bathyal and abyssal sediments. *Oceanologica Acta*, 7(4):399–408. 4, 28, 54

Beaulieu, S. E. (2002). Accumulation and fate of phytodetritus on the sea floor. *Oceanography and Marine Biology: An annual review*, 40:171–232. 26, 44

Beaulieu, S. E. (2003). Resuspension of phytodetritus from the sea floor: A laboratory flume study. *Limnology and Oceanography*, 48(3):1235–1244. 44

Benitez-Nelson, C. R. (2000). The biogeochemical cycling of phosphorus in marine systems. *Earth-Science Reviews*, 51:109–135. 3

Benoit, J. M., Torgersen, T., and Odonnell, J. (1991). An advection/diffusion model for ^{222}Rn transport in near-shore sediments inhabited by sedentary polychaetes. *Earth and Planetary Science Letters*, 105(4):463–473. 80

Berelson, W. M. (2002). Particle settling rates increase with depth in the ocean. *Deep Sea Research Part II: Topical Studies in Oceanography*, 49:237–251. 20

Berelson, W. M., Heggie, D., Longmore, A., Kilgore, T., Nicholson, G., and Skyring, G. (1998). Benthic nutrient recycling in Port Phillip Bay, Australia. *Estuarine Coastal and Shelf Science*, 46(6):917–934. 80

Berelson, W. M., Townsend, T., Heggie, D., Ford, P., Longmore, A., Skyring, G., Kilgore, T., and Nicholson, G. (1999). Modelling bioirrigation rates in the sediments of Port Phillip Bay. *Marine and Freshwater Research*, 50(6):573–579. 80

Berelson, W. T., McManus, J., Coale, K. H., Johnson, K. S., Kilgore, T., Burdige, D. J., and Pilskaln, C. H. (1996). Biogenic matter diagenesis on the sea floor: A comparison between two continental margin transects. *Journal of Marine Research*, 54:731–762. 74, 75

Berg, P., Risgaard-Petersen, N., and Rysgaard, S. (1998). Interpretation of measured concentration profiles in sediment pore water. *Limnology and Oceanography*, 43(7):1500–1510. 7

Berg, P., Røy, H., Janssen, F., Meyer, V., Jørgensen, B. B., Huettel, M., and de Beer, D. (2003a). Oxygen uptake by aquatic sediments measured with a novel non-invasive eddy-correlation technique. *Marine Ecology-Progress Series*, 261:75–83. 130

Berg, P., Rysgaard, S., and Funch, P. (2001). Effects of bioturbation on solutes solids in marine sediments. *Aquatic Microbial Ecology*, 26:81–94. 103

Berg, P., Rysgaard, S., and Thamdrup, B. (2003b). Dynamic modeling of early diagenesis and nutrient cycling. A case study in an Arctic marine sediment. *American Journal of Science*, 303(10):905–955. 9, 85

Berner, R. A. and Raiswell, R. (1983). Burial of organic carbon and pyrite sulfur in sediments over phanerozoic time: a new theory. *Geochimica et Cosmochimica Acta*, 47:855–862. 1

Berntsson, M., Tengberg, A., Hall, P. O. J., and Josefson, M. (1997). Multivariate experimental methodology applied to the calibration of a Clark type oxygen sensor. *Analytica Chimica Acta*, 355(1):43–53. 112, 118

Bird, F. L., Ford, P. W., and Hancock, G. J. (1999). Effect of burrowing macrobenthos on the flux of dissolved substances across the water-sediment interface. *Marine and Freshwater Research*, 50(6):523–532. 80

Blair, N. E., Levin, L. A., DeMaster, D. J., and Plaia, G. (1996). The short-term fate of fresh algal carbon in continental slope sediments. *Limnology and Oceanography*, 41(6):1208–1219. 27

Boschker, H. T. S., de Brouwer, J. F. C., and Cappenberg, T. E. (1999). The contribution of macrophyte-derived organic matter to microbial biomass in salt-marsh sediments: Stable carbon isotope analysis of microbial biomarkers. *Limnology and Oceanography*, 44(2):309–319. 30

Boschker, H. T. S. and Middelburg, J. J. (2002). Stable isotopes and biomarkers in microbial ecology. *FEMS Microbiology Ecology*, 40(2):85–95. 32

Boudreau, B. P. (1984). On the equivalence of nonlocal and radial diffusion models for porewater irrigation. *Journal of Marine Research*, 42(3):731–735. 81

Boudreau, B. P. (1997). *Diagenetic models and their implementation.* Springer, Berlin. 66, 69, 81, 85

Bouldin, D. R. (1968). Models for describing the diffusion of oxygen and other mobile consituents across the mud-water interface. *Journal of Ecology*, 56(1):77–87. 7

Bourget, E., Ardisson, P. L., Lapointe, L., and Daigle, G. (2003). Environmental factors as predictors of epibenthic assemblage biomass in the St.

Lawrence system. *Estuarine Coastal and Shelf Science*, 57(4):641–652. 118

Boyd, P. W. and Stevens, C. L. (2002). Modelling particle transformations and the downward organic carbon flux in the ne atlantic ocean. *Progress in Oceanography*, 52(1):1–29. 14

Briggs, R. and Viney, M. (1964). Design + performance of temperature compensated electrodes for oxygen measurements. *Journal of Scientific Instruments*, 41(2):78–83. 112

Brun, R., Kuhni, M., Siegrist, H., Gujer, W., and Reichert, P. (2002). Practical identifiability of ASM2d parameters - systematic selection and tuning of parameter subsets. *Water Research*, 36(16):4113–4127. 85

Brun, R., Reichert, P., and Kunsch, H. R. (2001). Practical identifiability analysis of large environmental simulation models. *Water Resources Research*, 37(4):1015–1030. 9, 82, 86, 87

Bühring, S. I., Lampadariou, N., Moodley, L., Tselepides, A., and Witte, U. (2006). Benthic microbial and whole-community responses to different amounts of ^{13}C-enriched algae: In situ experiments in the deep Cretan Sea (Eastern Mediterranean). *Limnology and Oceanography*, 51(1):157–165. 45

Burdige, D. J. (2005). Burial of terrestrial organic matter in marine sediment: A re-assessment. *Global Biogeochemical Cycles*, 19:GB4011. doi:10.1029/2004BG002368. 75

Burdige, D. J. (2007). Preservation of organic matter in marine sediments: Controls, mechanisms, and an imbalance in sediment organic carbon budgets? *Chemical Reviews*, 107(2):467–485. 27

Canfield, D. E. and Teske, A. (1996). Late Proterozoic rise in atmospheric oxygen concentration inferred from phylogenetic and sulphur-isotope studies. *Nature*, 382:127–132. 2

Catling, D. C. and Claire, M. W. (2005). How Earth's atmosphere evolved to an oxic state: A status report. *Earth and Planetary Science Letters*, 237:1–20. 1

Clark, L. C. J. (1959). Electrochemical device for chemical analysis. US patent number 2,913,386. 112

Conley, D. J., Humborg, C., Rahm, L., Savchuk, O. P., and Wulff, F. (2002). Hypoxia in the Baltic Sea and basin-scale changes in phosphorus biogeochemistry. *Environmental Science & Technology*, 36(24):5315–5320. 51

Conley, D. J., Stockenberg, A., Carman, C., Johnstone, R. W., Rahm, L., and Wulff, F. (1997). Sediment-water nutrient fluxes in the Gulf of Finland, Baltic Sea. *Estuarine Coastal and Shelf Science*, 45:591–598. 50, 64

Cowie, G. L., Calvert, S. E., Pedersen, T. F., Schulz, H., and von Rad, U. (1999). Organic content and preservational controls in surficial shelf and slope sediments from the Arabian Sea (Pakistan margin). *Marine Geology*, 161:23–38. 27

Dauwe, B., Middelburg, J. J., Herman, P. M. J., and Heip, C. H. R. (1999). Linking diagenetic alteration of amino acids and bulk organic matter reactivity. *Limnology and Oceanography*, 44(7):1809–1814. 20

del Giorgio, P. A. and Duarte, C. M. (2002). Respiration in the open ocean. *Nature*, 420(6914):379–384. 23

Demas, J. N., DeGraff, B. A., and Coleman, P. B. (1999). Oxygen sensors based on luminescence quenching. *Analytical Chemistry*, 71(23):793A–800A. 113, 114, 116

Devol, A. H. and Hartnett, H. E. (2001). Role of the oxygen-deficient zone in transfer of organic carbon to the deep ocean. *Limnology and Oceanography*, 46(7):1684–1690. 19, 44

Dowd, M. and Meyer, R. (2003). A Bayesian approach to the ecosystem inverse problem. *Ecological Modelling*, 168(1-2):39–55. 82

Dyrssen, D., Hall, P., and Westerlund, S. (1984). Benthic chamber chemistry. *Fresenius' Journal of Analytical chemistry*, 317(3-4):380–382. 4

Emerson, S., Jahnke, R., and Heggie, D. (1984). Sediment-water exchange in shallow-water estuarine sediments. *Journal of Marine Research*, 42(3):709–730. 80, 81, 102

Epping, E., van der Zee, C., Soetaert, K., and Helder, W. (2002). On the oxidation and burial of organic carbon in sediments of the Iberian margin and Nazare Canyon (NE Atlantic). *Progress in Oceanography*, 52(2-4):399–431. 4, 16, 103

Forster, S., Glud, R. N., Gundersen, J. K., and Huettel, M. (1999). In situ study of bromide tracer and oxygen flux in coastal sediments. *Estuarine Coastal and Shelf Science*, 49:813–827. 85, 101, 107

Forster, S., Khalili, A., and Kitlar, J. (2003). Variation of nonlocal irrigation in a subtidal benthic community. *Journal of Marine Research*, 61(3):335–357. 80, 81, 89, 104, 106

Francois, R., Honjo, S., Krishfield, R., and Manganini, S. (2002). Factors controlling the flux of organic carbon to the bathypelagic zone of the ocean. *Global Biogeochemical Cycles*, 16(4):1087. doi:10.1029/2001GB001722. 26, 118

Garcia, H. E. and Gordon, L. I. (1992). Oxygen solubility in seawater - better fitting equations. *Limnology and Oceanography*, 37(6):1307–1312. 118, 122, 123, 133

Gelman, A., Carlin, J. B., Stern, H. S., and Rubin, D. B. (2003). *Bayesian Data Analysis*. Chapman and Hall, London. 87

Gilks, W., Richardson, S., and Spiegelhalter, D. (1996). *Markov Chain Monte Carlo in practice*. Chapman and Hall, London. 88

Glud, R. N., Gundersen, J., and Ramsing, N. (2000). Electrochemical and optical oxygen microsensors for in situ measurements. In Buffle, J. and Horvai, G., editors, *In situ monitoring of aquatic systems: Chemical analysis and speciation*. Wiley, New York. 4, 112, 113, 114, 130

Glud, R. N., Gundersen, J. K., and Holby, O. (1999a). Benthic in situ respiration in the uppwelling area off central Chile. *Marine Ecology Progress Series*, 186:9–18. 112

Glud, R. N., Gundersen, J. K., Jørgensen, B. B., Revsbech, N. P., and Schulz, H. D. (1994). Diffusive and total oxygen-uptake of deep-sea sediments in the eastern South-Atlantic ocean - in-situ and laboratory measurements. *Deep Sea Research Part I: Oceanographic Research Papers*, 41(11-12):1767–1788. 4, 41

Glud, R. N., Gundersen, J. K., Revsbech, N. P., Jørgensen, B. B., and Hüttel, M. (1995). Calibration and performance of the stirred flux chamber from the benthic lander Elinor. *Deep Sea Research Part I: Oceanographic Research Papers*, 42(6):1029–1042. 29

Glud, R. N., Gundersen, J. K., Røy, H., and Jørgensen, B. B. (2003). Seasonal dynamics of benthic O_2 uptake in a semienclosed bay: Importance of diffusion and faunal activity. *Limnology and Oceanography*, 48(3):1265–1276. 7

Glud, R. N., Kühl, M., Kohls, O., and Ramsing, N. B. (1999b). Heterogeneity of oxygen production and consumption in a photosynthetic microbial mat as studied by planar optodes. *Journal of Phycology*, 35(2):270–279. 113

Glud, R. N., Tengberg, A., Kühl, M., Hall, P. O. J., Klimant, I., and Holst, G. (2001). An in situ instrument for planar O_2 optode measurements at benthic interfaces. *Limnology and Oceanography*, 46(8):2073–2080. 113

Glud, R. N., Wenzhofer, F., Tengberg, A., Middelboe, M., Oguri, K., and Kitazato, H. (2005). Distribution of oxygen in surface sediments from central Sagami Bay, Japan: In situ measurements by microelectrodes and planar optodes. *Deep Sea Research Part I: Oceanographic Research Papers*, 52(10):1974–1987. 113

Gneigner, E. and Forstner, H. (1983). *Polarographic oxygen sensors*. Springer, Heidelberg. 112

Gooday, A. J. (2002). Biological responses to seasonally varying fluxes of organic matter to the ocean floor: A review. *Journal of Oceanography*, 58(2):305–332. 26

Grigg, N. J., Boudreau, B. P., Webster, I. T., and Ford, P. W. (2005). The nonlocal model of porewater irrigation: Limits to its equivalence with

a cylinder diffusion model. *Journal of Marine Research*, 63(2):437–455. 83, 102

Gundersen, J. K., Ramsing, N. B., and Glud, R. N. (1998). Predicting the signal of O_2 microsensors from physical dimensions, temperature, salinity, and O_2 concentration. *Limnology and Oceanography*, 43(8):1932–1937. 112

Haake, B., Ittekkot, V., Rixen, T., Ramaswamy, V., Nair, R. R., and Curry, W. B. (1993). Seasonality and interannual variability of particle fluxes to the deep Arabian sea. *Deep Sea Research Part I: Oceanographic Research Papers*, 40(7):1323–1344. 26

Hall, P. O. J., Brunnegård, J., Hulthe, G., Martin, W. R., Stahl, H., and Tengberg, A. (2007). Dissolved organic matter in abyssal sediment: Core recovery artifacts. *Limnology and Oceanography*, 52(1):19–31. 4

Harmon, R. and Challenor, P. (1997). A Markov chain Monte Carlo method for estimation and assimilation into models. *Ecological Modelling*, 101(1):41–59. 82

Hartnett, H. E., Keil, R. G., Hedges, J. I., and Devol, A. H. (1998). Influence of oxygen exposure time on organic carbon preservation in continental margin sediments. *Nature*, 391(6667):572–574. 27, 47

Haus, F., Boissel, O., and Junter, G. A. (2003). Multiple regression modelling of mineral base oil biodegradability based on their physical properties and overall chemical composition. *Chemosphere*, 50(7):939–948. 118

Hedges, J. I. and Keil, R. G. (1995). Sedimentary organic-matter preservation - an assessment and speculative synthesis. *Marine Chemistry*, 49(2-3):81–115. 3

Hedges, J. I., S, H. F., Devol, A. H., Hartnett, H. E., Tsamakis, E., and Keil, R. G. (1999). Sedimentary organic matter preservation: A test for selective degradation under oxic conditions. *American Journal of Science*, 299(7-9):529–555. 47

Heinze, C., Maier-Raimer, E., Winguth, A. M. E., and Archer, D. (1999). A global oceanic sediment model for long-term climate studies. *Global Biogeochemical Cycles*, 13(1):221–250. 14, 18, 19

Heip, C. H. R., Duineveld, G., Flach, E., Graf, G., Helder, W., Herman, P. M. J., Lavaleye, M., Middelburg, J. J., Pfannkuche, O., Soetaert, K., Soltwedel, T., Stigter, H. d., Thomsen, L., Vanaverbeke, J., and de Wilde, P. (2001). The role of the benthic biota in sedimentary metabolism and sediment-water exchange processes in the goban spur area (ne atlantic). *Deep Sea Research Part II: Topical Studies in Oceanography*, 48(14-15):3223–3243. 14

Helly, J. J. and Levin, L. A. (2004). Global distribution of naturally occurring marine hypoxia on continental margins. *Deep Sea Research Part I: Oceanographic Research Papers*, 51(9):1159–1168. 27

Herman, P. M., Soetaert, K., Middelburg, J. J., Heip, C., Lohse, L., Epping, E., Antia, A. N., and Peinert, R. (2001). The seafloor as the ultimate sediment trap - using sediment properties to constrain benthic-pelagic exchange processes at the goban spur. *Deep Sea Research Part II: Topical Studies in Oceanography*, 48(14-15):3245–3264. 3, 14

Herman, P. M. J., Middelburg, J. J., Koppel, J. V. d., and Heip, C. H. R. (1999). Ecology of estuarine macrobenthos. *Advances in Ecological Research*, 29:195–240. 7, 80

Hitchman, M. L. (1978). *Measurements of dissolved oxygen*, volume 49 of *Chemical Analysis*. John Wiley, New York. 112

Holst, G., Glud, R. N., Kühl, M., and Klimant, I. (1997). A microoptode array for fine-scale measurement of oxygen distribution. *Sensors and Actuators B-Chemical*, 38(1-3):122–129. 113

Holst, G., Kohls, O., Klimant, I., Konig, B., Kühl, M., and Richter, T. (1998). A modular luminescence lifetime imaging system for mapping oxygen distribution in biological samples. *Sensors and Actuators B-Chemical*, 51(1-3):163–170. 113

Holst, G., Kühl, M., and Klimant, I. (1995). A novel measuring system for oxygen microoptodes based on a phase modulation technique. In

Scheggi, A. V., editor, *Proceedings SPIE Chemical, Biochemical, and Environmental Fiber Sensors VII*, volume 2508, pages 387–398. doi: 10.1117/12.221754. 113

Huber, C., Klimant, I., Krause, C., Werner, T., Mayr, T., and Wolfbeis, O. S. (2000). Optical sensor for seawater salinity. *Fresenius' Journal of Analytical chemistry*, 368(2-3):196–202. 113

Huber, C., Klimant, I., Krause, C., Werner, T., and Wolfbeis, O. S. (2001a). Nitrate-selective optical sensor applying a lipophilic fluorescent potential-sensitive dye. *Analytica Chimica Acta*, 449(1-2):81–93. 113

Huber, C., Klimant, I., Krause, C., and Wolfbeis, O. S. (2001b). Dual lifetime referencing as applied to a chloride optical sensor. *Analytical Chemistry*, 73(9):2097–2103. 113

Hulth, S., Aller, R. C., Engström, P., and Selander, E. (2002). A pH plate fluorosensor (optode) for early diagenetic studies of marine sediments. *Limnology and Oceanography*, 47(1):212–220. 113

Hulthe, G., Hulth, S., and Hall, P. O. J. (1998). Effect of oxygen on degradation rate of refractory and labile organic matter in contintental margin sediments. *Geochimica et Cosmochimica Acta*, 62(8):1319–1328. 48

Jackson, G. A. and Burd, A. B. (2002). A model for the distribution of particle flux in the mid-water column controlled by subsurface biotic interactions. *Deep Sea Research Part II: Topical Studies in Oceanography*, 49:193–217. 20

Jahnke, R. A. (1996). The global ocean flux of particulate organic carbon: Areal distribution and magnitude. *Global Biogeochemical Cycles*, 10(1):71–88. 21, 23

Jahnke, R. A. (2005). Transport processes and organic matter cycling in coastal sediments. In Robinson, A. R. and Brink, K. H., editors, *The Sea*, volume 13. Harvard University Press. 138, 142

Jahnke, R. A., Reimers, C. E., and Craven, S. B. (1990). Intensification of recycling of organic matter at the sea floor near ocean margins. *Nature*, 348:50–54. 3

Jørgensen, B. B. and Revsbech, N. P. (1985). Diffusive boundary-layers and the oxygen-uptake of sediments and detritus. *Limnology and Oceanography*, 30(1):111–122. 6

Jørgensen, B. B. (1983). Processes at the sediment-water interface. In Bolin, B. and Cook, R. B., editors, *The major biogeochemical cycles and their interactions*, pages 477–515. Wiley, New York. 5, 7

Kamp, A. and Witte, U. (2005). Processing of ^{13}C-labelled phytoplankton in a fine-grained sandy-shelf sediment (North sea): relative importance of different macrofauna species. *Marine Ecology Progress Series*, 297:61–70. 46

Kanwisher, J. (1959). Polarographic oxygen electrode. *Limnology and Oceanography*, 4(2):210–217. 112

Karlson, K., Rosenberg, R., and Bonsdorff, E. (2002). Temporal and spatial large-scale effects of eutrophication and oxygen deficiency on benthic fauna in Scandinavian and Baltic waters - a review. *Oceanography and Marine Biology: An annual review*, 40:427–489. 51

Kautsky, H. (1939). Quenching of luminescence by oxygen. *Transactions of the Faraday Society*, 35:216–219. 112

Kawamiya, M. and Oschlies, A. (2003). An eddy-permitting, coupled ecosystem-circulation model of the Arabian Sea: comparison with observations. *Journal of Marine Systems*, 38(3-4):221–257. 26

Keeling, R. F. and Garcia, H. E. (2002). The change in oceanic O_2 inventory associated with recent global warming. *Proceedings of the National Academy of Sciences of the United States of America*, 99(12):7848–7853. 27

Kemp, W. M., Boynton, W. R., Adolf, J E Boesch, D. F., Boicourt, W. C., Brush, G., Cornwell, J. C., Fisher, T. R., Glibert, P Mand Hagy, J. D., Harding, L. W., Houde, E. D., Kimmel, D. G., Miller, W. D., Newell, R.

I. E., Roman, M. R., Smith, E. M., and JC, S. (2005). Eutrophication of Chesapeake Bay: historical trends and ecological interactions. *Marine Ecology Progress Series*, 303:1–29. 3

Kemp, W. M., Sampou, P., Caffrey, J., Mayer, M., Henriksen, K., and Boynton, W. R. (1990). Ammonium recycling versus denitrification in Chesapeake Bay sediments. *Limnology and Oceanography*, 35(7):1545–1563. 3

Kiirikki, M., Inkala, A., Kuosa, H., Pitkänen, H., Kuusisto, M., and Sarkkula, J. (2001). Evaluating the effects of nutrient load reductions on the biomass of toxic nitrogen-fixing cyanobacteria in the Gulf of Finland, Baltic Sea. *Boreal Environmental Research*, 6(2):131–146. 50

Kiirikki, M., Lehtoranta, J., Inkala, A., Pitkänen, H., Hietanen, S., Hall, P. O. J., Tengberg, A., Koponen, J., and Sarkkula, J. (2006). A simple sediment process description suitable for 3D-ecosystem modelling - Development and testing in the Gulf of Finland. *Journal of Marine Systems*, 61(1-2):55–66. 50

Klimant, I., Huber, C., Liebsch, G., Neurauter, G., Stangelmayer, A., and Wolfbeis., O. S. (2000). Dual lifetime referencing (dlr) - a new scheme for converting fluorescence intensity into a frequency-domain or time-domain information. In Valeur, B. and Brochon, C., editors, *Fluorescence Spectroscopy: New Methods and Applications*. Springer, Berlin. 113

Klimant, I., Kühl, M., Glud, R. N., and Holst, G. (1997). Optical measurement of oxygen and temperature in microscale: strategies and biological applications. *Sensors and Actuators B: Chemical*, 38(1-3):29–37. 113, 114, 132

Klimant, I., Meyer, V., and Kühl, M. (1995). Fiber-optic oxygen microsensors, a new tool in aquatic biology. *Limnology and Oceanography*, 40(6):1159–1165. 112, 113

Knoll, A. H. and Carroll, S. B. (1999). Early animal evolution: Emerging views from comparative biology and geology. *Science*, 284(5423):2129–2137. 1

Koop, K., Boynton, W. R., Wulff, F., and Carman, R. (1990). Sediment-water oxygen and nutrient exchanges along a depth gradient in the Baltic Sea. *Marine Ecology Progress Series*, 63(1):65–77. 50, 64

Körtzinger, A., Hedges, J. I., and Quay, P. D. (2001). Redfield ratios revisited: Removing the biasing effect of anthropogenic CO_2. *Limnology and Oceanography*, 46(4):964–970. 23

Körtzinger, A., Schimanski, J., and Send, U. (2005). High quality oxygen measurements from profiling floats: A promising new technique. *Journal of Atmospheric and Oceanic Technology*, 22(3):302–308. 120

Körtzinger, A., Schimanski, J., Send, U., and Wallace, D. (2004). The ocean takes a deep breath. *Science*, 306(5700):1337–1337. 120

Kriest, I. and Evans, G. T. (1999). Representing phytoplankton aggregates in biogeochemical models. *Deep Sea Research Part I: Oceanographic Research Papers*, 46(11):1841–1859. 26

Kristensen, E., Ahmed, S. I., and Devol, A. H. (1995). Aerobic and anaerobic decomposition of organic matter in marine sediment: Which is fastest? *Limnology and Oceanography*, 40(8):1430–1437. 48

Kuhrts, C., Fennel, W., and Seifert, W. (2004). Model studies of transport of sedimentary material in the Western Baltic. *Journal of Marine Systems*, 52:167–190. 75

Lampitt, R. S., Raine, R. C. T., Billett, D. S. M., and Rice, A. L. (1995). Material supply to the european continental slope: A budget based on benthic oxygen demand and organic supply. *Deep Sea Research Part I: Oceanographic Research Papers*, 42(11-12):1865–1880. 3

Lenton, T. M. (2003). The coupled evolution of life and atmospheric oxygen. In Rothschild, L. and Lister, A., editors, *Evolution on planet Earth: the impact of the physical environment*, pages 35–53. Academic Press, London. 1

Levin, L., Blair, N., DeMaster, D., Plaia, G., Fornes, W., Martin, C., and Thomas, C. (1997). Rapid subduction of organic matter by maldanid

polychaetes on the North Carolina slope. *Journal of Marine Research*, 55:596–611. 46

Levin, L. A. (2003). Oxygen minimum zone benthos: Adaptation and community response to hypoxia. *Oceanography and Marine Biology: An annual review*, 41:1–45. 3, 133

Logan, G. B., Hayes, J. M., Hieshima, G. B., and Summons, R. (1995). Terminal Proterozoic reorganization of biogeochemical cycles. *Nature*, 376:53–56. 2

Malve, O., Laine, M., and Haario, H. (2005). Estimation of winter respiration rates and prediction of oxygen regime in a lake using bayesian inference. *Ecological Modelling*, 182(2):183–197. 83

Martin, J. H., Knauer, G. A., Karl, D. M., and Broenkow, W. W. (1987). VERTEX: Carbon cycling in the northeast Pacific. *Deep-Sea Research*, 34:267–285. 15, 18, 19

Martin, W. R. and Banta, G. T. (1992). The measurement of sediment irrigation rates - a comparison of the Br^- tracer and $^{222}Rn/^{226}Ra$ disequilibrium techniques. *Journal of Marine Research*, 50(1):125–154. 80, 81, 84, 85

Mayer, L. M. (1994). Surface area control of organic carbon accumulation in continental shelf sediments. *Geochimica et Cosmochimica Acta*, 58(4):1271–1284. 20

Meile, C., Berg, P., Van Cappellen, P., and Tuncay, K. (2005). Solute-specific pore water irrigation: Implications for chemical cycling in early diagenesis. *Journal of Marine Research*, 63(3):601–621. 83, 102

Meile, C. and Van Cappellen, P. (2003). Global estimates of enhanced solute transport in marine sediments. *Limnology and Oceanography*, 48(2):777–786. 85

Meysman, F. J., Galaktionov, O. S., Gribsholt, B., and Middelburg, J. J. (2006). Bio-irrigation in permeable sediments: Advective pore water transport induced by burrow ventilarion. *Limnology and Oceanography*, 51:142–156. 2, 81

Meysman, F. J. R., Middelburg, J. J., Herman, P. M. J., and Heip, C. H. R. (2003). Reactive transport in surface sediments. ii. media: an object-oriented problem-solving environment for early diagenesis. *Computers and Geosciences*, 29(3):301–318. 9

Middelburg, J. J. (1989). A simple rate model for organic-matter decomposition in marine-sediments. *Geochimica et Cosmochimica Acta*, 53(7):1577–1581. 20

Middelburg, J. J., Barranguet, C., Boschker, H. T. S., Herman, P. M. J., Moens, T., and Heip, C. H. R. (2000). The fate of intertidal microphytobenthos carbon: An in situ ^{13}c-labeling study. *Limnology and Oceanography*, 45(6):1224–1234. 30

Middelburg, J. J. and Meysman, F. J. R. (2007). Burial at sea. *Science*, 316:1294–1295. 1

Middelburg, J. J., Soetaert, K., and Herman, P. M. (1997). Empirical relationships for use in global diagenetic models. *Deep Sea Research Part I: Oceanographic Research Papers*, 44(2):327–344. 5, 16, 23

Middelburg, J. J., Soetaert, K., Herman, P. M., and Heip, C. H. (1996). Denitrification in marine sediments: A model study. *Global Biogeochemical Cycles*, 10(4):661–673. 3, 72

Millerway, T., Boland, G., Rowe, G. T., and Twilley, R. R. (1994). Sediment oxygen-consumption and benthic nutrient fluxes on the Louisiana continental-shelf - a methodological comparison. *Environmental Science & Technology*, 17(4):809–815. 5

Miyajima, T., Yamada, Y., Hanba, Y. T., Yoshii, K., Koitabashi, T., and Wada, E. (1995). Determining the stable-isotope ratio of total dissolved inorganic carbon in lake water by GC/C/IRMS. *Limnology and Oceanography*, 40(5):994–1000. 55

Moodley, L., Boschker, H. T. S., Middelburg, J. J., Pel, R., Herman, P. M. J., de Deckere, E., and Heip, C. H. R. (2000). Ecological significance of benthic foraminifera: ^{13}c labelling experiments. *Marine Ecology Progress Series*, 202:289–295. 27, 31

Moodley, L., Middelburg, J. J., Boschker, H. T. S., Duineveld, G. C. A., Pel, R., Herman, P. M. J., and Heip, C. H. R. (2002). Bacteria and foraminifera: key players in a short-term deep-sea benthic response to phytodetritus. *Marine Ecology Progress Series*, 236:23–29. 26, 27, 46

Moodley, L., Middelburg, J. J., Soetaert, K., Boschker, H. T. S., Herman, P. M. J., and Heip, C. H. R. (2005). Similar rapid response to phytodetritus deposition in shallow and deep-sea sediments. *Journal of Marine Research*, 63(2):457–469. 26, 32, 47

Mortazavi, B. and Chanton, J. P. (2004). Use of Keeling plots to determine sources of dissolved organic carbon in nearshore and open ocean systems. *Limnology and Oceanography*, 49(1):102–108. 56, 74

Mucci, A., Sundby, B., Gehlen, M., Arakaki, T., Zhong, S., and Silverberg, N. (2000). The fate of carbon in continental shelf sediments of eastern Canada: a case study. *Deep Sea Research Part II: Topical Studies in Oceanography*, 47:733–760. 75

Munk, W. H. (1966). Abyssal recipes. *Deep-Sea Research*, 13:707–730. 21, 22

Naqvi, S. W. A., Jayakumar, D., Narvekar, P., Naik, H., Sarma, V. V. S. S., D'Souza, W., Joseph, S., and George, M. D. (2000). Increased marine production of N_2O due to intensifying anoxia on the Indian continental shelf. *Nature*, 408:346–349. 27

Neumann, T. (2000). Towards a 3D-ecosystem model of the Baltic Sea. *Journal of Marine Systems*, 25(3):405–419. 50

Nieuwenhuize, J., Maas, Y. E. M., and Middelburg, J. J. (1994). Rapid analysis of organic carbon and nitrogen in particulate materials. *Marine Chemistry*, 45(3):217–224. 55

Omlin, M., Brun, R., and Reichert, P. (2001). Biogeochemical model of lake zurich: sensitivity, identifiability and uncertainty analysis. *Ecological Modelling*, 141(1-3):105–123. 85, 87

O'Sullivan, D. W. and Millero, F. J. (1998). Continual measurement of the total inorganic carbon in surface seawater. *Marine Chemistry*, 60:75–83. 55

Pamatmat, M. M. and Banse, K. (1969). Oxygen consumption by the seabed. II. *in situ* measurements to a depth of 180 m. *Limnology and Oceanography*, 14(2):250–259. 4

Pitkänen, H., Lehtoranta, J., and Räike, A. (2001). Internal nutrient fluxes counteract decreases in external load: the case of the estuarial eastern Gulf of Finland, Baltic Sea. *Ambio*, 30(4):195–201. 50

Plummer, M., Best, N., Cowles, K., and Vines, K. (2006). *coda: Output analysis and diagnostics for MCMC*. R package version 0.10-7. 88

R Development Core Team (2007). *R: A Language and Environment for Statistical Computing*. R Foundation for Statistical Computing, Vienna, Austria. ISBN 3-900051-07-0. 91

Raftery, A. E. and Lewis, S. M. (1996). Implementing MCMC. In Gilks, W., Richardson, S., and Spiegelhalter, D., editors, *Markov chain Monte Carlo in practice*, pages 115–130. Chapman, London. 88

Rao, A. M. F. and Jahnke, R. A. (2004). Quantifying porewater exchange across the sediment-water interface in the deep sea with in situ tracer studies. *Limnology and Oceanography: Methods*, 2:75–90. 54, 81, 82, 101

Revsbech, N. P. (1989). An oxygen microsensor with a guard cathode. *Limnology and Oceanography*, 34(2):474–478. 130

Revsbech, N. P., Sorensen, J., Blackburn, T. H., and Lomholt, J. P. (1980). Distribution of oxygen in marine-sediments measured with microelectrodes. *Limnology and Oceanography*, 25(3):403–411. 6

Rowe, G. T., Cruz-Kaegi, M. E., Morse, J. W., Boland, G. S., and Escobar Briones, E. G. (2002). Sediment community metabolism associated with continental shelf hypoxia, Northern Gulf of Mexico. *Estuaries*, 25:1097–1106. 64, 72

Røy, H., Huettel, M., and JøRgensen, B. B. (2005). The influence of topography on the functional exchange surface of marine soft sediments, assessed from sediment topography measured in situ. *Limnology and Oceanography*, 50(1):106–112. 80

Røy, H., Hüttel, M., and JøRgensen, B. B. (2002). The role of small-scale sediment topography for oxygen flux across the diffusive boundary layer. *Limnology and Oceanography*, 47(3):837–847. 80

Rysgaard, S., Risgaard-Petersen, N., Sloth, N. P., Jensen, K., and Nielsen, L. P. (1994). Oxygen regulation of nitrification and denitrification in sediments. *Limnology and Oceanography*, 39(7):1643–1652. 3

Savchuk, O. and Wulff, F. (2001). A model of the biogeochemical cycles of nitrogen and phosphorus in the Baltic. In Wulff, F., Rahm, L., and Larssson, P., editors, *A systems analysis of the Baltic Sea*, volume 148 of *Ecological studies*, pages 373–415. Springer. 50

Savchuk, O. P. (2002). Nutrient biogeochemical cycles in the Gulf of Riga: scaling up field studies with a mathematical model. *Journal of Marine Systems*, 32(4):253–280. 50

Sayles, F. L. and Martin, W. R. (1995). In situ tracer studies of solute transport across the sediment-water interface at the Bermuda time series site. *Deep Sea Research Part II: Topical Studies in Oceanography*, 42(1):31–52. 81

Sayles, F. L., Martin, W. R., and Deuser, W. G. (1994). Response of benthic oxygen-demand to particulate organic-carbon supply in the deep-sea near Bermuda. *Nature*, 371(6499):686–689. 14, 26

Schabenberger, O. and Pierce, F. J. (2001). *Contemporary statistical models for the plant and soil sciences*. CRC Press, London. 16

Schneider, B., Nagel, K., and Struck, U. (2000). Carbon fluxes across the halocline in the eastern Gotland Sea. *Journal of Marine Systems*, 25:261–268. 77

Schwartz, M., Smith, J., Woulds, C., and Cowie, G. (2007). Laboratory incubations with regulated oxygen concentrations used to measure benthic biogeochemical fluxes in parallel with autonomous lander studies. *Limnology and Oceanography: Methods*, In revision. 29

Seifert, T., Tauber, F., and Kayser, B. (2001). A high resolution spherical grid topography of the Baltic sea, 2nd edition. Baltic Sea Science Congress, Stockholm 25-29. November, Poster #147,http://www.io-warnemuende.de/iowtopo. 52

Short, D. L. and Shell, G. S. G. (1984). Fundamentals of Clark membrane configuration oxygen sensors - some confusion clarified. *Journal of Physics E-Scientific Instruments*, 17(11):1085–1092. 112

Skjelhaugen, O. J. (1999). Thermophilic aerobic reactor for processing organic liquid wastes. *Water Research*, 33(7):1593–1602. 121

Smith, K. L. (1992). Benthic boundary-layer communities and carbon cycling at abyssal depths in the central North Pacific. *Limnology and Oceanography*, 37(5):1034–1056. 26

Smith, K. L., Baldwin, R. J., and Williams, P. M. (1992). Reconciling particulate organic-carbon flux and sediment community oxygen-consumption in the deep North Pacific. *Nature*, 359(6393):313–316. 14

Soetaert, K., deClippele, V., and Herman, P. (2002). Femme, a flexible environment for mathematically modelling the environment. *Ecological Modelling*, 151(2-3):177–193. 91

Soetaert, K., Herman, P. M., Middelburg, J. J., and Heip, C. (1998). Assessing organic matter mineralization, degradability and mixing rate in an ocean margin sediment (Northeast Atlantic) by diagenetic modeling. *Journal of Marine Research*, 56(2):519–534. 9, 85

Soetaert, K., Herman, P. M. J., and Middelburg, J. J. (1996a). Dynamic response of deep-sea sediments to seasonal variations: A model. *Limnology and Oceanography*, 41(8):1651–1668. 26, 66

Soetaert, K., Herman, P. M. J., and Middelburg, J. J. (1996b). A model of early diagenetic processes from the shelf to abyssal depths. *Geochimica et Cosmochimica Acta*, 60(6):1019–1040. 7, 9, 66, 85, 89

Stahl, H., Tengberg, A., Brunnegard, J., Bjornbom, E., Forbes, T. L., Josefson, A. B., Kaberi, H. G., Hassellov, I. M. K., Olsgard, F., Roos, P., and Hall, P. O. J. (2004a). Factors influencing organic carbon recycling and burial in Skagerrak sediments. *Journal of Marine Research*, 62(6):867–907. 74

Stahl, H., Tengberg, A., Brunnegard, J., and Hall, P. O. J. (2004b). Recycling and burial of organic carbon in sediments of the Porcupine abyssal plain, NE Atlantic. *Deep Sea Research Part I: Oceanographic Research Papers*, 51(6):777–791. 54, 89

Stigebrandt, A. and Wulff, F. (1987). A model for the dynamics of nutrients and oxygen in the Baltic proper. *Journal of Marine Research*, 45:729–759. 50

Stoer, J. and Bulirsch, R. (1983). *Introduction to Numerical analysis*. Springer, New York. 89

Stokes, M. D. and Romero, G. N. (1999). An optical oxygen sensor and reaction vessel for high-pressure applications. *Limnology and Oceanography*, 44(1):189–195. 113, 114, 132

Suess, E. (1980). Particulate organic-carbon flux in the oceans - surface productivity and oxygen utilization. *Nature*, 288(5788):260–263. 6, 14, 18, 19, 21

Tengberg, A., Almroth, E., and Hall, P. (2003). Resuspension and its effects on organic carbon recycling and nutrient exchange in coastal sediments: in situ measurements using new experimental technology. *Journal of Experimental Marine Biology and Ecology*, 285-286:119–142. 75

Tengberg, A., De Bovee, F., Hall, P., Berelson, W., Chadwick, D., Ciceri, G., Crassous, P., Devol, A., Emerson, S., Gage, J., Glud, R., Graziottin, F., Gundersen, J., Hammond, D., Helder, W., Hinga, K., Holby, O.,

Jahnke, R., Khripounoff, A., Lieberman, S., Nuppenau, V., Pfannkuche, O., Reimers, C., Rowe, G., Sahami, A., Sayles, F., Schurter, M., Smallman, D., Wehrli, B., and Wilde, P. D. (1995). Benthic chamber and profiling landers in oceanography - a review of design, technical solutions and functioning. *Progress in Oceanography*, 35(3):253–294. 4, 14

Tengberg, A., Hovdenes, J., Andersson, H. J., Brocandel, O., Diaz, R., Hebert, D., Arnerich, T., Huber, C., Körtzinger, A., Khripounoff, A., Rey, F., Rönning, C., Schimanski, J., Sommer, S., and Stangelmayer, A. (2006). Evaluation of a lifetime-based optode to measure oxygen in aquatic systems. *Limnology and Oceanography: Methods*, 4:7–17. 55, 58, 71

Ullman, W. J. and Aller, R. C. (1982). Diffusion coefficients in nearshore marine sediments. *Limnology and Oceanography*, 27(3):552–556. 85

Underwood, A. J. (1997). *Experiments in ecology: their logical design and interpretation using analysis of variance*. Cambridge Unviversity Press, Cambridge, U.K. 8, 9

Vallius, H. (2006). Permanent seafloor anoxia in coastal basins of the northwestern Gulf of Finland, Baltic Sea. *Ambio*, 35(3):105–108. 53

van Cappellen, P. and Wang, Y. (1996). Cycling of iron and manganese in surface sediments: A general theory for the coupled transport and reaction of carbon, oxygen, nitrogen, sulfur, iron and manganese. *American Journal of Science*, 296:197–243. 72

van Oevelen, D., Middelburg, J. J., Soetaert, K., and Moodley, L. (2006). The fate of bacterial carbon in an intertidal sediment: Modeling an in situ isotope tracer experiment. *Limnology and Oceanography*, 51(3):1302–1314. 83

van Weering, T. C. E., De Stigter, H. C., Balzer, W., Epping, E. H. G., Graf, G., Hall, I. R., Helder, W., Khripounoff, A., Lohse, L., McCave, N., Thomsen, L., and Vangries, A. (2001). Benthic dynamics and carbon fluxes on the NW European continental margin. *Deep Sea Research Part II: Topical Studies in Oceanography*, 48(14-15):3191–3221. 3

Voipio, A. (1981). *The Baltic Sea*. Elsevier, Amsterdam. 51

Volk, T. and Hoffert, M. I. (1985). Ocean carbon pumps: Analysis of relative strengths and efficiencies in ocean-driven atmospheric CO_2 change. In Sundquist, E. T. and Broecker, W. S., editors, *The Carbon cycle and atmosheric CO_2 : Natural variations Archean to present*, pages 99–110. American Geophysical Union, Washington. 14, 15, 18

von Bultzingslowen, C., McEvoy, A. K., McDonagh, C., MacCraith, B. D., Klimant, I., Krause, C., and Wolfbeis, O. S. (2002). Sol-gel based optical carbon dioxide sensor employing dual luminophore referencing for application in food packaging technology. *Analyst*, 127(11):1478–1483. 113

Weiss, R. F. (1970). Solubility of nitrogen, oxygen and argon in water and seawater. *Deep-Sea Research*, 17(4):721–735. 118

Wenzhöfer, F. and Glud, R. N. (2002). Benthic carbon mineralization in the Atlantic: a synthesis based on in situ data from the last decade. *Deep Sea Research Part II: Topical Studies in Oceanography*, 49(7):1255–1279. 80

Wenzhöfer, F., Holby, O., and Kohls, O. (2001). Deep penetrating benthic oxygen profiles measured in situ by oxygen optodes. *Deep Sea Research Part I: Oceanographic Research Papers*, 48(7):1741–1755. 112

Weston, N. B. and Joye, S. B. (2005). Temperature-driven decoupling of key phases of organic matter degradation in marine sediments. *Proceedings of the National Academy of Sciences of the United States of America*, 102(47):17036–17040. 47, 138, 142

Westrich, J. T. and Berner, R. A. (1984). The role of sedimentary organic-matter in bacterial sulfate reduction - the G model tested. *Limnology and Oceanography*, 29(2):236–249. 20

Westrich, J. T. and Berner, R. A. (1988). The effect of temperature on rates of sulfate reduction in marine sediments. *Geomicrobiology Journal*, 6(2):99–117. 47

Wiggert, J. D., Hood, R. R., Banse, K., and Kindle, J. C. (2005). Monsoon-driven biogeochemical processes in the Arabian Sea. *Progress in Oceanography*, 65(2-4):176–213. 26

Wijsman, J. W. M., Herman, P. M. J., Middelburg, J. J., and Soetaert, K. (2002). A model for early diagenetic processes in sediments of the continental shelf of the Black Sea. *Estuarine Coastal and Shelf Science*, 54(3):403–421. 72

Winkler, L. W. (1888). Die bestimmung des im wasser gelösten sauerstoffes. *Berichte der deutschen chemischen Gesellschaft*, 21:2843–2846. doi:10.1002/cber.188802102122. 112

Witte, U., Aberle, N., Sand, M., and Wenzhöfer, F. (2003a). Rapid response of a deep-sea benthic community to POM enrichment: an in situ experimental study. *Marine Ecology Progress Series*, 251:27–36. 46

Witte, U., Wenzhofer, F., Sommer, S., Boetius, A., Heinz, P., Aberle, N., Sand, M., Cremer, A., Abraham, W. R., JøRgensen, B. B., and Pfannkuche, O. (2003b). In situ experimental evidence of the fate of a phytodetritus pulse at the abyssal sea floor. *Nature*, 424(6950):763–766. 26, 27

Wolfbeis, O. (1991). *Fiber optic chemical sensors and biosensors*, volume I + II. CRC Press, Boca Raton. 113

Wollast, R. and Chou, L. (2001). Ocean margin exchange in the northern Gulf of Biscay: OMEX I. an introduction. *Deep Sea Research Part II: Topical Studies in Oceanography*, 48(14-15):2971–2978. 15

Woulds, C., Cowie, G. L., Levin, L. A., Andersson, J. H., Middelburg, J. J., Vandewiele, S., Lamont, P. A., Larkin, K. E., Gooday, A. J., Schumacher, S., Whitcraft, C., Jeffreys, R., and Schwartz, M. (2007). Oxygen as a control on sea floor faunal communities and their roles in sedimentary carbon cycling. *Limnology and Oceanography*, 52(4):1698–1709. 11, 34, 41, 46

Wulff, F., Bonsdorff, E., Gren, I. M., Johansson, S., and Stigebrandt, A. (2001). Giving advice on cost effective measures for a cleaner Baltic Sea: A challenge for science. *Ambio*, 30(4-5):254–259. 50

Wulff, F. and Stigebrandt, A. (1989). A time-dependent budget model for nutrients in the Baltic Sea. *Global Biogeochemical Cycles*, 3:63–78. 50

Yamanaka, Y. and Tajika, E. (1996). The role of the vertical fluxes of particulate organic matter and calcite in the oceanic carbon cycle: Studies using an ocean biogeochemical general circulation model. *Global Biogeochemical Cycles*, 10(2):361–382. 14